FIELDIANA

Geology

NEW SERIES, NO. 28

Osteology of *Simosaurus gaillardoti* and the Relationships of Stem-Group Sauropterygia

Olivier Rieppel

December 30, 1994
Publication 1462

PUBLISHED BY FIELD MUSEUM OF NATURAL HISTORY

Information for Contributors to Fieldiana

General: *Fieldiana* is primarily a journal for Field Museum staff members and research associates, although manuscripts from nonaffiliated authors may be considered as space permits.

The Journal carries a page charge of $65.00 per printed page or fraction thereof. Payment of at least 50% of page charges qualifies a paper for expedited processing, which reduces the publication time. Contributions from staff, research associates, and invited authors will be considered for publication regardless of ability to pay page charges, however, the full charge is mandatory for nonaffiliated authors of unsolicited manuscripts. Three complete copies of the text (including title page and abstract) and of the illustrations should be submitted (one original copy plus two review copies which may be machine-copies). No manuscripts will be considered for publication or submitted to reviewers before all materials are complete and in the hands of the Scientific Editor.

Manuscripts should be submitted to Scientific Editor, *Fieldiana*, Field Museum of Natural History, Chicago, Illinois 60605-2496, USA.

Text: Manuscripts must be typewritten double-spaced on standard-weight, 8½- by 11-inch paper with wide margins on all four sides. If typed on an IBM-compatible computer using MS-DOS, also submit text on 5¼-inch diskette (WordPerfect 4.1, 4.2, or 5.0, MultiMate, Displaywrite 2, 3 & 4, Wang PC, Samna, Microsoft Word, Volkswriter, or WordStar programs or ASCII).

For papers over 100 manuscript pages, authors are requested to submit a "Table of Contents," a "List of Illustrations," and a "List of Tables" immediately following title page. In most cases, the text should be preceded by an "Abstract" and should conclude with "Acknowledgments" (if any) and "Literature Cited."

All measurements should be in the metric system (periods are not used after abbreviated measurements). The format and style of headings should follow that of recent issues of *Fieldiana*.

For more detailed style information, see *The Chicago Manual of Style* (13th ed.), published by The University of Chicago Press, and also recent issues of *Fieldiana*.

References: In "Literature Cited," book and journal titles should be given in full. Where abbreviations are desirable (e.g., in citation of synonymies), authors *consistently* should follow *Botanico-Periodicum-Huntianum* and *TL-2 Taxonomic Literature* by F. A. Stafleu & R. S. Cowan (1976 *et seq.*) (botanical papers) or *Serial Sources for the Biosis Data Base* (1983) published by the BioSciences Information Service. Names of botanical authors should follow the "Draft Index of Author Abbreviations, Royal Botanic Gardens, Kew," 1984 edition, or *TL-2*.

References should be typed in the following form:

Croat, T. B. 1978. Flora of Barro Colorado Island. Stanford University Press, Stanford, Calif., 943 pp.

Grubb, P. J., J. R. Lloyd, and T. D. Pennington. 1963. A comparison of montane and lowland rain forest in Ecuador. I. The forest structure, physiognomy, and floristics. Journal of Ecology, **51:** 567-601.

Langdon, E. J. M. 1979. Yage among the Siona: Cultural patterns in visions, pp. 63-80. *In* Browman, D. L.,and R. A. Schwarz, eds., Spirits, Shamans, and Stars. Mouton Publishers, The Hague, Netherlands.

Murra, J. 1946. The historic tribes of Ecuador, pp. 785-821. In Steward, J. H., ed., Handbook of South American Indians. Vol. 2, The Andean Civilizations. Bulletin 143, Bureau of American Ethnology, Smithsonian Institution, Washington, D.C.

Stolze, R. G. 1981. Ferns and fern allies of Guatemala. Part II. Polypodiaceae. Fieldiana: Botany, n.s., **6:** 1-522.

Illustrations: Illustrations are referred to as "figures" in the text (not as "plates"). Figures must be accompanied by some indication of scale, normally a reference bar. Statements in figure captions alone, such as "× 0.8," are not acceptable. Captions should be typed double-spaced and consecutively. See recent issues of *Fieldiana* for details of style.

All illustrations should be marked on the reverse with author's name, figure number(s), and "top."

Figures as submitted should, whenever practicable, be 8½ × 11 inches (22 × 28 cm), and may not exceed 11½ × 16½ inches (30 × 42 cm). Illustrations should be mounted on boards in the arrangement to be obtained in the printed work. This original set should be suitable for transmission to the printer as follows: Pen and ink drawings may be originals (preferred) or photostats; shaded drawings must be originals, but within the size limitation; and photostats must be high-quality, glossy, black-and-white prints. Original illustrations will be returned to the corresponding author upon publication unless otherwise specified.

Authors who wish to publish figures that require costly special paper or color reproduction must make prior arrangements with the Scientific Editor.

Page Proofs: *Fieldiana* employs a two-step correction system. The corresponding author will normally receive a copy of the edited manuscript on which deletions, additions, and changes can be made and queries answered. Only one set of page proofs will be sent. All desired corrections of type must be made on the single set of page proofs. Changes in page proofs (as opposed to corrections) are very expensive. Author-generated changes in page proofs can only be made if the author agrees in advance to pay for them.

THIS PUBLICATION IS PRINTED ON ACID-FREE PAPER.

FIELDIANA

Geology

NEW SERIES, NO. 28

Osteology of *Simosaurus gaillardoti* and the Relationships of Stem-Group Sauropterygia

Olivier Rieppel

Department of Geology
Field Museum of Natural History
Roosevelt Road at Lake Shore Drive
Chicago, Illinois 60605-2496
U.S.A.

Accepted July 19, 1994
Published December 30, 1994
Publication 1462

PUBLISHED BY FIELD MUSEUM OF NATURAL HISTORY

Library of Congress Catalog Card Number: 94-61792
ISSN 0096-2651
PRINTED IN THE UNITED STATES OF AMERICA

Table of Contents

List of Illustrations

List of Tables

Osteology of *Simosaurus gaillardoti* and the Relationships of Stem-Group Sauropterygia

Olivier Rieppel

Abstract

Simosaurus gaillardoti H.v. Meyer, 1842, is recognized as the only species of its genus. An amended diagnosis of the genus is given here. *Simosaurus mougeoti* H.v. Meyer, 1842, is a lower jaw of *Nothosaurus*; *Simosaurus guilielmi* H.v. Meyer, 1847–1855, is a junior synonym of *Simosaurus gaillardoti*. The skeletal morphology of *Simosaurus* is redescribed in detail and compared to that of other stem-group (non plesio- and pliosaur) Sauropterygia (including *Placodus*). Ninety-four skeletal characters are defined and used in a phylogenetic analysis. *Placodus* is shown to be the sister-taxon of the Eosauropterygia, placodonts and eosauropterygians together constituting the monophyletic Sauropterygia. Within the Eosauropterygia, *Corosaurus* is the sister-taxon of an unnamed clade comprising Pachypleurosauroidea plus Eusauropterygia. *Simosaurus* is the sister-taxon to all other eusauropterygians included in the analysis (the *Cymatosaurus–Nothosaurus–Lariosaurus–Pistosaurus* clade). Functional morphological correlates of the skeleton suggest that *Simosaurus* was capable of sustained swimming in the shallow epicontinental sea in pursuit of prey such as "holostean"-grade fishes and, perhaps, ammonites.

Zusammenfassung

Simosaurus gaillardoti H.v. Meyer, 1842 wird als alleiniger Vertreter seiner Gattung anerkannt. *Simosaurus mougeoti* H.v. Meyer, 1842, ist ein Unterkieferrest von *Nothosaurus*; *Simosaurus guilielmi* H.v. Meyer, 1847–1855, ist ein jüngeres Synonym von *Simosaurus gaillardoti*. Die Gattung *Simosaurus* wird durch eine erweiterte Diagnose besser begründet. Die Morphologie des Skelettes von *Simosaurus* wird neu beschrieben und mit dem Skelett anderer Stammgruppen-Vertreter der Sauropterygia, und mit *Placodus*, verglichen. Die phylogenetische Analyse weist die Placodontier als Schwestergruppe der Eosauropterygia aus; beide Gruppen zusammen bilden die monophyletische Gruppe der Sauropterygia. Innerhalb der Sauropterygier erweist sich *Corosaurus* als Schwestergruppe eines unbenannten Taxons, das die Pachypleurosauroidea und die Eusauropterygia umfasst. *Simosaurus* ist die Schwestergruppe aller andern in der Analyse berücksichtigten Eusauropterygier (*Cymatosaurus Nothosaurus Lariosaurus Pistosaurus*). Funktionell-morphologische Betrachtungen lassen *Simosaurus* als ausdauernden Schwimmer erscheinen, der im flachen epicontinentalen Meer Ganoidfische und, vielleicht, Ammoniten gejagt haben mag.

Introduction

The Sauropterygia are a group of marine Mesozoic reptiles with a fossil record dating back to the uppermost Lower Triassic and a first radiation in the lower Muschelkalk (lower Anisian) of central Europe. The Sauropterygia include a diversity of taxa such as the enigmatic genera *Cymatosaurus* and *Pistosaurus* (Sues, 1987a) from the Middle Triassic, the relatively small pachypleurosaurs from the Middle Triassic (Rieppel, 1987), the Triassic nothosaurs (*Ceresiosaurus, Lariosaurus, Notho-*

saurus, Paranothosaurus; Rieppel, 1994a) extending from the lower Anisian (possibly uppermost Scythian) to the uppermost Carnian, the Middle Triassic genus *Simosaurus,* and the crown-group plesio- and pliosaurs with a fossil record extending from the Triassic–Jurassic boundary (Storrs & Taylor, 1993) to the Upper Cretaceous. (For a complete and annotated list of generic names for Triassic Sauropterygia, see Storrs, 1991.) Whereas the crown-group plesio- and pliosaurs show a cosmopolitan distribution, the stem-group taxa listed above are restricted to the Old World with the exception of *Corosaurus* from the upper Scythian of Wyoming (Storrs, 1991). Recent fieldwork, however, indicates the presence of other stem-group sauropterygians in the Middle Triassic (Anisian) of northwestern Nevada (Sander et al., 1994).

The monophyly of the Sauropterygia has been recognized for a long time, but the relationships of the Sauropterygia to placodonts, a group of durophagous marine reptiles extending from the uppermost Scythian to the Rhaetian (Pinna, 1990), have remained controversial to the present date. The discussion of phylogenetic interrelationships of the Sauropterygia (Fig. 1) has had a long history (summarized, in part, by Rieppel, 1989a). Owen (1860) recognized the relationships of "nothosaurs" and plesiosaurs with placodonts and included these taxa with some other enigmatic fossils in his Sauropterygia. A revised concept of the Sauropterygia was proposed by Williston (1925), who included the nothosaurs, plesiosaurs, and placodonts in the Synaptosauria (a term taken from Baur, 1887) on the basis of the presence of a single upper temporal fossa. Williston's (1925) Synaptosauria were renamed as Euryapsida by Colbert (1955), and the Lower Permian genus *Araeoscelis* (Williston, 1914; Vaughn, 1955) was included within the group, as it shares the presence of a single upper temporal fossa (Romer, 1968).

The concept of the Euryapsida (including *Araeoscelis,* Sauropterygia, and Placodontia) contrasts with the hypothesis of a diapsid relation of the Sauropterygia (not the placodonts), first proposed by Jaekel (1910) following his investigation of the cranial structure of the pachypleurosaur *Anarosaurus* and of *Simosaurus.* A diapsid derivation of sauropterygians was further supported by Kuhn-Schnyder (1967, 1980), who again used the skull of *Simosaurus* (Kuhn-Schnyder, 1961) to support Jaekel's (1910) hypothesis of the loss of a lower temporal arch in the Sauropterygia. Following the description of the marine diapsid genus *Claudiosaurus* from the Permo-Triassic of Madagascar, Carroll (1981) further supported the diapsid status of the Sauropterygia.

Subsequent cladistic analysis of reptile interrelationships (Gauthier, 1984; Reisz et al., 1984; Benton, 1985; Evans, 1988) showed *Araeoscelis* to be a stem-group diapsid and modified the diagnosis of the Diapsida to refer to the presence of an upper temporal fossa (among other characters) since the lower temporal fossa is a plesiomorphic trait at the level of the Diapsida. The relations of the Sauropterygia within the Diapsida were not addressed in any of these cladistic analyses, and although the Placodontia were recognized as diapsids (Sues, 1987b), a close relationship between them and sauropterygians continued to be rejected (Kuhn-Schnyder, 1967, 1980; Sues, 1987b; Carroll & Currie, 1991).

The most recent published contributions to sauropterygian interrelationships, presented in a cladistic framework, are those of Sues (1987a), S. Schmidt (1987), Rieppel (1987, 1989a), Tschanz (1989), and Storrs (1991, 1993a). An important insight was the recognition (by Sues, 1987a; see also S. Schmidt, 1987) of the monophyly of the "Nothosauridae" (including *Ceresiosaurus, Lariosaurus, Nothosaurus,* and *Paranothosaurus*; see also Rieppel, 1994a, for additional synapomorphies of Nothosauridae), and the corroboration of a basal dichotomy, the Pachypleurosauroidea representing the sister-group of all other sauropterygians, the Eusauropterygia (Tschanz, 1989). Within the Eusauropterygia, *Simosaurus* was hypothesized to represent the sister-group of all other taxa (included in the Nothosauria *sensu* Tschanz, 1989). Rieppel (1989a) defended a sister-group relationship of the Placodontia and Sauropterygia, resurrecting the Euryapsida as a subgroup of the Diapsida (see also Zanon, 1989), but Storrs' (1991, 1993a) analysis showed the placodonts to be the sister-group of the Eusauropterygia within the Sauropterygia (Storrs, 1991, grouped the Placodontia and Eusauropterygia in a new taxon, the Nothosauriformes). In view of these competing hypotheses (Fig. 1), I reanalyzed Storrs' data matrix using the same software package as he did (Swofford, 1990) and obtained the same results, which persisted even after manipulation of his data matrix in a critical reassessment of character definitions and/or polarities (Rieppel, 1993a). Characters supporting the position of placodonts as sister-group of the Eusauropterygia are few and in some cases problematical: the enlarged upper temporal fossa, the elongated mandibular symphysis, the

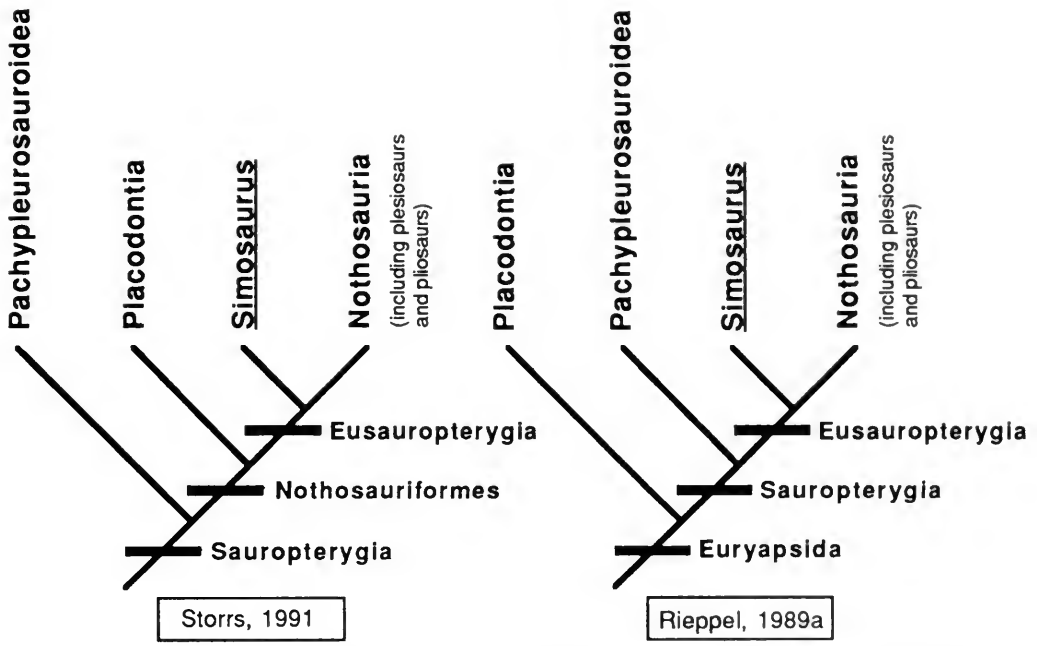

FIG. 1. Competing hypotheses of sauropterygian interrelationships. For further discussion, see text.

robust and distinctly curved humerus, and the approximately equal length of radius and ulna. Among these characters, temporal elongation and elongation of the mandibular symphysis may be functionally correlated characters, as an increase in the physiological cross-section of the jaw adductor musculature may require increased stability of the lower jaw in these durophagous reptiles. Humerus morphology and limb proportions may again reflect functional demands of aquatic locomotion; furthermore, these characters have been shown to be sexually dimorphic in at least some sauropterygian taxa (Rieppel, 1989a, 1993b; Sander, 1989), which adds to the problem of character definitions.

In view of possible functional constraints in secondarily aquatic tetrapods, the problem of convergence must be addressed by inspection of the original material, by increased scrutiny of character definitions, and by the attempt to broaden the data base for testing homology versus homoplasy (convergence or reversals) by congruence. This study is designed to test the interrelationships of Triassic Sauropterygia by a critical reevaluation of the characters taken from the literature by Storrs (1991, 1993a) and Rieppel (1993a). The osteology of *Simosaurus* will be reviewed in detail, in view of the hypothesized crucial position of the genus as sister-taxon to all other eusauropterygians (Sues, 1987a; S. Schmidt, 1987; Tschanz, 1989) and the fact that *Simosaurus* is known from complete and partially articulated specimens. A close comparison of the osteology of *Simosaurus* to that of *Nothosaurus* will provide the basis for a critical characterization of eusauropterygian morphology. *Placodus*, again known from at least one complete skeleton (Drevermann, 1933), is here chosen as a paradigm for placodont morphology and is compared to isolated placodont material in the effort to characterize the basal placodont morphology (a complete skeleton of *Paraplacodus* [Kuhn-Schnyder, 1942] remains inaccessible for study at this time; see also Zanon, 1989). The Pachypleurosauroidea will be used as a terminal taxon even though some of the genera referred to this taxon are poorly known and future revision of the pachypleurosaurs (Rieppel, work in progress) may alter our current understanding of the group. Accordingly, characters for the Pachypleurosauroidea will be taken from *Dactylosaurus* (Sues & Carroll, 1985, and pers. obs.) and the well-known *Serpianosaurus–Neusticosaurus* clade (Rieppel, 1989a; Sander, 1989).

The material described and illustrated in this study is listed in Appendix II, which also provides the relevant institutional abbreviations.

Systematic Paleontology

Sauropterygia Owen, 1860

DEFINITION—A monophyletic group of Mesozoic marine reptiles including the Placodontia and Eosauropterygia.

DIAGNOSIS—Premaxillae large, forming most of the snout; anterior teeth procumbent; lacrimal lost; clavicles positioned anteroventral to interclavicle; clavicles applied to medial surface of scapula; posterior stem of interclavicle reduced or absent; coracoid foramen enclosed between coracoid and scapula; pectoral girdle fenestrate; three or more sacral ribs.

Eosauropterygia, new taxon

DEFINITION—A monophyletic group including *Corosaurus,* Pachypleurosauroidea, and Eusauropterygia.

DIAGNOSIS—Lateral basioccipital tubera in complex relation to pterygoid; zygosphene-zygantrum articulation present; expanded articular facets of centrum support neural arch; clavicles with expanded anterolateral corners; scapular blade reduced.

Eusauropterygia Tschanz, 1989

DEFINITION—A monophyletic group including *Ceresiosaurus, Cymatosaurus, Lariosaurus, Nothosaurus, Pistosaurus, Simosaurus,* and all plesio- and pliosaurs.

DIAGNOSIS—Frontal in contact with premaxilla; frontals fused (in adult); parietal fused (in adult); vertebrae platycoelous.

Simosaurus H.v. Meyer, 1842

TYPE SPECIES—*Simosaurus gaillardoti* H.v. Meyer, 1842, from the upper Muschelkalk (Ladinian) of Lunéville, France (the holotype is now lost; see discussion below).

DIAGNOSIS—Large (3–4 m total length) eusauropterygians with a brevirostrine skull; tooth crowns broad and blunt, distinctly set off from tooth base, enamel distinctly striated; snout not constricted; upper temporal fossae much larger than orbits; pineal foramen displaced posteriorly; mandibular articulation displaced to a level well behind the occipital condyle, occiput deeply excavated; squamosal with distinct lateral process; vertebrae platycoelous and non-notochordal with infraprezygapophysis and infrapostzygapophysis in addition to zygosphene and zygantrum; clavicle with short anterolateral process; humerus without entepicondylar foramen; ulna with broad proximal head.

DISTRIBUTION—Middle Triassic of central Europe.

Simosaurus gaillardoti H.v. Meyer, 1842

1844 *Simosaurus gaillardoti,* H.v. Meyer & T. Plieninger, pp. 45–47, Pl. 11, Fig. 1.
1847 *Simosaurus gaillardoti,* Giebel, p. 162.
1847–1855 *Simosaurus gaillardoti,* H.v. Meyer, p. 86, Pl. 65, Figs. 1–2.
1847–1855 *Simosaurus guilielmi,* H.v. Meyer, p. 93, Pl. 20, Fig. 1.
1859 *Simosaurus gaillardoti,* Gervais, 1859, pp. 475–476, Pl. 55, Fig. 2, Pl. 56, Figs. 1–4.
1864 *Simosaurus gaillardoti,* v. Alberti, p. 225.
1864 *Simosaurus guilielmi,* v. Alberti, p. 225.
1896 *Simosaurus gaillardoti,* Fraas, p. 11, Pl. 3.
1896 *Simosaurus guilielmi,* Fraas, p. 13.
1899 *Simosaurus gaillardoti,* Schrammen, Pl. 24, Figs. 2a–c.
1905 *Simosaurus gaillardoti,* Jaekel, pp. 60, 72, Figs. 4–7.
1910 *Simosaurus gaillardoti,* Jaekel, pp. 327, 72, Fig. 3.
1914 *Simosaurus gaillardoti,* Schröder, p. 96, text Figs. 14, 28.
1921 *Simosaurus gaillardoti,* Huene, pp. 201–239, Figs. 1–13, Pls. I–III.
1921 *Simosaurus guilelmi,* Huene, pp. 227–228, Fig. 14.
1924 *Simosaurus gaillardoti,* Arthaber, p. 470, Figs. 8–9.
1924 *Simosaurus guilelmi,* Arthaber, p. 470.
1928 *Simosaurus gaillardoti,* Corroy, p. 122, Fig. 11.
1928 *Simosaurus guilielmi,* Corroy, pp. 122–123.
1928 *Simosaurus gaillardoti,* M. Schmidt, p. 404, Fig. 1134.
1928 *Simosaurus guillelmi,* M. Schmidt, pp. 404–405, Fig. 1135.
1934 *Simosaurus gaillardotii,* Kuhn, p. 38.

1934 *Simosaurus guillelmi,* Kuhn, p. 39.
1935 *Simosaurus gaillardoti,* Edinger, p. 330, Figs. 6, 9a.
1948 *Simosaurus gaillardoti,* Huene, p. 41, Fig. 1.
1952 *Simosaurus gaillardoti,* Huene, p. 163ff., Figs. 1–66.
1956 *Simosaurus gaillardoti,* Huene, p. 390, Fig. 429.
1956 *Simosaurus guilelmi,* Huene, p. 390.
1959 *Simosaurus guilielmi* var. *angusticeps,* Huene, pp. 180–184, Figs. 1–3, Pl. 19.
1961 *Simosaurus gaillardoti,* Kuhn-Schnyder, p. 95ff., Figs. 1–3, 4a, 5, 7b, 8, Pls. 9–10.
1962 *Simosaurus gaillardoti,* Kuhn-Schnyder, p. 135, Figs. 1–2.
1963 *Simosaurus gaillardoti,* Kuhn-Schnyder, Figs. 1a, 2a, 3a.
1965 *Simosaurus gaillardoti,* Kuhn-Schnyder, p. 153, Fig. 7.
1967 *Simosaurus gaillardoti,* Kuhn-Schnyder, p. 342, Figs. 7a, 8b.
1970 *Simosaurus gaillardoti,* Schultze, pp. 230–231, Fig. 15.
1987 *Simosaurus guilielmi,* Wild, pp. 19–20, Fig. 8.
1989a *Simosaurus gaillardoti,* Rieppel, p. 61, Fig. 15a.
1994a *Simosaurus gaillardoti,* Rieppel, p. 9ff., Figs. 2B, 3B, 4, 5A, 6.

HOLOTYPE—The original skull from the Muschelkalk of Lunéville (France), described by Meyer (1842) as *Simosaurus gaillardoti,* can no longer be located today, but the description and illustrations given by Meyer (1847–1855) validate the name. The holotype of *Simosaurus guilielmi* Meyer, 1847–1855, a subjective junior synonym of *Simosaurus gaillardoti,* is kept at the Staatliches Museum für Naturkunde Stuttgart (SMNS 16700) and is considered to be the neotype of *Simosaurus gaillardoti.*

LOCUS TYPICUS—Upper Muschelkalk (Ladinian) of Lunéville, France.

DISTRIBUTION—Upper Muschelkalk (Ladinian, Middle Triassic) of eastern France, Württemberg and Franconia, SW Germany; Lettenkeuper and Gipskeuper (restricted to upper Ladinian: H. Hagdorn, in lit. 7 Apr. 1994) of Württemberg, Germany (Fig. 2).

The occurrence of *Simosaurus* in the upper Muschelkalk of Württemberg (Germany) is correlated with particular ammonite faunas within the "Discoceratitenschichten" (H. Hagdorn, in lit. 18 Dec. 1993). The genus is first recorded from the *nodosus* biozone (*Ceratites* [*Ceratites*] *nodosus*) of the upper Ceratitenschichten (Wenger, 1957; Hagdorn, 1991) of the upper Muschelkalk and is most frequently encountered in the *dorsoplanus* biozone, characterized by *Ceratites* (*Discoceratites*) *dorsoplanus.* In the *semipartitus* biozone (*Ceratites* [*Discoceratites*] *semipartitus*), *Simosaurus* becomes rare again and remains so until the end of the Muschelkalk. *Simosaurus* is exceedingly rare in the Keuper.

DIAGNOSIS—Same as for genus, of which this is the only known species.

COMMENTS—The genus *Simosaurus* was first described by Meyer (1842) on the basis of specimens from the Muschelkalk of Lunéville, France. Meyer (1842) provided no formal diagnosis and no illustration of the holotype of the genotypical species, but he recognized *Simosaurus gaillardoti* as very distinct from *Nothosaurus* by its broad, flat, and brevirostrine skull with a deeply excavated occiput (type species by priority on p. 192; named after Claude Antoine Gaillardot [1774–1833]). The holotype is now lost, but the description and illustrations provided by Meyer (1847–1855) validate the species.

Announcing his work on the fossil reptiles from Lunéville to F.v. Andriani, Meyer wrote in a letter dated 27 December 1841 that he was surprised not to find *Nothosaurus* as part of the fauna; he indicated, however, that he recognized two species of *Simosaurus, S. gaillardoti* and *S. mougeoti* (Freyberg, 1972, p. 25). *Simosaurus mougeoti* was based on a mandibular symphysis and was formally described by Meyer in 1842. The same specimen was later figured by Meyer (1847–1855, Pl. 15, Fig. 3) but designated as *Nothosaurus mougeoti* in the figure caption (p. 165). In the text, Meyer (1847–1855, p. 19) referred to the specimen as "the first fragment of the lower jaw of *Nothosaurus* ever found." Indeed, the characteristic elongation of the symphyseal area of the lower jaw with, in its posterior part, large alveoli for fangs opposing the paired maxillary fangs is diagnostic for the genus *Nothosaurus* (Fig. 3B). Again, the holotype of *Simosaurus mougeoti* can no longer be located today.

A skull of *Simosaurus* (Fig. 4) from the Lettenkeuper of Hoheneck near Ludwigsburg, Baden-Württemberg, was sent to H.v. Meyer by the Duke Wilhelm of Württemberg (Meyer, in lit. to F.v. Andriani, 25 Jan. 1842; Freyberg, 1972, p. 26) and first described by Meyer and Plieninger (1844).

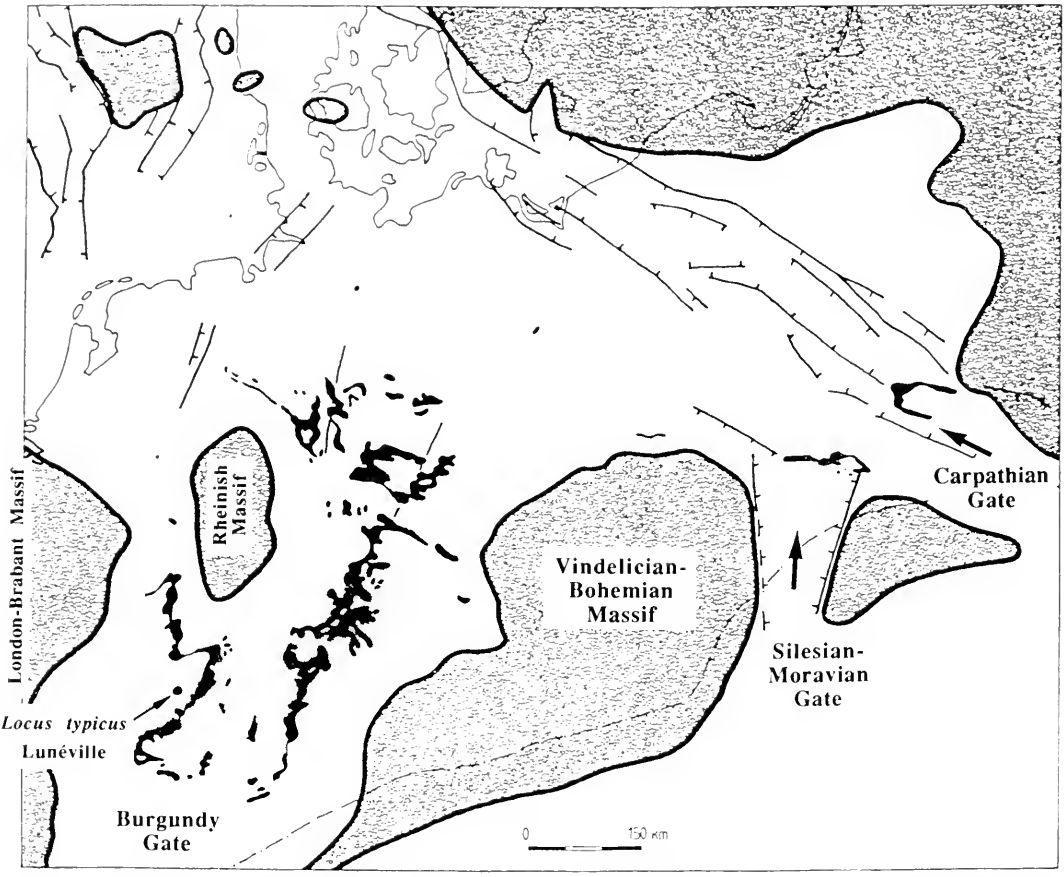

FIG. 2. Distribution of outcrops yielding *Simosaurus* in the upper Muschelkalk basin. Dotted: upper Muschelkalk; black: Keuper. (Courtesy of H. Hagdorn, Ingelfingen.)

Coming from the Lettenkeuper, this specimen was geologically younger than other *Simosaurus* specimens from the upper Muschelkalk. Meyer and Plieninger (1844, p. 46) mentioned problems of preparation and described proportional relations that differed from the skull of *Simosaurus gaillardoti*. Their final conclusion was, however, that "all of those differences, including the different contours of the upper temporal fossae, are not sufficient to refer the skull from Ludwigsburg to a species separate from *Simosaurus gaillardoti*." Later, Meyer (1847–1855, p. 93, Pl. 20, Fig. 1) changed his views and named a new species, *Simosaurus guilielmi*, to refer to the skull from Ludwigsburg. The diagnosis of *Simosaurus guilielmi* is to be deduced from its comparison with *Simosaurus gaillardoti* (Meyer, 1847–1855, p. 72): the skull of *Simosaurus gaillardoti* is generally larger and is said to have a broader and less pointed snout, a less deeply excavated occiput, and relatively larger upper temporal fenestrae (whose longitudinal diameter exceeds twice the longitudinal diameter of the orbit); the distance from the posterior margin of the orbit to the anterior margin of the upper temporal fossa, compared to the distance from the posterior margin of the external naris to the anterior margin of the orbit, is larger in *Simosaurus gaillardoti*; and the dorsal bridge (frontal bone) between the orbits is relatively broader in *Simosaurus gaillardoti*. Huene (1921, pp. 227–228) confirmed the validity of the new species (which he misspelled as *Simosaurus guilelmi*) on the basis of differences in the cranial suture pattern that he claimed to be able to identify on the holotype. M. Schmidt (1928) again listed *Simosaurus guilielmi* (which he misspelled as *Simosaurus guillelmi*) as a separate species based on the proportional differences listed by Meyer (1847–1855).

Inspection of the holotype of *Simosaurus gui-*

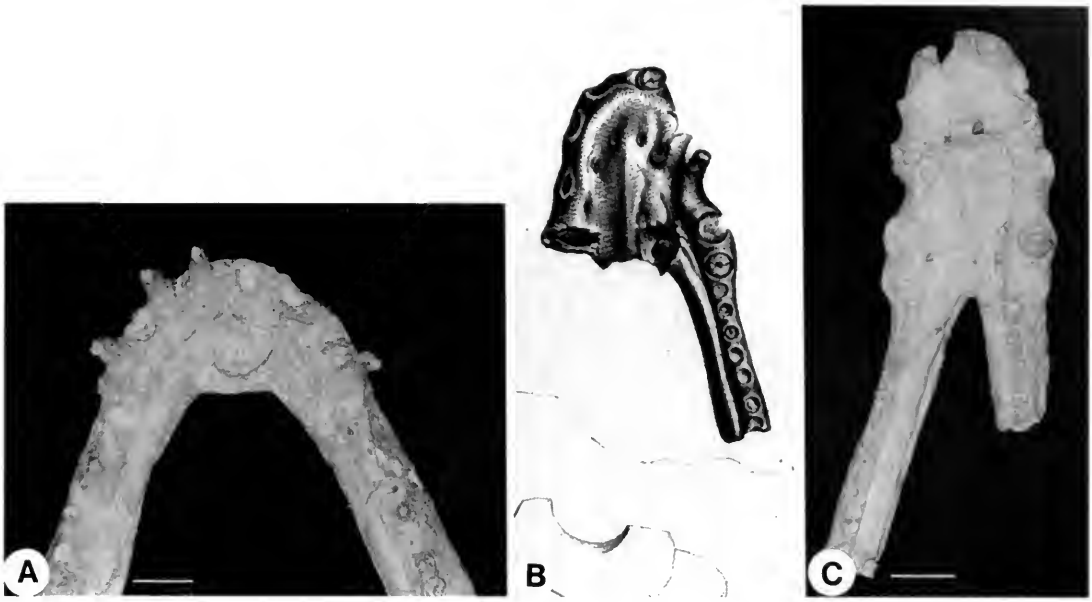

FIG. 3. Mandibular symphysis in dorsal view. **A**, *Simosaurus* (SMNS 7861, upper Muschelkalk, Crailsheim; original of Fraas, 1896, Pl. 3); **B**, *Nothosaurus mougeoti* (from Meyer, 1847–1855, Pl. 15, Fig. 3); **C**, *Nothosaurus mirabilis* (SMNS 59817, upper Muschelkalk [*nodosus* biozone], Hegnabrunn). Scale bar = 20 mm.

lielmi (SMNS 16700), and its comparison with all other *Simosaurus* skulls from the upper Muschelkalk deposited in public repositories, shows that this species must be considered a junior synonym of *Simosaurus gaillardoti*. Absolute size differs considerably among the skulls from the upper Muschelkalk (usually referred to *Simosaurus gaillardoti*), some of them being as small as the skull of *Simosaurus guilielmi*, indicating ontogenetic variation. The holotype of *Simosaurus guilielmi* does not show an appreciably more pointed snout than is observed in the skulls from the upper Muschelkalk. The holotype of *Simosaurus guilielmi* is very poorly prepared (see Meyer & Plieninger, 1844, p. 46), with most of the bone surface severely damaged. The natural bone surface is damaged all around the contours of the snout, rendering the assessment of its natural shape problematical. Preparation may also account for the apparent slight constriction of the snout referred to by M. Schmidt (1928). What little can be identified of the sutural pattern does not support Huene's (1921) observation (Fig. 5). The posterior projection of the jugal is very distinct, as is the suture between premaxilla and maxilla at the anterolateral edge of the external naris. In front of the right orbit there is a vague indication of a contact of the prefrontal with the nasal. This character does not differentiate *Simosaurus guilielmi* from *Simosaurus gaillardoti*, since the latter shows bilateral variability in at least one of the skulls (SMNS 10360, see Kuhn-Schnyder, 1961, Pl. 9, contra Kuhn-Schnyder, 1961, Fig. 2; see also Figs. 8–9 of this paper). The second specimen, *Simosaurus guilielmi* var. *angusticeps* (Fig. 6), described by Huene (1959) from the lower Gipskeuper of Obersontheim, is very poorly preserved and allows no identification of sutural details in the skull.

To use cranial proportional relations in the diagnosis of different species of *Simosaurus* is highly problematical, because of 1) incomplete preservation of most skulls, 2) extensive crushing and deformation of the skulls during fossilization, and 3) poor preparation. In the holotype of *Simosaurus guilielmi*, the margins of the external nares, orbits, and upper temporal fossae are, partially at least, severely damaged, and the skull dorsoventrally compressed, rendering proportional relations unclear. With reference to the proportional relations considered to be diagnostic at the species level by Meyer (1847–1855), the following are considered to be least affected by crushing and flattening of the skull: 1) longitudinal diameter of the upper temporal fossa in relation to the longitudinal diameter of the orbit; 2) width of the postorbital arch in relation to the distance between the exter-

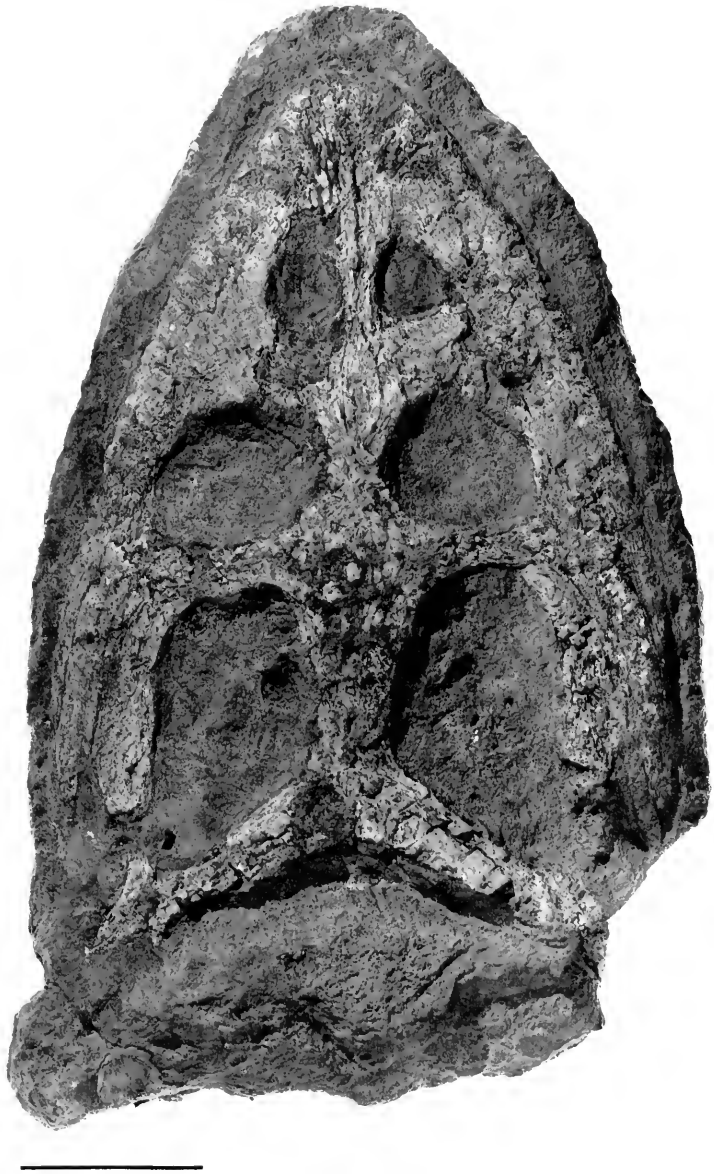

FIG. 4. Holotype of *Simosaurus guilielmi* (Meyer, 1847–1855), from the Lettenkeuper of Hoheneck near Ludwigsburg (SMNS 16700). Scale bar = 50 mm.

nal naris and the orbit; and 3) width of the frontal bone between the orbits, related to the width of the bony bridge separating the external nares. Measurements were taken from a total of 12 *Simosaurus* skulls deposited in public repositories (see Appendix II for the material included in this study). For measurements that differ on the left and right side of the skull, the arithmetic mean of the two values was used.

The ratio (longitudinal diameter of upper tem-

poral fossa/longitudinal diameter of orbit) ranges from 1.48 to 2.44. The value for the holotype of *Simosaurus guilielmi* (SMNS 16700) is 2.01, and the Tübingen specimen of *Simosaurus guilielmi* shows a ratio of 1.48, whereas the ratios represented by skulls from the upper Muschelkalk of Crailsheim range from 1.53 (SMNS 18274) to 2.44 (original of Meyer, 1847–1855, p. 86ff., Pl. 65, Figs. 1–2; SMNS uncatalogued). The ratio (width of postorbital arch/distance between external naris and orbit) ranges from 0.44 to 1.15. The value for the holotype of *Simosaurus guilielmi* (SMNS 16700) is 0.52, and the same ratio is shown by the Tübingen specimen of *Simosaurus guilielmi*. The ratios represented by skulls from the upper Muschelkalk of Crailsheim range from 0.44 (SMNS 16639) to 1.15 (BSP 1932.1.13). The ratio (width of frontal bridge between orbits/width of bony bridge between external nares) ranges from 1.38 to 2.44. The value for the holotype of *Simosaurus guilielmi* (SMNS 16700) is 2.0, and the Tübingen specimen of *Simosaurus guilielmi* shows a ratio of 1.70, whereas the ratios represented by skulls from the upper Muschelkalk of Crailsheim range from 1.38 (BSP 1932.1.13) to 2.44 (SMNS 18550). As far as they can be established with any degree of confidence, proportional relations in the skull lend no support to the validity of two separate species of *Simosaurus*.

Opeosaurus suevicus is a genus and species described by Meyer (1847–1855, p. 82, Pl. 14, Figs. 7–9) on the basis of lower jaw fragments, including parts of both left and right dentary, from the upper Muschelkalk of Stuttgart–Zuffenhausen (SMNS 4141). An alleged diagnostic feature is a "mandibular fenestra" in the posterior part of the left dentary. Preservation and/or preparation of the specimen is very poor, and the mandibular fenestra is an artifact. The genus was considered a possible junior synonym of *Simosaurus* by Kuhn (1934, p. 40; see also Arthaber, 1924, p. 470; Huene, 1956, p. 390; Storrs, 1991, p. 137), but tooth fragments preserved on both dentaries indicate that *Opeosaurus* must be a junior synonym of *Nothosaurus* (pers. obs.). Fraas (1896, p. 9) considered *Opeosaurus suevicus* a junior synonym of *Nothosaurus aduncidens* (see also Schrammen, 1899, p. 408; Romer, 1956, p. 662). The lower jaw is not diagnostic, and *Opeosaurus* and *suevicus* are nomina dubia (Storrs, 1991, p. 137).

Another taxon questionably considered a junior synonym of *Simosaurus* by Kuhn (1934, p. 38; see also Arthaber, 1924, pp. 470–471) is *Lamprosauroides goepperti* (*Lamprosauroides* K. P. Schmidt, 1927, replaces *Lamprosaurus* Meyer, 1860), represented by a right maxilla from the lower Muschelkalk of Upper Silesia (now Poland) and first described by Meyer (1860) (the holotype is at the Institute of Geological Sciences of the University of Wroclaw, MGU Wr. 3871_S). If that and similar specimens (Fig. 7) were, indeed, *Simosaurus*, it would significantly extend the geological range of that genus from the upper down into the lower Muschelkalk. The teeth, however, are different from those of *Simosaurus* (slender and pointed), and *Lamprosauroides goepperti* Meyer (1860) may be a senior synonym of *Cymatosaurus* Fritsch (1894; see also Schrammen, 1899, p. 408) if it is not, in fact, a nomen dubium. The consequences of such synonymy for the validity of the genus name *Cymatosaurus* must await the proper assessment of the type material of *Conchiosaurus clavatus* Meyer (1834), which may include *Cymatosaurus* material (R. Wild, in lit. 7 Oct. 1993).

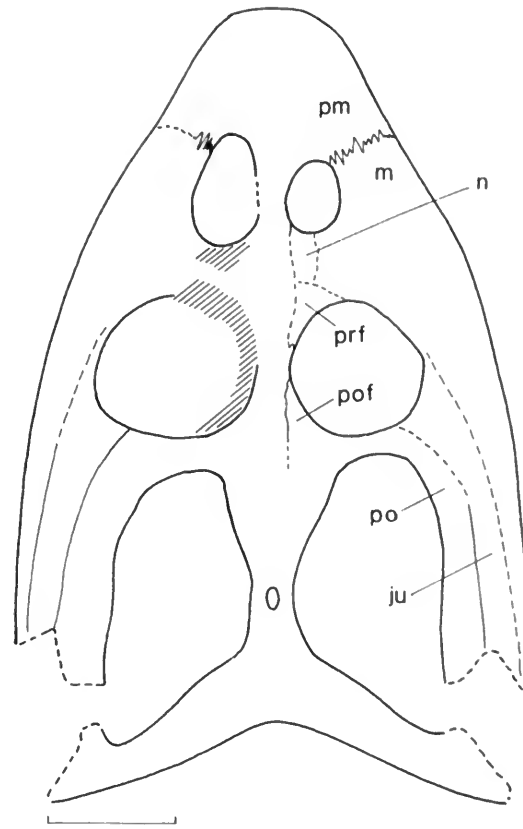

FIG. 5. Sutures identified on the holotype of *Simosaurus guilielmi* (SMNS 16700). Abbreviations: ju, jugal; m, maxilla; n, nasal; pm, premaxilla; po, postorbital; pof, postfrontal; prf, prefrontal. Scale bar = 40 mm.

FIG. 6. Skull of the holotype of *Simosaurus gutlielmi* var. *angusticeps* (Huene, 1959) from the lower Gipskeuper of Obersontheim (Geologisch–Paläontologisches Institut und Museum, University of Tübingen, uncatalogued). Scale bar = 50 mm.

Morphological Description

Skull

The skull of *Simosaurus* has been the object of a large number of studies. The most important specimen is SMNS 10360 (Figs. 8–10). It was donated to the Staatliches Museum für Naturkunde in Stuttgart by R. Blezinger in 1901 and formed the original of Jaekel's (1905; see also Jaekel, 1907, Fig. 19) description. Huene (1921, p. 222) described a second skull (SMNS 11364), erroneously identifying it as Jaekel's (1905) specimen. Jaekel's (1905) original specimen was reprepared and redescribed by Huene (1952). The same specimen was later used by Romer (1956) and, after acid preparation, by Kuhn-Schnyder (1961; see also Kuhn-Schnyder, 1962, 1963, 1965, 1967) and Rieppel (1989a, 1994a) in their discussion of cranial anatomy.

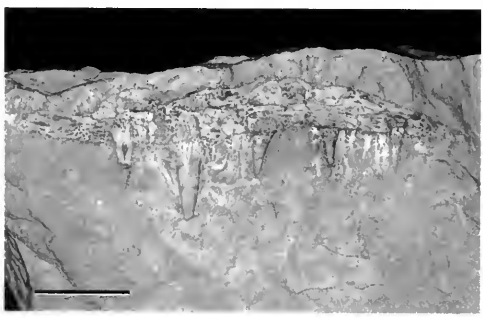

FIG. 7. Jaw fragment of cf. *Lamprosauroides goepperti* (Meyer, 1860) (lower Muschelkalk [mu1], Sacrau near Gogolin [Poland], BGR uncatalogued).

DORSAL VIEW (Fig. 9)—The skull of *Simosaurus* is broad and flat, with large and oval temporal fossae and a short and broad rostrum. A rostral constriction of the skull at the level of the anterior margin of the external nares is absent or only very weakly developed. The premaxilla meets the maxilla at the anterolateral edge of the oval external naris. Posterior (nasal) processes of the premaxillae (identified as nasals by Jaekel, 1905; see Kuhn-Schnyder, 1961) extend backward between the external nares to meet the frontal at a level shortly behind the posterior margin of the external nares. The nasals (identified as postnasals by Jaekel, 1905; see Kuhn-Schnyder, 1961) are relatively small triangular elements defining the posteromedial margin of the external naris; the posteriorly pointing apex of the nasal is embraced between anteromedial and anterolateral processes of the frontal.

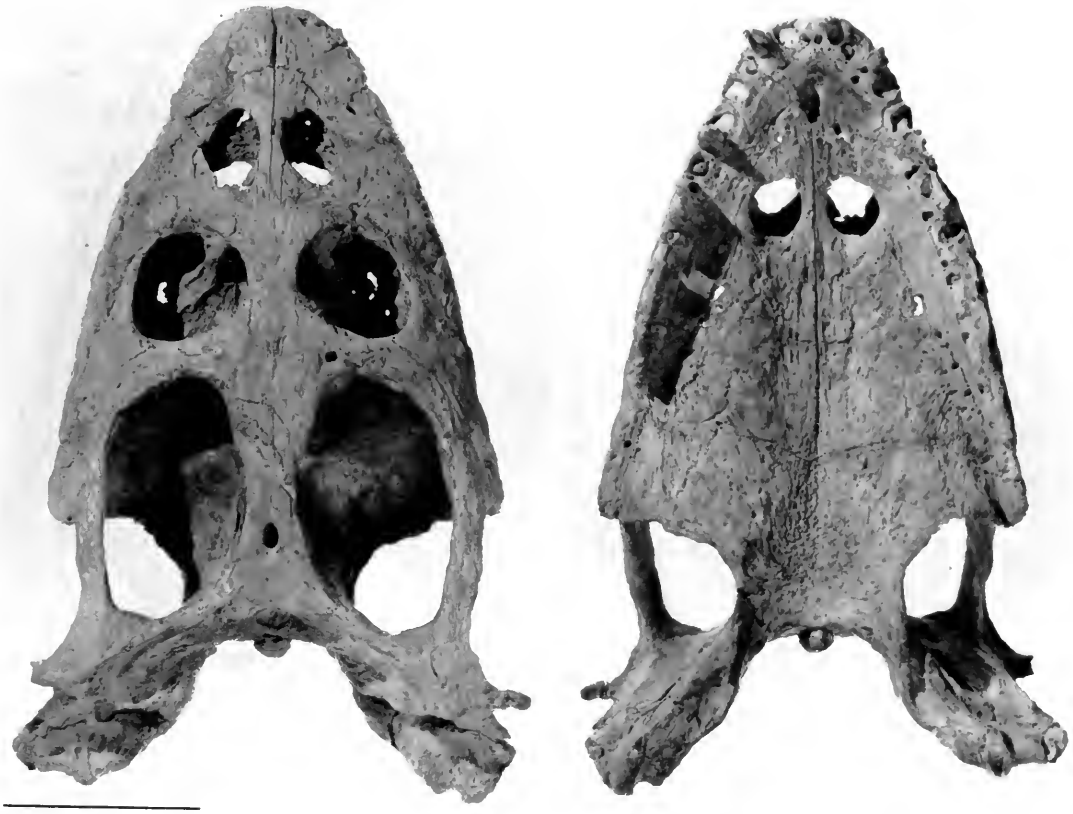

FIG. 8. Skull of *Simosaurus gaillardoti* (SMNS 10360) in dorsal (left) and ventral (right) views. Scale bar = 50 mm. (Dorsal view: SMNS neg. #9160; ventral view SMNS neg. #9159.)

The prefrontal (identified as lacrimal by Jaekel, 1905; see Kuhn-Schnyder, 1961) defines the anteromedial margin of the orbit. It remains separated from the postfrontal along the dorsal margin of the orbit. SMNS 10360 is interesting because it shows an asymmetry of the anterior relations of the prefrontal on the right and left side of the skull. Jaekel (1905, Fig. 4) showed the prefrontal in contact with the nasal on both sides of the skull, whereas Kuhn-Schnyder (1961, Fig. 2) reconstructed the skull with a contact of the anterolateral process of the frontal with the maxilla, separating the prefrontal from the nasal on both sides. In fact, the skull shows the prefrontal in contact with the nasal on the right side, whereas the anterolateral process of the frontal reaches the maxilla on the left side (Fig. 9; see also Kuhn-Schnyder, 1961, Pl. 9).

The prefrontal meets the palatine by means of a distinct yet slender pillar-like structure (identified as lacrimal by Huene, 1921), which in its dorsal part carries a depression, or one or two small foramina (Huene, 1921). This prefrontal–palatine pillar divides the anteroventral part of the orbit into two large openings, a lateral one situated between the ascending process of the maxilla (not lacrimal, as claimed by Kuhn-Schnyder, 1961) and the palatine–prefrontal pillar, the medial one located medial to the palatine–prefrontal pillar. The lateral opening represents the infraorbital foramen (*sensu* Oelrich, 1956), which in *Simosaurus* is confluent with the lacrimal foramen and, hence, served the passage of the lacrimal duct in its dorsal part and the passage of the superior alveolar nerve (maxillary division of the trigeminal nerve) along with its artery in its ventral part. The medial opening may have served the passage of the palatine nerve and of the ophthalmic division of the trigeminal nerve.

The frontals are fused and define the concave dorsal margin of the orbit (between prefrontal and postfrontal). The bone lacks clearly defined pos-

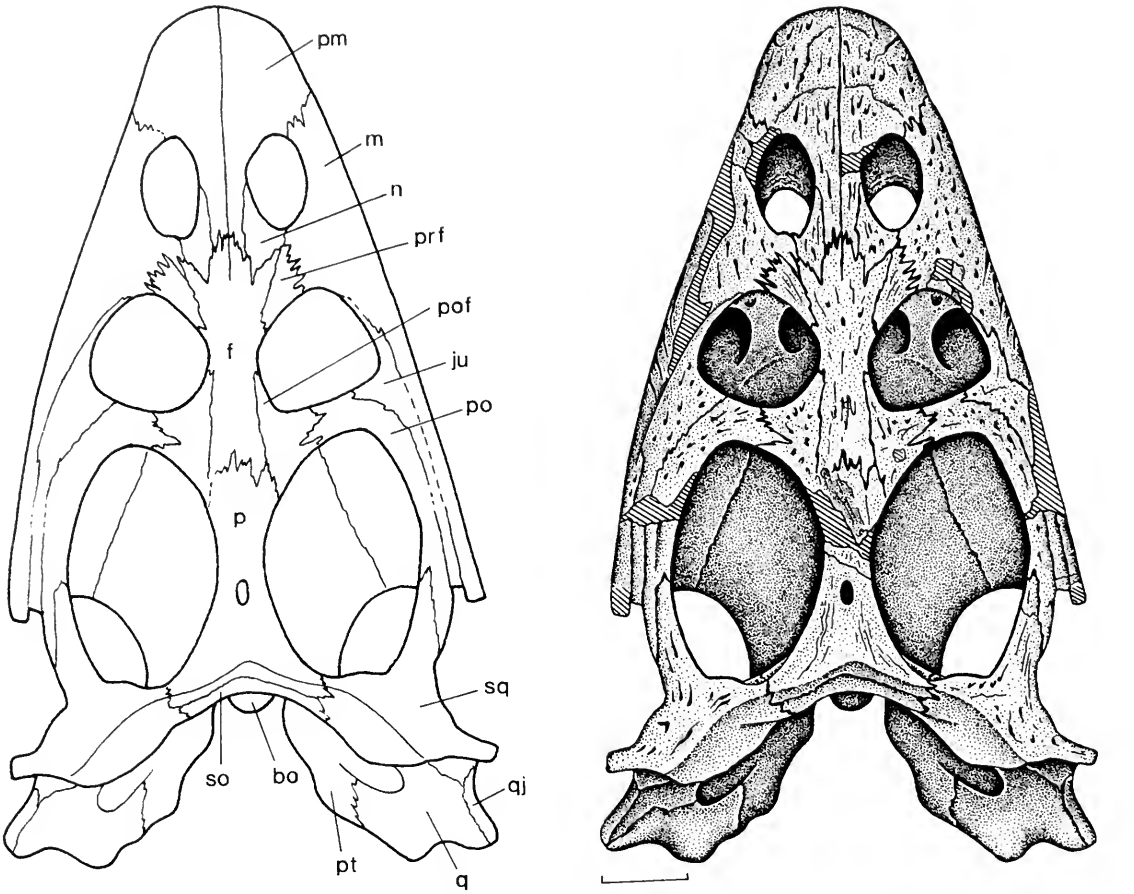

FIG. 9. Skull of *Simosaurus gaillardoti* (SMNS 10360) in dorsal view. Abbreviations: bo, basioccipital; f, frontal; ju, jugal; m, maxilla; n, nasal; p, parietal; pm, premaxilla; po, postorbital; pof, postfrontal; prf, prefrontal; pt, pterygoid; q, quadrate; qj, quadratojugal; so, supraoccipital; sq, squamosal. Scale bar = 40 mm.

terolateral processes and meets the parietal in a deeply interdigitating suture somewhat behind the level of the anterior margin of the upper temporal fossa. The postfrontal defines the posteromedial margin of the orbit as well as the anteromedial margin of the upper temporal fossa, forming the dorsal part of the narrow postorbital arch. The ventral process of the postfrontal embraces a tapering dorsal process of the postorbital. The postorbital is a curved (rather than triradiate) element defining the anterolateral and most of the lateral margin of the upper temporal fossa through its participation in the formation of the upper temporal arch. Anteriorly, the postorbital has a relatively narrow exposure at the posterior margin of the orbit, between the postfrontal and jugal bone.

The jugal is a fairly prominent element in *Simosaurus*. A slender anterior process extends along the entire lateral (morphologically ventral) margin of the orbit but does not reach the prefrontal anteriorly. The width of the jugal is increased at the posterolateral margin of the orbit, but the element becomes narrow again as it extends farther posteriorly, situated between the postorbital and the maxilla. The maxilla forms the greater part of the lateral (morphologically ventral) margin of the external naris and expands to form a low ascending process (topologically a medial process) between the external naris and the orbit. Behind the orbit, the bone shows a narrow lateral exposure and extends backward , below the jugal, to a level slightly in front of the squamosal–postorbital suture within the upper temporal arch. The anterior half of the upper temporal fossa is thus closed laterally by a bony arcade composed of postorbital, jugal, and maxilla, the maxillary tooth row thus extending backward to a level well behind the orbit. The jugal, together with the maxilla, forms a short,

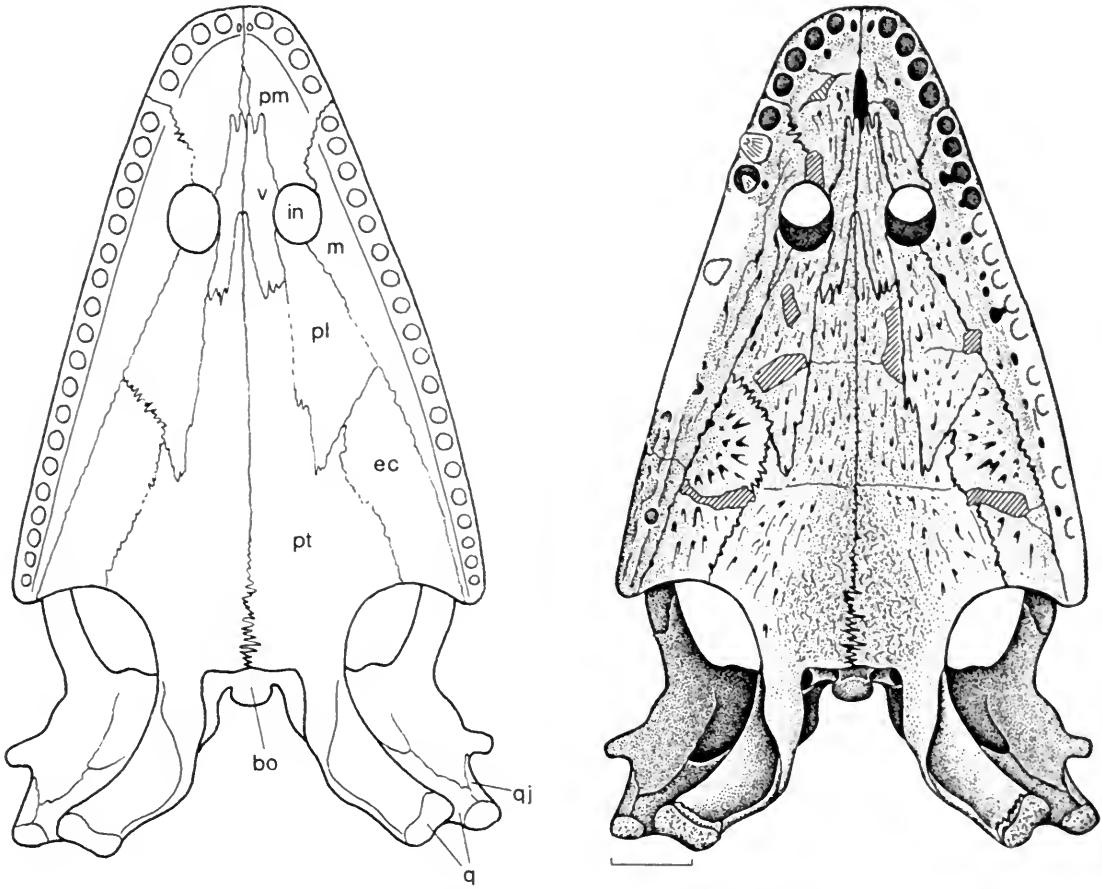

FIG. 10. Skull of *Simosaurus gaillardoti* (SMNS 10360) in ventral view. Abbreviations: bo, basioccipital; ec, ectopterygoid; in, internal naris; m, maxilla; pl, palatine; pm, premaxilla; pt, pterygoid; q, quadrate; qj, quadratojugal; v, vomer. Scale bar = 40 mm.

free-ending posterior process (broken in many specimens), which prompted Jaekel (1910) to postulate a diapsid derivation for the Sauropterygia.

The parietal is unpaired (fused) and forms a narrow bridge between the upper temporal fossae. The pineal foramen is displaced to a position somewhat behind the midpoint of the parietal skull table. Posteriorly, the parietal is broadened, with a concave posterior margin. A poorly defined occipital crest (for the insertion of the spinalis capitis muscle) separates the parietal skull table from the occipital exposure of the parietal (identified as postparietal by Kuhn-Schnyder, 1961; but see Schultze, 1970). The parietal forms a laterally descending flange along the medial and posteromedial margin of the upper temporal fossa for the origin of the deep jaw adductor musculature (m. adductor mandibulae externus medialis and, possibly, m. pseudotemporalis superficialis; Rieppel, 1989a).

The squamosal caps the quadrate suspension and defines the posterolateral margin of the upper temporal fossa. Posterolateral to the upper temporal fossa, the squamosal is drawn out into a distinct but small lateral projection. The poorly defined and shallow occipital crest separates the dorsal exposure of the squamosal from its occipital exposure (identified as tabular by Kuhn-Schnyder, 1961; but see Schultze, 1970). The quadrate bone is covered in lateral view by a descending process of the squamosal. The latter meets a small quadratojugal bone, positioned lateral to the ventral part of the quadrate bone, immediately above the mandibular condyles of the quadrate. The quadratojugal of *Simosaurus* was first identified by Schultze (1970, Fig. 15; see also Sues, 1987a).

VENTRAL VIEW (Fig. 10)—The palate of *Simosaurus* is characterized by relatively small internal nares of almost circular contours. The internal nares are separated by the paired vomers, which are

long and slender elements. Anteriorly, the vomers reach a gap separating the premaxillaries along the midline (see below). Posteriorly, the vomers embrace an anteromedial projection of the pterygoids.

The premaxillae show five tooth positions on an "alveolar ridge." Behind the alveolar ridge, a gap in the ossification results in the formation of a "foramen incisivum" enclosed between the two premaxillaries and closed posteriorly by the vomers. Between the vomer and maxilla, the premaxilla extends backward, entering (and defining) the anterior margin of the internal naris.

The palatal shelf of the maxilla is broadest in its anterior part, where it forms the lateral margin of the internal naris. From there it tapers toward its posterior tip along a gently curved medial margin, which establishes sutural contact with the palatine (anteriorly) and ectopterygoid (posteriorly). The palatine is an almost triangular or trapezoidal element, wedged in between the vomer and pterygoid medially, the maxilla laterally, and the ectopterygoid posteriorly. It defines the posterior margin of the internal naris. The ectopterygoid lies behind the palatine and between the pterygoid (medially) and the maxilla (laterally). It defines the anterolateral margin of the subtemporal fossa.

The pterygoids are the dominant elements in the dermal palate. The bones meet in a ventromedial suture, obliterating the interpterygoid fossa and covering the basicranium in ventral view. Only the basioccipital is narrowly exposed behind their posterior border. The palate is akinetic due to the fusion of the pterygoids with the basicranium.

The anterior (palatine) processes of the two pterygoids form a combined anteromedial process that enters between the vomers, extending to a level between the internal nares. Transverse processes of the pterygoid are weakly expressed and meet the ectopterygoid laterally. There is no ventral flange of the pterygoids for the origin of the pterygoideus externus muscle. In front of the anterior margin of the subtemporal fossa, the palate (pterygoid and ectopterygoid) is characteristically vaulted, which results from a depression of the dorsal surface of the palate in the corresponding area. This indicates the presence of a well-developed dorsal (anterior) portion of m. pterygoideus externus, which took its origin from the dorsal surface of the pterygoid and ectopterygoid behind the orbit. The quadrate ramus of the pterygoid defines the medial margin of the subtemporal fossa and carries a well-developed ventral flange along the medial margin of its anterior part from which originated m. pterygoideus internus.

Occipital View and Braincase—The occiput of *Simosaurus* was described by Schultze (1970) and Rieppel (1994a), who also described braincase structure in detail. The present account will emphasize the discussion of characters not dealt with in detail in these publications but essential with respect to the definition of characters for phylogenetic analysis (see below). The occiput of *Simosaurus* is deeply concave due to the displacement of the mandibular articulation to a position well behind the occipital condyle. The posttemporal fossa is reduced to a small opening positioned between the occipital exposure of the opisthotic and squamosal. The occiput is essentially closed and platelike, and no well-defined paroccipital process is differentiated. A deep incisure separates the occipital exposure of the squamosal from the laterally descending process of the same bone covering the quadrate in lateral view. This incisure was identified by Kuhn-Schnyder (1961) as an "otic notch" and taken as evidence for the presence of a small (reduced?) and dorsally positioned tympanic membrane in *Simosaurus*. However, while showing a slight concavity of its posterior aspect, the quadrate of *Simosaurus* slants backward (in correlation with the posterior displacement of the mandibular joint), and it lacks the posterior concavity indicative of the presence of a tympanic membrane in other diapsids. A tympanic membrane most probably was absent in *Simosaurus,* as it presence would also interfere with the depressor mandibulae muscle (Rieppel, 1989a).

The occipital condyle is formed by the basioccipital only, which on either side of the condyle forms large lateral basioccipital tubera defining the medial margin of the eustachian foramen (Rieppel, 1994a). The exoccipitals do not meet dorsal to the occipital condyle. An ossified epipterygoid is absent in *Simosaurus* (Rieppel, 1994a).

Lower Jaw

The lower jaw of *Simosaurus* (Fig. 11) is slender and lacks a coronoid process. The greater part of the lateral surface of the lower jaw is covered by the dentary (anteriorly) and surangular (posteriorly). The angular forms the ventral margin of the lower jaw ramus below the surangular. The lateral exposure of the articular ossification below the mandibular joint and on the short retroarticular

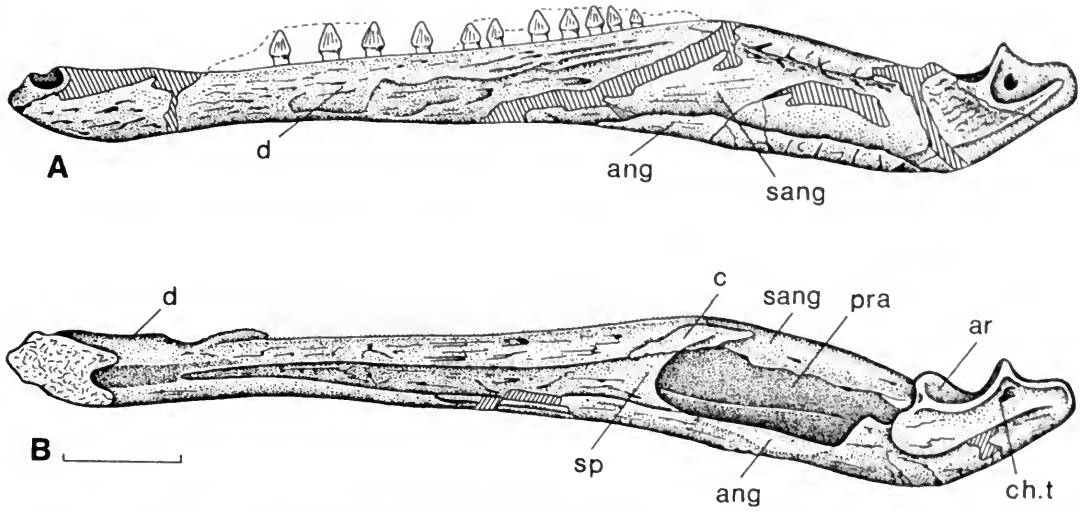

FIG. 11. Lower jaw of *Simosaurus gaillardoti* (SMNS 16638; original of Huene, 1952, Fig. 58). Abbreviations: ang, angular; ar, articular; c, coronoid; ch.t., chorda tympani foramen; d, dentary; pra, prearticular; sang, surangular; sp, splenial. Scale bar = 40 mm.

process cannot be delineated with any certainty (in *Nothosaurus,* the articular ossification is not exposed in lateral view, due to a posterior extension of the surangular; pers. obs.). The supposed anterior margin of the articular bone shown by Huene (1952, Fig. 58a, drawn from SMNS 16638) is a crack. A distinct ridge on the lateral surface of the surangular marks the ventral edge of the insertion area of the m. adductor mandibulae externus superficialis on the lateral surface of the lower jaw. The anterior and dorsal edge of the insertion area of the m. pterygoideus externus is indicated by a distinct, curved ridge on the posteroventrolateral aspect of the lower jaw, ventral to and in front of the mandibular articulation.

In medial view, the lower jaw shows the elongated splenial bone. Fairly high posteriorly, the bone defines the anterior margin of the adductor fossa. The bone closes the Meckelian canal medially, tapering anteriorly to a blunt tip. The splenial does not reach the mandibular symphysis (contra Huene, 1952). SMNS 16638 is the original of Huene (1952, Fig. 58). The mandibular ramus measures 366 mm in length, and the anterior tip of the splenial lies about 30 mm behind the symphysis. The splenial gains no ventral exposure along the ventral margin of the lower jaw.

In front of the splenials, Meckel's canal opens on the medial side of the lower jaw. Meckel's cartilage must have emerged from the anterior opening of the Meckelian canal to meet with its counterpart from the other side in the mandibular symphysis. The dentary provides a dermal covering of the lateral and ventral surface of Meckel's cartilage; each dentary also forms a medial symphyseal shelf covering the anterior tips of Meckel's cartilages dorsally. As the dentaries wrap around the anterior tips of Meckel's cartilages, the dermal mandibular symphysis appears recessed in posterior (medial) view. An anteroposterior elongation of the mandibular symphysis is not prominent in *Simosaurus.*

The coronoid is a small element lying at the anterodorsal margin of the adductor fossa. It gains no exposure on the lateral surface of the lower jaw. The prearticular is exposed within the adductor fossa. Along the ventral margin of the adductor fossa, the angular bone forms a distinct ledge that must have served for the insertion of the pterygoideus internus muscle.

The articular surface is saddle-shaped. Its anterior margin is relatively low compared to the distinctly elevated posterior margin. This morphology of the articular facet locks the lower jaw against the quadrate, blocking translational movement caused by the anterior pull of the pterygoideus muscle (which had a strongly developed dorsal [anterior] portion; see above).

The retroarticular process is present but short. Its lateral surface bears a deep facet, which must have served for the insertion of the depressor mandibulae muscle. Deep to this facet lies a distinct

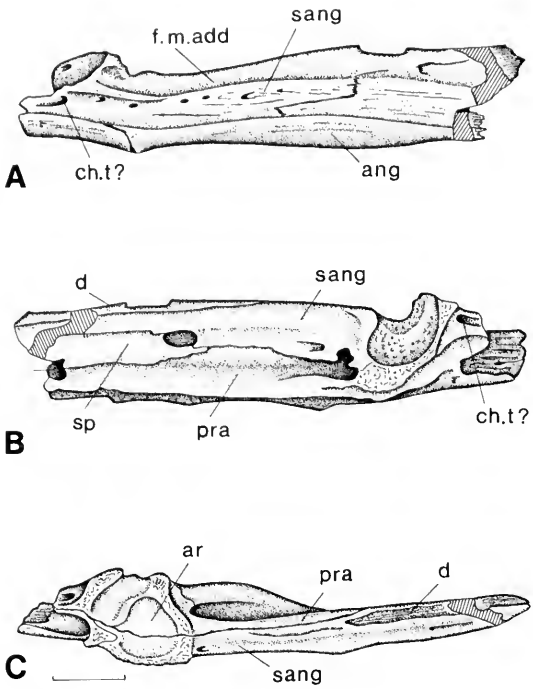

FIG. 12. Posterior part of the lower jaw of *Nothosaurus mirabilis* (SMNS 59818, upper Muschelkalk [*nodosus–spinosus* biozone], Hegnau). **A,** Left lateral view; **B,** medial view; **C,** dorsal view. Abbreviations: ang, angular; ar, articular; ch.t., chorda tympani foramen; d, dentary; f.m.add, facet for the insertion of superficial jaw adductor muscle fibers; pra, prearticular; sang, surangular; sp, splenial. Scale bar = 20 mm.

foramen. The medial surface of the retroarticular process, together with the medially overhanging mandibular articular facet, forms a deep recess that faces medioventrally and probably served as the insertion site of the m. pterygoideus internus (posterior fibers). Immediately posteroventral to the mandibular articular facet, the retroarticular process shows another distinct foramen (SMNS 16638) that lies in the classical position of the chorda tympani foramen. The foramen on the lateral surface of the retroarticular process cannot also serve the entry of the chorda tympani into the lower jaw and must therefore be interpreted as the posterior supra-angular foramen (*sensu* Oelrich, 1956). Although sutural relations are not distinct, the position of the posterior supra-angular foramen indicates a posterior extension of the surangular in a pattern similar to *Nothosaurus* (Fig. 12).

Postcranial Skeleton

The best preserved skeleton of *Simosaurus* is SMNS 14733 (Huene, 1952) from the upper Muschelkalk of Tiefenbach near Crailsheim. The skeleton is fairly complete but was fully disarticulated. The skull and the pectoral girdle were missing, but its association with teeth of *Simosaurus* allowed its unequivocal identification. The skeletal elements were completely removed from the matrix, but a cast was made of the specimen before its preparation in order to document the original position of its parts. This cast was lost during World War II. Only one photograph of the specimen in its original position survived, but in a very poor, almost unrecognizable condition. The original specimen was packed and sheltered during the war. In 1945, the specimen was returned to provisional quarters in Ludwigsburg. To make it available for description by Huene (1952), the specimen was unpacked by Dr. Staesche, Curator at the SMNS, and parts went on loan to Huene in Tübingen (R. Wild, pers. comm.). Redescription of this skeleton of *Simosaurus* below will be augmented by reference to additional material deposited in public repositories and referred to by the appropriate collection numbers.

Vertebral Column

SMNS 14733 provided six centra and three neural arches of the cervical region, 26 centra and 28 neural arches of the dorsal region, five vertebrae counted as sacrals by Huene (1952), and two proximal as well as one distal caudal vertebra. The articulated skeleton of *Simosaurus* from the Gipskeuper of Obersontheim (GTPI uncatalogued) shows a total of 32 dorsal vertebrae in situ (counting three rather than five sacral vertebrae; cf. Huene, 1959), with the possibility that there were one or two additional dorsal vertebrae in front of the preserved series. Huene (1959) estimated a similar number of elements (30–31) in the cervical vertebral column, but with no factual basis. The distance between the skull and the preserved torso as reconstructed for the specimen was estimated and not based on the position of the parts in the field (see discussion below).

The cervical vertebrae (Fig. 13) show a weakly amphicoelous and non-notochordal centrum with a slightly constricted middle portion. The ventral surface of the centrum is distinctly keeled. The length of the centra increases from front to back. Centrum #124a (SMNS 14733), an anterior cervical element, measures 16 mm in length, whereas centrum #130 (SMNS 14733), located more posteriorly within the cervical series, is 20.5 mm long. The neural spines slant slightly backward. Their an-

terior edges are thin, and the posterior margins are thickened. The height of the neural spines increases from front to back: 47.5 mm is the total height of a neural arch from the middle of the cervical region (the dorsal tip of a neural spine from a more anterior position is broken); total arch height increases to 55 mm in the posterior cervical region. In addition to the zygapophyseal articulations, the neural arches of the cervical region show the accessory zygosphene–zygantrum articulation, but not the differentiation of infrapre- and infrapostzygapophyses (see below). Width across the postzygapophyses is slightly larger than across the prezygapophyses, but pre- as well as postzygapophyses are generally wider (45–47 mm) than the centra (26–28 mm). The articular surface of the prezygapophyses in the cervical region is slightly inclined facing dorsomedially (approx. 30° from the horizontal in the midcervical region); the postzygapophyses correspondingly face ventrolaterally. The neurocentral suture is unfused in the cervical region (allowing the neural arches to separate from the centra). The dorsal surface of the centrum is broadened and flattened, providing a platform for articulation with the neural arch. This character is further accentuated in the dorsal region, as will be discussed below.

The centra of the dorsal vertebral column (Fig. 14) average 26–27 mm in length, 33–35 mm in height, and 21–29 mm in width. The central part of the centrum is constricted in ventral view, the articular surfaces are weakly amphicoelous or platycoelous, and the centra are non-notochordal. The available neural arches show differences in height of the neural spine, indicating that the neural spines were somewhat higher in the pectoral region than elsewhere in the dorsal region. The total height of the dorsal neural arches is 72–77 mm, the total width across the transverse processes is 55–59 mm, and the average total width across the pre- and postzygapophyses is 35–40 mm. The zygapophyses are hence generally broader than the centrum, but this character depends on the inclination of the articular surfaces, which increases from front to back, and may be reversed in the sacral and caudal regions (see below). In an anterior dorsal neural arch, the articular surface of the prezygapophysis is inclined by approximately 30° from the horizontal (facing dorsomedially); in a posterior neural arch, the inclination increases to approximately 40° from the horizontal. Neural arches of the dorsal region differ from those of the cervical region by the development of infrapre- and infrapostzygapophyses (Huene, 1952, p. 167) as accessory articulations in addition to the zygosphene–zygantrum articulation (Fig. 15). The neurocentral suture is open throughout the dorsal region, as is again indicated by the separation of the neural arches from the centra. The dorsal surface of the centrum is conspicuously widened, providing a very characteristic "cruciform" or "butterfly-shaped" platform for the articulation with the neural arch. This platform, increasing in width along an anteroposterior gradient, is traversed by the longitudinal neural canal (forming a longitudinal groove on the centrum, which is somewhat broader and deeper than in *Nothosaurus*), and its surface bears a pattern of radiating grooves and ridges participating in sutural interdigitation (Fig. 16). Posterolaterally, the articular platform carries triangular areas on both sides with a conspicuous pattern of pitting; similar pitted areas, but much smaller and less well defined, are located in the anterolateral corner of the articular surface.

FIG. 13. Cervical vertebra of *Simosaurus gaillardoti* (SMNS 14733). Left: centrum in dorsal view (#130 of Huene, 1952); right: neural arch in anterior view (#144 of Huene, 1952). Scale bar = 20 mm.

The interpretation of the sacral region of *Simosaurus* remains problematical to some degree. Huene (1952) counted five sacral vertebrae, but a count of three sacral vertebrae is probably correct. Two vertebrae of SMNS 14733 (with no individual numbers) are unquestionably sacral elements, and they were interpreted as such by Huene (1952, Fig. 19). The vertebrae (Fig. 17) are in articulation, and the neural arches have not separated from the centrum, although the neurocentral suture remains visible. It passes through the lower part of the rib articulation, the centrum thus contributing to the formation of a short yet high transverse process. The infrapre- and infrapostzygapophyses are reduced as compared to those of the dorsal neural arches. The dorsomedial inclination of the articular surface on the prezygapophysis (laterolateroventral inclination of the articular surface on the

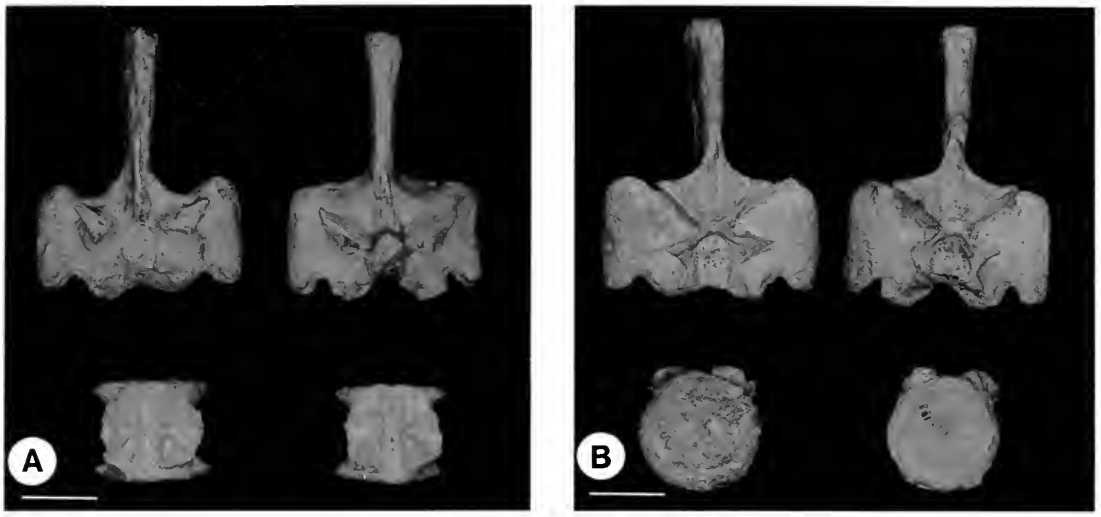

FIG. 14. Dorsal vertebrae of *Simosaurus gaillardoti* (SMNS 14733). **A,** Neural arches in anterior view, centra in dorsal view; **B,** neural arches in posterior view, centra in posterior view. Scale bar = 20 mm.

postzygapophysis) is very pronounced, and the width across the zygapophyses no longer exceeds the width across the platycoelous articular surface of the centrum. The width across the pre- or postzygapophyses of these two vertebrae ranges from 21.5 to 23 mm, and the width across the articular surface of the centrum measures 28–29 mm. The middle portion of the centrum is constricted in ventral view.

The isolated vertebra #147 (SMNS 14733) (Fig. 17) was not figured by Huene (1952). It shows reduced infrapre- and infrapostzygapophyses, the articular surface of the prezygapophysis is strongly inclined dorsomedially (approximately 45° from the horizontal), and the neural arch has not separated from the centrum. The transverse process is high dorsoventrally but short proximodistally, and the neurocentral suture passes through its middle portion, indicating that the centrum contributes to the rib support. This indicates that the element derives from the far posterior dorsal series and/or may represent the first sacral vertebra.

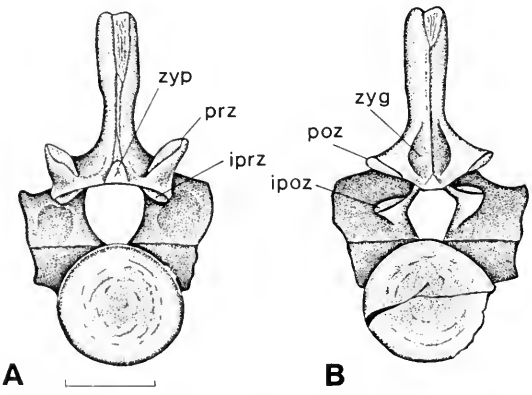

FIG. 15. Sacral vertebrae of *Simosaurus gaillardoti* (SMNS 14733, #147 of Huene, 1952). **A,** Anterior view; **B,** posterior view. Abbreviations: ipoz, infrapostzygapophysis; iprz, infraprezygapophysis; poz, postzygapophysis; prz, prezygapophysis; zyg, zygantrum; zyp, zygosphene. Scale bar = 20 mm.

Vertebra #113 (SMNS 14733) shows even more reduced infrapre- and infrapostzygapophyses, and the articular surface of the prezygapophysis is even more inclined than in vertebra #147 (approximately 55° from the horizontal). Again, the neural arch has not separated from the centrum, and again, the neurocentral suture passes through the middle of the short yet high transverse process, the centrum thus contributing to the rib support. Huene (1952, Fig. 18) interpreted the vertebra as a "caudosacral element," which is here interpreted to mean an anterior caudal. As the centrum shows no clear-cut posteroventral articular facets for the chevron bone, the element could also represent the posteriormost of four sacral vertebrae.

Huene (1952, p. 168) considered vertebra #153 (SMNS 14733) as the first sacral element, a claim that cannot be supported on morphological grounds. The inclination of the articular surface of the prezygapophysis indicates a position in the posterior dorsal region, the neural arch has sepa-

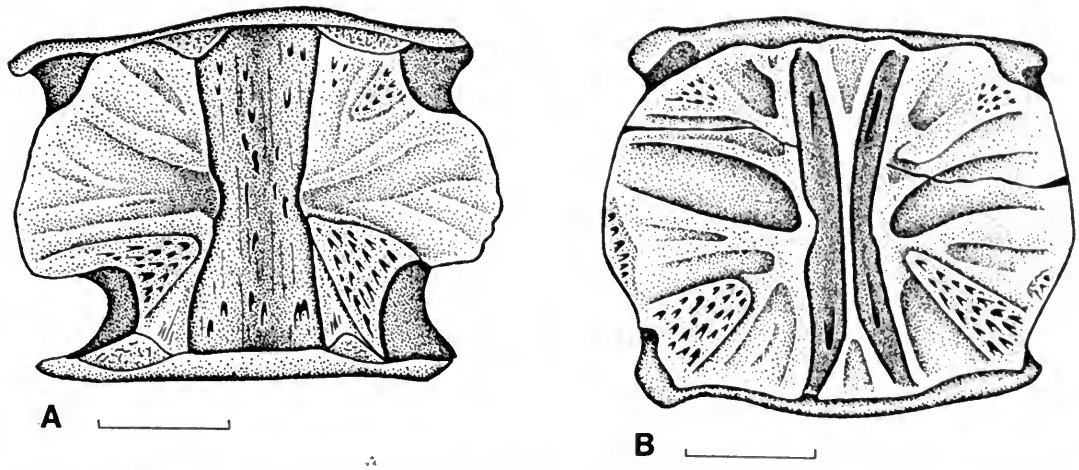

FIG. 16. **A,** Dorsal centrum of *Simosaurus gaillardoti* (SMNS 54763; upper Muschelkalk, Hildesheim) in dorsal view. **B,** Dorsal centrum of *Nothosaurus* sp. in dorsal view (SMNS 59819, upper Muschelkalk, Bindlach near Bayreuth). Anterior is at the top. Scale bar = 20 mm.

rated from the centrum, and the centrum did not contribute significantly to the formation of the articular facet for the rib at the distal end of the transverse process. On morphological grounds, no more than four vertebrae can possibly be interpreted as sacral vertebrae of *Simosaurus*. On functional grounds, *Simosaurus* may have had no more than three sacral vertebrae (see the discussion of sacral ribs and of the ilium, below), with the consequence that the first caudal element would not bear a chevron. The problem with the identification of the number of sacral elements in sauropterygians (and other reptiles in general) is that posteriormost dorsal and/or anteriormost caudal ribs may converge on the ilium in addition to the genuine sacral ribs.

The tail of SMNS 14733 is very incompletely preserved. Vertebra #98 represents an isolated distal tail vertebra. It is relatively long (26.2 mm) in relation to its total height (36 mm; neural arch somewhat incomplete) and total width (approximately 11 mm across the prezygapophyses). The neural arch has not separated from the centrum, and the prezygapophyses are almost vertically oriented and hence do not exceed the width of the centrum. The middle part of the centrum is constricted in ventral view, and the ventral surface is keeled. The keel bifurcates and diverges toward

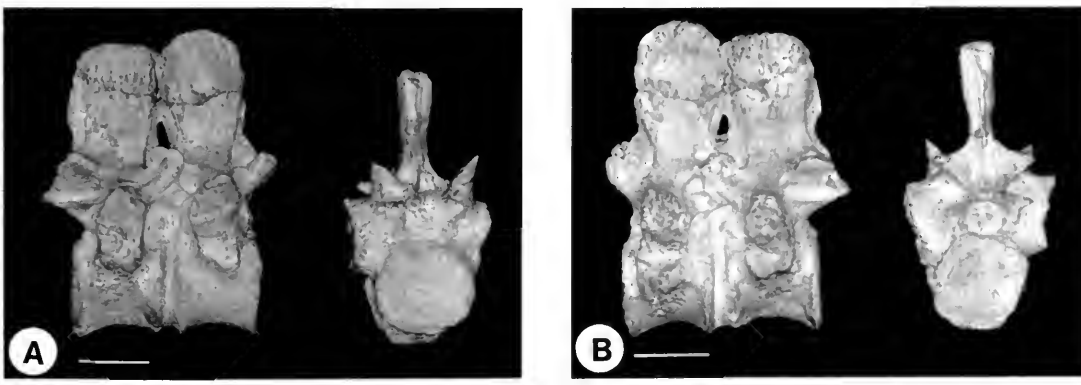

FIG. 17. Sacral vertebrae of *Simosaurus gaillardoti* (SMNS 14733). **A,** Sacral vertebrae in right lateral view (left, original of Huene, 1952, Fig. 19), vertebra #147 (right, original of Huene, 1952) in anterior view. **B,** Sacral vertebrae in left lateral view (left, original of Huene, 1952, Fig. 19), vertebra #147 (right, original of Huene, 1952) in posterior view. Scale bar = 20 mm.

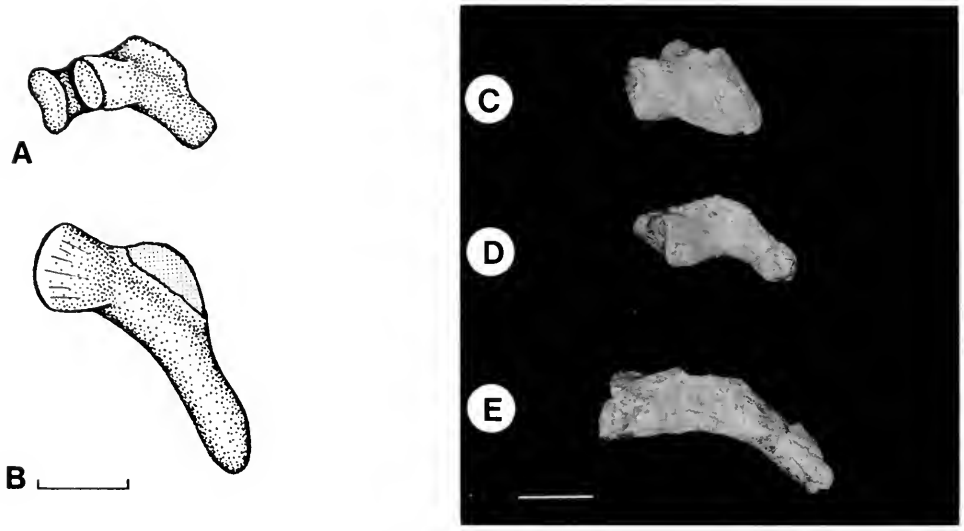

FIG. 18. Cervical ribs of *Simosaurus gaillardoti* (SMNS 14733). **A,** Anterior cervical rib (#140?); **B,** posterior cervical rib (#150); **C,** #19 of Huene, 1952; **D,** #140? of Huene, 1952; **E,** #150 of Huene, 1952. Scale bar = 10 mm.

the posterior margin of the centrum, where its limbs expand into articular facets for the chevron.

Ribs

A total of four cervical ribs are available (SMNS 14733, #19, #140, #145, and #150; Fig. 18), of which the anteriormost one is the smallest and shortest. It is dichocephalous, whereas in the more posterior cervical ribs the tuberculum and capitulum tend to become confluent. All cervical ribs show an expanded (broadened) "shoulder," but none shows a distinct free anterior process. Whether this is the natural condition or due to breakage (incurred during casting or an incident in which the cabinet holding the specimen was overturned) can no longer be determined. However, Huene (1952, Fig. 21) figured such a process in at least one anterior cervical rib, and a free anterior process on cervical ribs is a general feature of sauropterygians (Fig. 19).

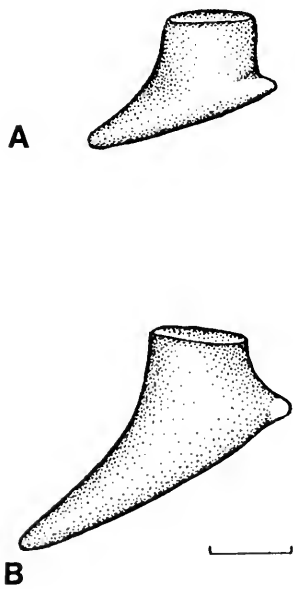

FIG. 19. Cervical ribs of *Nothosaurus* sp. (MB R.150, lower Muschelkalk [Schaumkalk], Oberdorla, Thüringen; original of Peyer, 1939, Fig. 23). Scale bar = 10 mm.

The dorsal ribs (Fig. 20G) are holocephalous, evenly curved, and show a sharp and slightly overhanging posterior margin. The anterior dorsal ribs show a moderate distal expansion. Posterior dorsal ("lumbar") ribs are distinctly reduced in size (see also Huene, 1959) and lack the distal expansion.

Problems surface again with identification of sacral ribs (Figs. 20–21). Among the available skeletal elements of SMNS 14733, a total of seven sacral ribs (both left and right) have been identified, distributed over an assumed total of five sacral ribs on each side by Huene (1952). Among these, rib #11 (Huene, 1952, Fig. 30) is the principal sacral rib. It is a very robust and stout element with a length of 70 mm and a distinct proximal and distal expansion (proximal width: 29.9 mm; minimal width at middiaphysis: 12.7 mm; distal width: 23.5

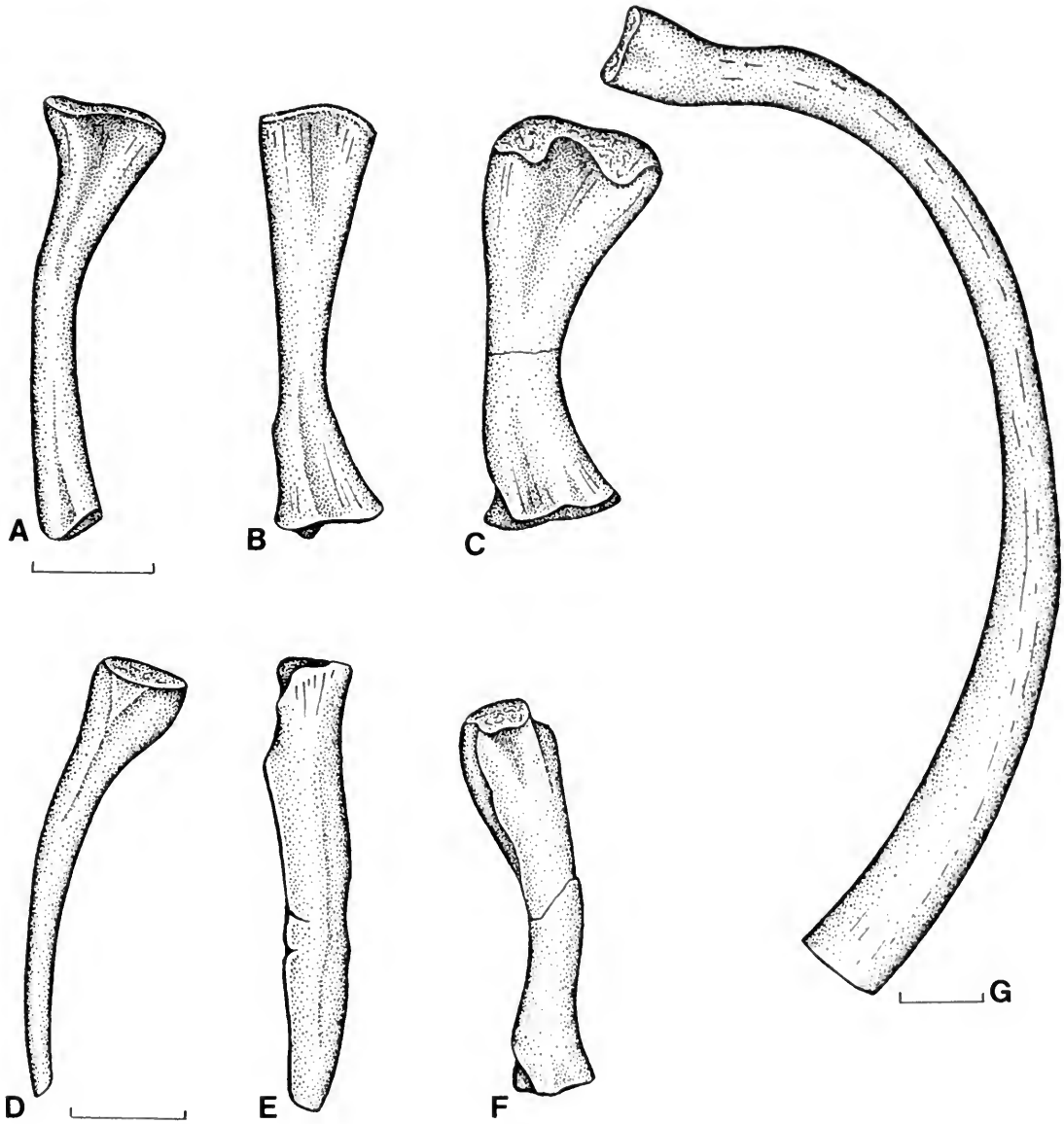

FIG. 20. Ribs of *Simosaurus gaillardoti* (SMNS 14733). **A**, Sacral rib (#73 of Huene, 1952) in lateral view; **B**, sacral rib (#65 of Huene, 1952) in lateral view; **C**, sacral rib (#11 of Huene, 1952) in lateral view; **D**, anterior caudal rib (#102 of Huene, 1952) in lateral view; **E**, anterior caudal rib (#102 of Huene, 1952) in dorsal view; **F**, sacral rib (#11 of Huene, 1952) in dorsal view; **G**, dorsal rib. Scale bar = 20 mm.

mm). A second sacral rib, not as robust as #11 but still more massive than all others, is rib #65 (Huene, 1952, Fig. 31), with a length of 75.0 mm, a proximal width of 21.1 mm, a distal width of 19.3 mm, and a width at middiaphysis of 9.3 mm. A third sacral rib, identifiable by the presence of both proximal and distal expansions, is rib #73 (Huene, 1952, Fig. 33), with a length of 73.2 mm, a proximal width of 23.5 mm, a distal width of 13 mm, and a width at middiaphysis of 8.3 mm. Assuming three sacral ribs to be the plesiomorphic condition at the level of the Eusauropterygia (with reference to pachypleurosaurs and *Placodus*), these three elements (#11, #65, and #73) would be the "ancestral" sacral ribs, and the question arises whether *Simosaurus* has added additional sacral ribs to the plesiomorphic number by "sacralization" of a posterior dorsal or an anterior caudal pair of ribs.

FIG. 21. Sacral ribs of *Simosaurus gaillardoti* (SMNS 14733). **A**, #11 of Huene, 1952; **B**, #65 of Huene, 1952; **C**, #73 of Huene, 1952. Scale bar = 20 mm.

Because a posterior dorsal or anterior caudal rib would have to converge on the ilium in a posterolateral or anterolateral direction, respectively (rather than being more or less transversely oriented, as are the three principal sacral ribs), one would expect the fourth pair of sacral ribs to be longer than the elements described above. Besides the three ribs just described (#11, #65, and #73), a total of four additional ribs (without separate numbers) have been described, two of which are shorter than (65.5 mm and 68 mm, respectively) and two the same length as (both 73.5 mm) the sacral ribs identified above. All four show a proximal and distal expansion, but the two longer elements (of these four) are distinctly more robust, their proximal and distal expansion is more pronounced, and their curvature is less, although one side is strongly concave. These two pairs of ribs may represent posteriormost dorsal ("lumbar") or anteriormost caudal ribs converging toward the ilium without providing much further support (see description of the ilium, below). Five pairs of ribs are converging toward the ilium in the skeleton from the Gipskeuper described by Huene (1959), but, judged by the size of the ilium, a maximum of three sacral ribs could possibly have supported

FIG. 22. Caudal ribs of *Simosaurus gaillardoti* (SMNS 14733). **A**, #102 of Huene, 1952; **B**, #168 of Huene, 1952. Scale bar = 20 mm.

the bone. Ilium morphology also indicates that the most massive of the three sacral ribs (#11) would be the posteriormost one of the three, articulating in the large posterior articular facet on the medial side of the ilium (see below).

Typical caudal ribs are rather straight elements with an expanded proximal articular head that does not fuse with the transverse process of the respective vertebral element (Fig. 22). The caudal ribs retain a broad but not expanded distal tip in dorsal or ventral view. The posterior margin of the rib continues to provide a sharp and slightly overhanging rim, as is the case in the dorsal ribs.

Gastral ribs were present in *Simosaurus,* but none is well enough preserved to allow a detailed description of their morphology. Huene (1952, p. 170) mentioned that medial gastral rib elements may co-ossify, a phenomenon also reported for *Nothosaurus* (Fig. 23; see also Koken, 1893, Pl. 11, Figs. 7–9) and *Corosaurus* (Storrs, 1991).

Pectoral Girdle

The dermal pectoral girdle is composed of the interclavicle and the clavicle (Fig. 24). The interclavicle is essentially a T-shaped element, with a broad anterior portion extending into tapering lateral processes and a relatively short yet distinct posterior stem. A complete interclavicle (SMNS 15995) measures 158 mm across the tips of the tapering anterior lateral processes, while the total length of the element is 88.3 mm (with the posterior stem approximately 68 mm long). The entire element is thus distinctly wider than long. Huene (1952, p. 174, Fig. 62) figured an isolated inter-

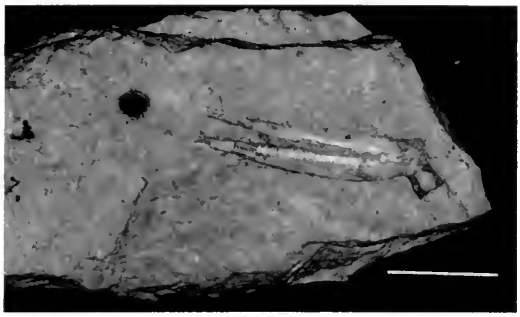

FIG. 23. Medial element of a gastral rib of *Nothosaurus* sp. (MB R.714, upper Muschelkalk, Bayreuth; original of Koken, 1893, Pl. 11, Fig. 9). Scale bar = 20 mm.

clavicle of large size from the Grenzbonebed of the upper Muschelkalk separating the Muschelkalk from the Keuper, which shows a relatively much longer posterior stem than is observed in SMNS 15995 and which may or may not be attributable to *Simosaurus*. Variation is also observed in the anterior part of the interclavicle as SMNS 15995 is compared to SMNS 7862 (Fig. 25). In the latter specimen, the anterolateral processes are relatively shorter and do not taper to a pointed tip, while the posterior stem (judged by its relative width at the posterior break) may well have been relatively longer than would appear in SMNS 15995.

The clavicles (Figs. 25A,C) are rather distinct, curved elements that are received in an anteroventral facet on the interclavicle and that established a broad mutual contact along the ventral midline of the body in front of the interclavicle. The anterolateral edge of the interclavicle is expanded into a distinct blade forming the "clavicular corner" described by Storrs (1991, 1993a). A character diagnostic (autapomorphic) for *Simosaurus* is a small anterior process projecting from the anterior edge of the clavicle. The posterior ramus of the clavicle tapers to a blunt tip as it trends in a posterodorsal direction. It is received in a distinct facet on the anterior and medial surface of the dorsal scapular wing.

The endochondral pectoral girdle is composed of two elements ossifying separately, the scapula and coracoid (Fig. 26). The dorsal wing (scapular blade) of the scapula is much reduced, forming essentially a posterodorsally ascending process. At its anterior base, this process expands into the ventral portion of the scapula, contributing to the formation of the glenoid laterally and to the closure of the coracoid foramen posteromedially. The anterior aspect of the dorsal wing supports the posterior process of the clavicle. The clavicular

FIG. 24. Pectoral girdle of *Simosaurus gaillardoti* (SMNS 7862, upper Muschelkalk, Crailsheim; original of Fraas, 1896, p. 12; Huene, 1952, Fig. 59). Scale bar = 50 mm.

facet expands onto the medial surface of the anterior part of the dorsal wing up to the deep furrow separating the dorsal wing from the expanded ventral portion of the scapula.

The coracoid is a characteristically waisted bone with distinctly concave anterior and posterior margins and convex lateral and medial margins. The lateral margin is thickened anteriorly where it participates in the formation of the glenoid facet. Immediately behind the latter, the lateral margin of the coracoid is notched, forming the medial margin of the coracoid foramen. Measurements for two well-preserved coracoids are given in Table 1.

Pelvic Girdle

The ilium of *Simosaurus* (Figs. 27–28) is a small element with a much reduced iliac blade. The latter is short and separated from the expanded ventral portion by a distinct constriction ("neck"). Both ends of the dorsal portion taper to a pointed tip, the anterior one corresponding to the spina pracacetabuli (Siebenrock, 1894), and the posterior one pointing in a posterodorsal direction but not quite reaching the level of the posterior margin of the expanded ventral portion. The ventral portion of the ilium participates in the formation of the acetabulum, but no supra-acetabular buttress is developed. The medial surface of the ventral portion of the ilium shows a complex morphology indicating a maximum of three articular facets for sacral ribs. The first and second sacral ribs artic-

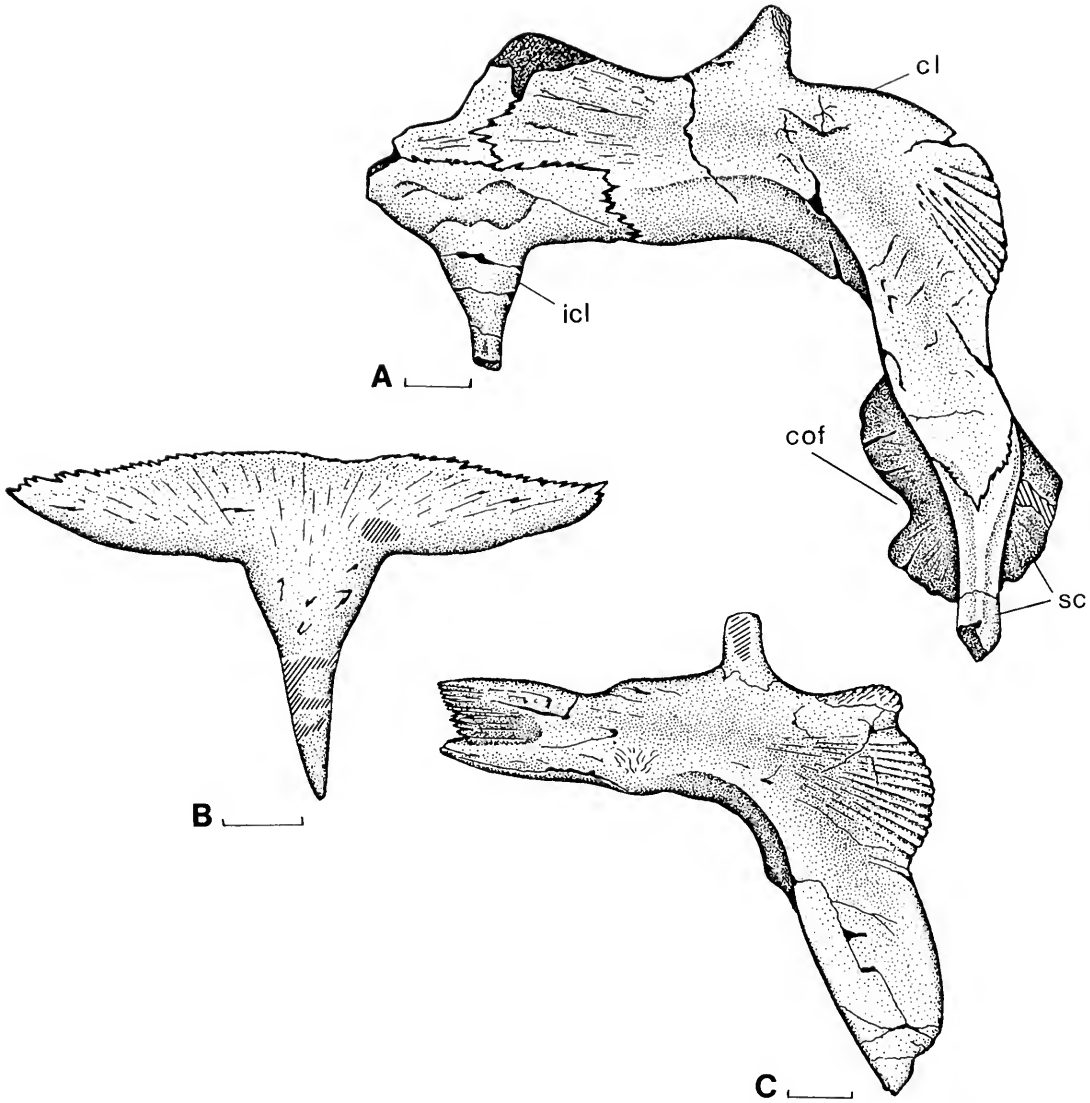

FIG. 25. The dermal pectoral girdle of *Simosaurus gaillardoti*. **A**, Interclavicle, clavicle, and scapula (SMNS 7862, upper Muschelkalk, Crailsheim; original of Fraas, 1896, p. 12; Huene, 1952, Fig. 59); **B**, interclavicle (SMNS 15995, upper Muschelkalk, Tiefenbach near Crailsheim); **C**, clavicle (SMNS 17097, upper Muschelkalk, Tiefenbach near Crailsheim). Abbreviations: cl, clavicle; cof, coracoid foramen; icl, interclavicle; sc, scapula. Scale bar = 20 mm.

ulated in two facets arranged one above the other on the anterior part of the ventral portion of the ilium. A third articular facet lies behind the two anterior ones, separated from the latter by a deep groove (or furrow). The morphology of the ilium thus indicates the presence of three functional sacral ribs in *Simosaurus*, and the same number is indicated for *Nothosaurus* by the articulated skeleton of *Nothosaurus* "*raabi*" (MB I.007.18) described by Schröder (1914; see discussion below and Fig. 51). Isolated ilia of *Nothosaurus* show a morphology almost identical to that of *Simosaurus*, although the deep furrow separating the anterior two from the posterior articular facet is absent (see discussion below and Fig. 50). There is one single or poorly subdivided articular facet on the medial surface of the ilium of *Nothosaurus*, offering room for no more than three functional sacral ribs.

The pubis of *Simosaurus* (Fig. 28) shows deeply

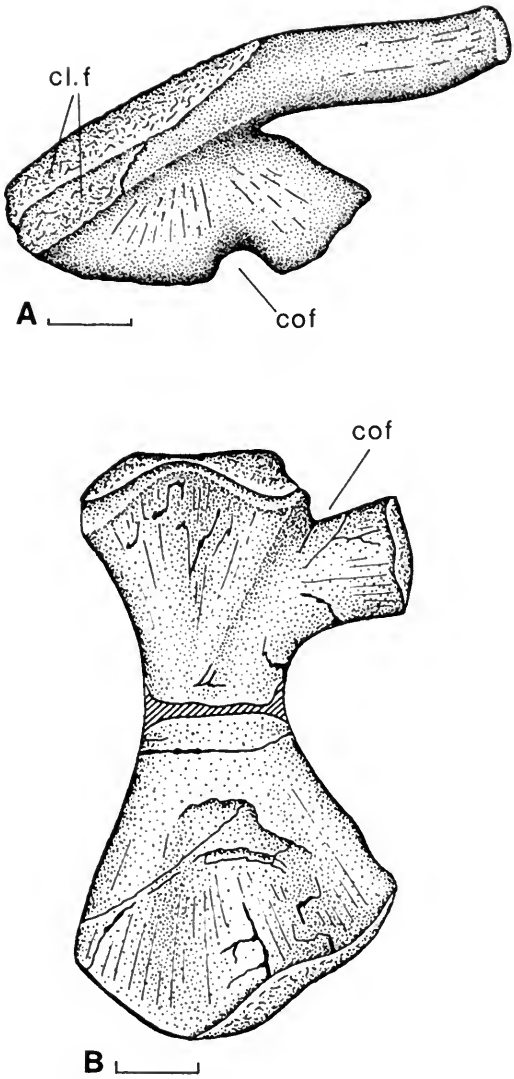

FIG. 26. The endochondral pectoral girdle of *Simosaurus gaillardoti*. **A**, Right scapula, medial view (composite, mainly based on SMNS 18373 from upper Muschelkalk, Heldenmühle); **B**, right coracoid, lateral (ventral) view (SMNS 10046, upper Muschelkalk, Crailsheim; original of Huene, 1952, Fig. 64). Abbreviations: cl.f, clavicular facet on scapula; cof, coracoid foramen. Scale bar = 20 mm.

concave anterior and posterior margins and expanded lateral (morphologically dorsal) and medial (morphologically ventral) heads. The lateral (dorsal) head is expanded as it participates in the formation of the acetabulum. The obturator foramen is located immediately anteroventral to the acetabulum and is completely enclosed by bone. The medial (ventral) margin shows a generally

TABLE 1. Measurements (in millimeters) for two well-preserved coracoids of *Simosaurus gaillardoti*.

Specimen number	Coracoid measurements			
	Length	Lateral width	Minimal width	Medial width
SMNS 10046	139	83	36.5	81.8
SMNS 16736	218	125	44.5	106.7

convex margin, which is distinctly notched, however. A similar notch (concavity) is observed in the medial (ventral) margin of the pubis of *Nothosaurus*, which shows an open (slitlike) obturator foramen in specimens of variable size (Fig. 29).

The ischium is again similar to that of *Nothosaurus* (Fig. 28) with strongly concave anterior and posterior margins, a thickened lateral (morphologically dorsal) head participating in the formation of the acetabulum, and a widely expanded medial (morphologically ventral) portion with an evenly convex margin. The concavity of the posterior margin of the pubis and anterior margin of the ischium indicates the presence of a large thyroid fenestra in *Simosaurus*. Measurements for well-preserved pelvic elements are given in Table 2.

Forelimb

The humerus is represented by a number of specimens (see Appendix II and Table 3). The element is generally wider distally than proximally. The proximal head is thicker, however, and the distal end is rather flat. The humerus shows a distinct curvature, with the posterior (postaxial) margin being evenly concave, while the anterior (preaxial) margin shows a distinct angulation between the first and second thirds of its length. The deltopectoral crest is fairly strongly developed and expanded into an anterior ledge accentuating the angulation of the humerus (Fig. 30A). Huene (1952) described an entepicondylar foramen in the humerus of *Simosaurus* that is, in fact, absent. The specimen described by Huene (1952; SMNS 14733) was reprepared, and the entepicondylar foramen described by Huene (1952) turned out to be a shallow groove at best. A shallow groove may also be observed in SMNS 52095 and SMNS 17590, whereas all other humeri investigated (see Appendix II) show no sign of an entepicondylar foramen or groove. Both proximal and distal articular surfaces are covered by unfinished bone. The distal artic-

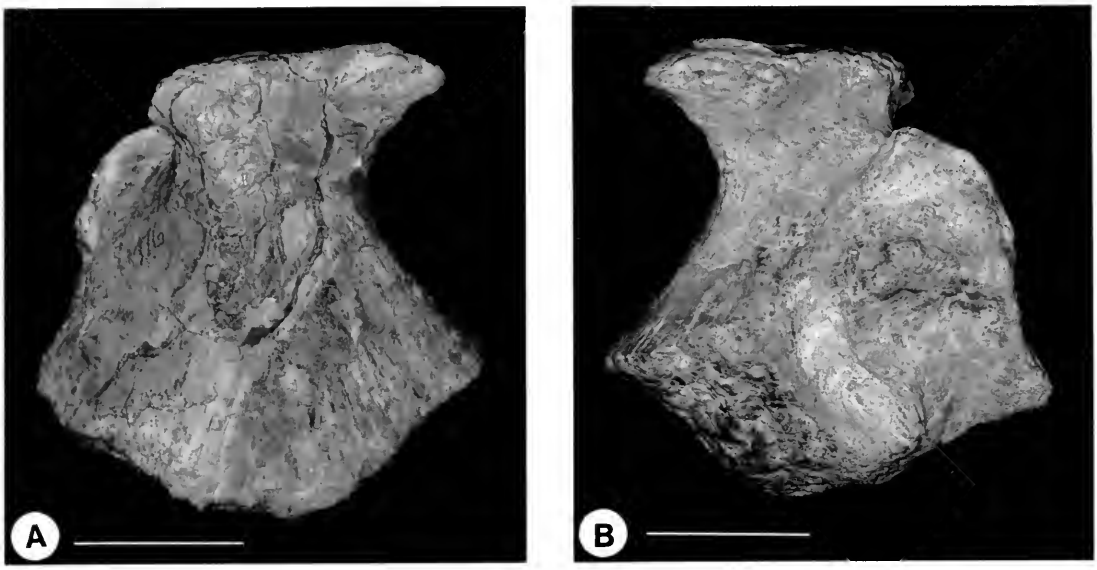

FIG. 27. Left ilium of *Simosaurus gaillardoti* (SMNS 14733). **A,** Lateral view; **B,** medial view. Scale bar = 20 mm.

ular surface is evenly rounded with no apparent separation of radial or ulnar condyles.

Among pachypleurosaurs, a sexual dimorphism in skeletal morphology was observed that is best expressed in proportional relations of the humerus (Rieppel, 1989a, 1993b; Sander, 1989), one sex (sex y) showing a greater degree of distal expansion of the humerus than the other (sex x). The sample of humeri of *Simosaurus* is rather restricted and hence not well suited for the analysis of sexual dimorphism in this genus. Additional problems were created by crushing of the bones during fossilization. Nevertheless, there is a distinct discrepancy in the values obtained for the ratio of humerus length/distal width. The ratio is 5.91 for SMNS 7956 and 5.02 for an uncatalogued SMNS specimen, whereas for five other intact humeri the ratio ranges from 4.17 to 4.5. This may be taken as indication that sexual dimorphism cannot be ruled out for *Simosaurus*.

The radius (Table 4) is a rather featureless bone (Fig. 30B) with the proximal head slightly more expanded than the distal end. The outer (preaxial) margin is somewhat angulated; the inner (postaxial) margin is evenly concave.

The most striking feature of the ulna (Fig. 30C and Table 5) is the distinct expansion of the proximal head and a much lesser expansion of the distal end. The anterior (preaxial) margin is strongly concave, which, together with the concavity of the postaxial margin of the radius, contributes to the formation of a distinct spatium interosseum. The posterior (postaxial) margin of the ulna is more or less straight.

The manus was completely disarticulated, which renders its reconstruction problematical. Huene (1952) assumed the presence of three ossified carpal elements, a reasonable assumption in view of the similar condition known from articulated *Nothosaurus* specimens (*Nothosaurus* "*raabi*," MB I.007.18; see Schröder, 1914). One of the carpal elements (#210) can safely be interpreted as the intermedium on the basis of its shape, which includes a concavity on the proximal margin (Fig. 31). The maximal diameter of the element is 30.5 mm and its thickness is 7.5 mm. It was situated distal to the spatium interosseum, and the concavity of its proximal margin indicates that the perforating artery passed proximal to the intermedium between the distal heads of radius and ulna (Rieppel, 1993c). The other two carpals most probably represent the ulnare (#212) and distal carpal 4 (#154). Additional carpal elements, if present, remain unknown.

Five metacarpals are known and have been arranged by Huene (1952) from digits I through V as follows (Fig. 32): #16 (50.4 mm), #112 (53 mm), #37 (58.5 mm), #151 (53.5 mm), and #42 (53 mm). Following that reconstruction, metacarpal I would be the shortest, metacarpal III the longest in the series. The phalangeal formula of the manus is unknown.

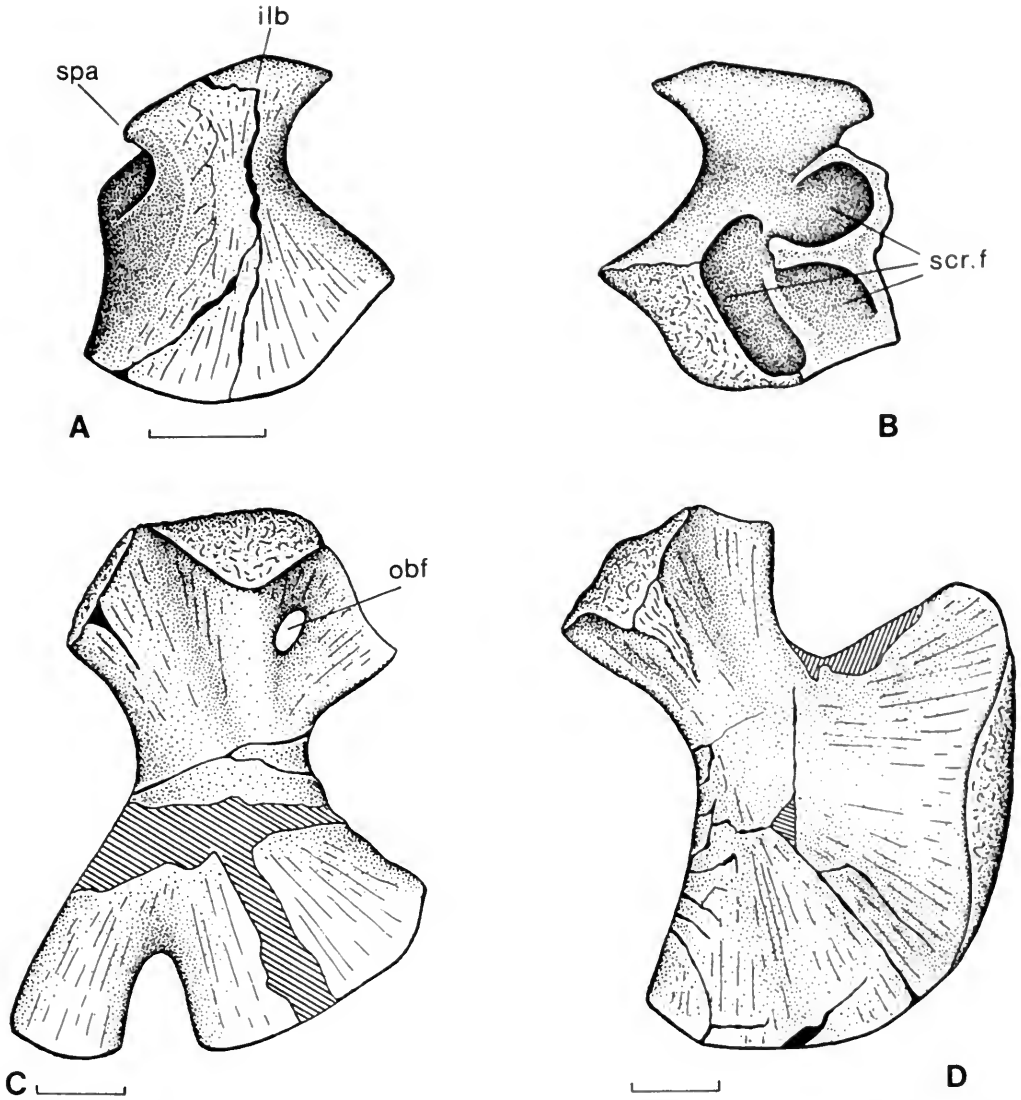

FIG. 28. The pelvic girdle of *Simosaurus gaillardoti* (SMNS 14733). **A**, Left ilium, lateral view; **B**, left ilium, medial view; **C**, right pubis, lateral (ventral) view; **D**, right ischium, lateral (ventral) view. Abbreviations: ilb, iliac blade; obf, obturator foramen; scr.f, sacral rib facets; spa, spina praeacetabuli. Scale bar = 20 mm.

Hindlimb

The femur (Table 6) of *Simosaurus* is a slender and only very weakly curved bone (Fig. 33A). In the associated material of SMNS 14733, the femur (#81) is distinctly shorter than the humerus and less expanded both proximally and distally (the same is true for the specimen described by Huene, 1959). Relating the distal expansion to the length of the bone, however, the ratio for the femur (4.1–5.3) is not significantly different from the ratio obtained for the humerus (4.2–5.9). The same results if distal width is related to proximal width (femur: 1.1–1.2; humerus: 0.8–1.2). The slender appearance of the femur results from a greater degree of constriction in the middiaphyseal part. If minimal width of the femur is related to the length of the bone, the ratio ranges from 8.6 through 11.9; comparable values (length/minimal width) for the humerus are 6.8–9.5.

The ventral side of the proximal head shows a fairly well developed trochanter, but the latter's

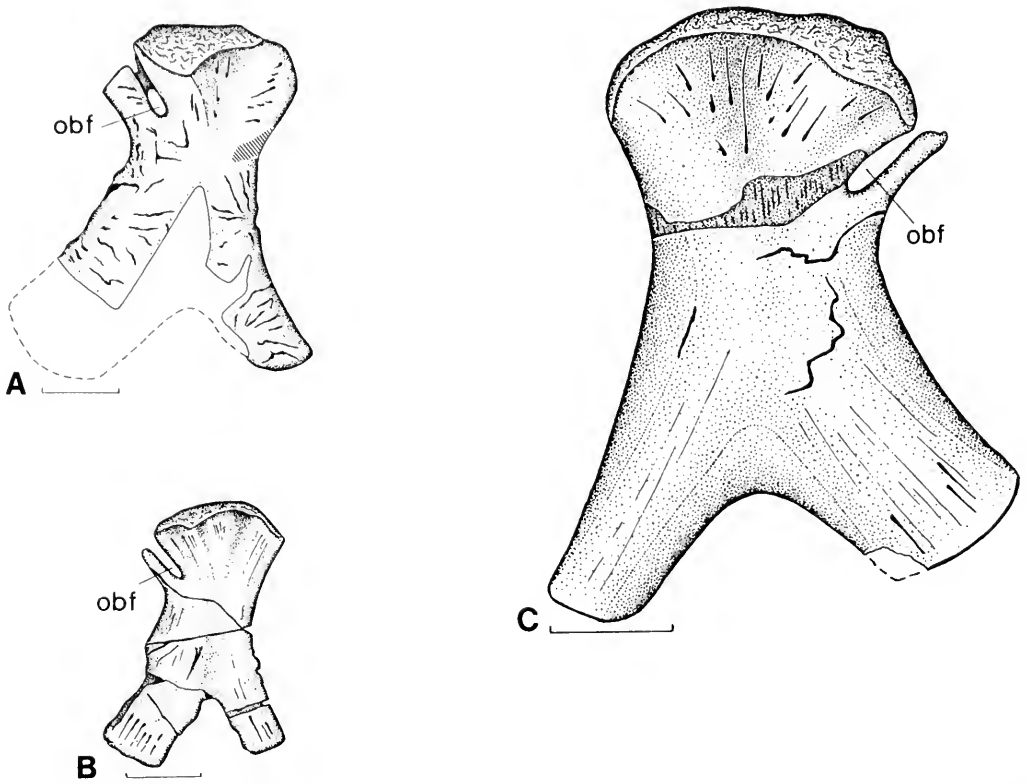

FIG. 29. The pubis of *Nothosaurus* sp. **A,** SMNS 18516, upper Muschelkalk, Heldenmühle near Crailsheim; **B,** SMNS 55853, Grenzbonebed, Zwingelhausen; **C,** Oberfränkisches Erdgeschichtliches Museum, Bayreuth, BT uncatalogued (original of Meyer, 1847–1855, Pl. 41, Fig. 3). Abbreviation: obf, obturator foramen. Scale bar = 20 mm.

head is not distinctly set off from the shaft of the femur by a deep intertrochanteric fossa. The development of the trochanter results in a triangular cross-section of the proximal head of the femur. The articular condyles for tibia and fibula are not separated from one another and in level; there is, however, a shallow intercondylar fossa separating the tibial and fibular articulations.

The tibia (Table 7) is a relatively robust element, generally thicker than the fibula, with rather straight lateral edges and only weakly expanded proximal and distal articular heads (Fig. 33B). The fibula (#182; length: 90 mm; proximal width: 26 mm; minimal width: 12.5 mm; distal width: 26.5 mm) is of similar length to the tibia, but generally more slender and distinguished by a strongly concave anterior (preaxial margin) (Fig. 33C). The latter contributes to the formation of a spatium interosseum but also emphasizes the appearance of markedly expanded proximal and distal articular heads.

The pes, again, is fully disarticulated, but the tarsus certainly had three ossifications (astragalus, calcaneum, and distal tarsal 4); Huene (1952) entertained the possibility of the presence of a fourth ossification in the tarsus (distal tarsal 3). As a general rule, however, the carpus retains a greater number of ossifications in those sauropterygians with a different number of ossified elements in the carpus and tarsus. With a disarticulated hand and foot, the morphology of the hand and foot may never be completely known, but the logical alter-

→

FIG. 30. The forelimb of *Simosaurus gaillardoti* (SMNS 14733). **A,** Left humerus (#1 of Huene, 1952); **B,** left radius (#89 of Huene, 1952); **C,** left ulna (#93 of Huene, 1952). Abbreviations: dpcr, deltopectoral crest; ecg, ectepicondylar groove. Scale bar = 20 mm.


A


B
C

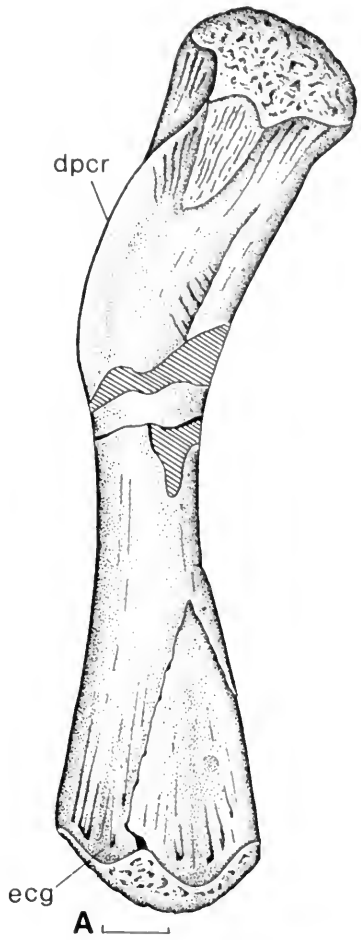
dpcr
ecg
A

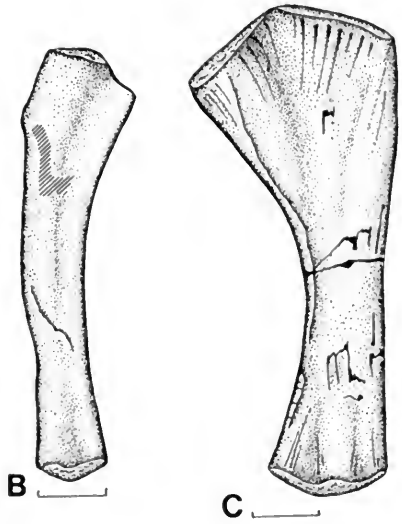
B
C

TABLE 2. Measurements (in millimeters) of the pubis and ischium of *Simosaurus gaillardoti* (SMNS 14733).

Specimen part	Measurements			
	Breadth	Lateral length	Minimal length	Medial length
Left pubis	116	72.5	37.8	98
Right pubis	118	70.9	39	95.5
Left ischium	—	51.7	31.5	119.5
Right ischium	121	52.5	31	118.5

TABLE 4. Measurements (in millimeters) of the radius of *Simosaurus gaillardoti* (SMNS 14733).

Specimen part	Measurements			
	Length	Lateral width	Minimal width	Medial width
#112, right	128	31.5	15.5	20.5
#89, left	126	30.5	15	22

natives available are 1) *Simosaurus* presents an exception to the rule, with three carpal and four tarsal ossifications, 2) the carpus of *Simosaurus* is incompletely preserved, or 3) the fourth tarsal ossification counted by Huene (1952) has a different identity.

One of the tarsal elements (#123) can unequivocally be identified as the astragalus (Figs. 31B, 34). It is larger than the intermedium, with a maximal diameter of 33.8 mm and a thickness of 15 mm, but it shares with the latter bone a distinct concavity on its proximal margin. This indicates, again, that the perforating artery did not pass between the astragalus and calcaneum, but proximal to the astragalus through the spatium interosseum between the distal heads of the tibia and fibula.

A total of six metatarsals are preserved, out of which four elements (Fig. 35) can be attributed to the left metatarsus (R. Wild, pers. comm.). Proceeding from digits I through V, their respective absolute length is as follows: #101, 38.5 mm; #192, 44.5 mm; #66, 46 mm; metatarsal 4, missing; and #55, 31 mm. Following this reconstruction, metatarsal 3 is the longest and metatarsal 5 the shortest of the series. The phalangeal formula of the pes is unknown.

Functional Morphological Correlates in the Skeleton of *Simosaurus gaillardoti*

Simosaurus gaillardoti was a sauropterygian of fairly large size (Fig. 36). The trunk of the subadult specimen from the Gipskeuper of Obersontheim measures 120 cm. Huene (1959) reconstructed the specimen with a cervical vertebral column of similar length as the trunk. This claim may be supported with reference to the articulated skeleton of *Nothosaurus raabi* (MB I.1007.18; Schröder, 1914), whose glenoid–acetabulum length measures approximately 255 mm and the neck region approximately 225 mm. In that specimen, the neck is therefore approximately 88% of trunk length. In the largest pachypleurosaur (*Neusticosaurus edwardsii*; Carroll & Gaskill, 1985), the neck is relatively shorter, on the average about 55% of trunk length. In view of other close skeletal resemblances with *Nothosaurus* (see the cladistic analysis below), similar body proportions may be proposed for *Simosaurus,* which results, for the subadult specimen of Obersontheim (Huene, 1952, measured 19 cm for basicranial length), in an approximate snout–vent length of 248 cm. *Paranothosaurus amsleri* (Peyer, 1939; probably congeneric

TABLE 3. Measurements (in millimeters) of the humerus of *Simosaurus gaillardoti.*

Specimen number	Measurements			
	Length	Proximal width	Minimal width	Distal width
SMNS 14733	262	56	27.5	59.5
SMNS 14733	261	52	28	60.5
SMNS 7956	270	53.5	31.3	45.7
SMNS 17590	342	65	45	82
SMNS 18287	288	57.9	37.5	64
SMNS 18658	210	39.5	29	ca. 48.5
SMNS 18686	ca. 307	ca. 67	45.2	—
SMNS 52095	ca. 315	59.9	43.9	—
SMNS uncatalogued	276	51	38	53

TABLE 5. Measurements (in millimeters) of the ulna of *Simosaurus gaillardoti* (SMNS 14733).

Specimen part	Measurements			
	Length	Lateral width	Minimal width	Medial width
#74, right	127.5	43.5	17.7	27.4
#93, left	127.5	44.6	16.9	28.7

TABLE 6. Measurements (in millimeters) of the femur of *Simosaurus gaillardoti*.

Specimen number	Measurements			
	Length	Proximal width	Minimal width	Distal width
SMNS 14733	203	46	17	39
SMNS 17223	ca. 215	ca. 49.5	21	41
SMNS 18038	142	34	14	ca. 28.8
SMNS 18676	129	29.5	12.7	24.3
SMNS 18689a	219	51.9	25.5	49
SMNS 19052	256	—	25.5	62

with *Nothosaurus*: Rieppel & Wild, 1994) is a nothosaur from the Alpine Triassic of Europe known from complete and articulated specimens. In the adult specimen described by Peyer (1939), tail length averages about 65% of trunk length. A fully grown *Simosaurus* may thus have reached a total length of up to 4 m. The skeletal reconstruction on display at the Stuttgart Museum measures approximately 3 m.

The shape of the distally expanded dorsal ribs results in a broad, somewhat dorsoventrally flattened body in the skeletal reconstruction. The skull is brevirostrine, broad, and flat in general outline, with a relatively long temporal region, large upper temporal fossae, and posteriorly displaced mandibular articulation. As is characteristic for some eusauropterygians, the tooth row is extended backward well beyond the posterior margin of the orbit, indeed well beyond the anterior margin of the upper temporal fossa. The anterior teeth of *Simosaurus* are somewhat enlarged and procumbent, suited for prey capture. The lateral teeth are rather short and blunt, characterized by an expanded and strongly striated crown. The morphology and vertical position of the lateral teeth of *Simosaurus*, correlated with a vertical mode of tooth replacement (Jaekel, 1905, 1907), are a striking contrast to the laterally directed and needle-shaped teeth of *Nothosaurus* and potentially indicative of durophagous habits in *Simosaurus*.

Mandibular mechanics appear less well suited to crush hard-shelled prey, however. Durophagy in reptiles is generally correlated with a deep lower jaw, a high coronoid process, and a load arm that is relatively short compared to the force arm (Rieppel & Labhardt, 1979, and references therein). None of these features is observed in *Simosaurus*. The lower jaw is a slender, almost delicate structure without a coronoid process, and the posterior extension of the tooth row results in a short force arm relative to a potentially very long load arm. A short force arm relative to a potentially long load arm is usually correlated with a quick snapping bite (Robinson, 1973). The mechanical

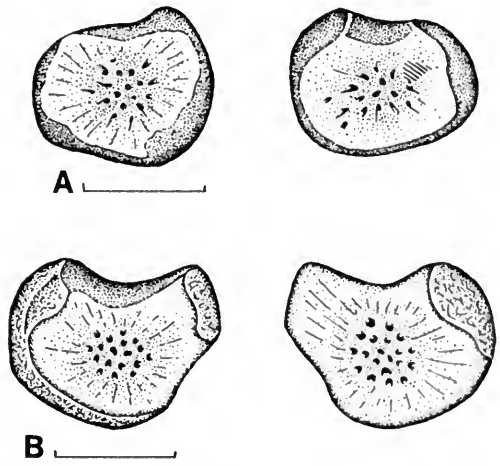

FIG. 31. **A**, Intermedium of *Simosaurus gaillardoti* (SMNS 14733, #210 of Huene, 1952), in dorsal (left) and ventral (right) views; **B**, astragalus of *Simosaurus gaillardoti* (SMNS 14733, #173 of Huene, 1952), in dorsal (left) and ventral (right) views. Scale bar = 20 mm.

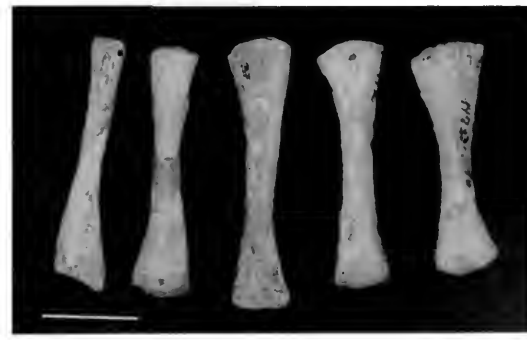

FIG. 32. Metacarpal series of *Simosaurus gaillardoti* (SMNS 14733). Scale bar = 20 mm.

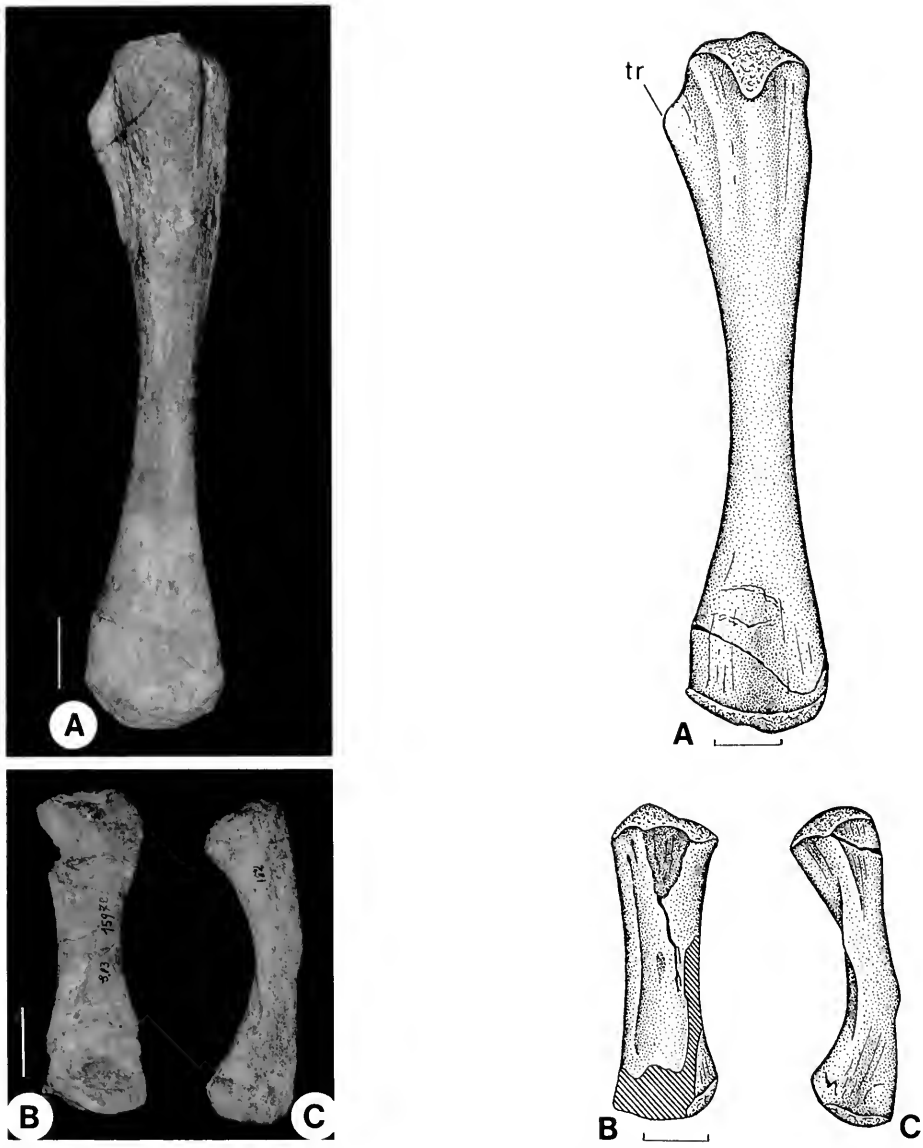

FIG. 33. Hindlimb of *Simosaurus gaillardoti* (SMNS 14733). **A**, Right femur (#81 of Huene, 1952); **B**, tibia (#51 of Huene, 1952); **C**, fibula (#182 of Huene, 1952). Abbreviation: tr, trochanter. Scale bar = 20 mm.

advantage of the jaw adductor musculature is dependent on two principal parameters: 1) the insertional angle of the jaw adductor muscle fibers and/or of their insertional tendon, relative to the long axis of the lower jaw, and 2) the distance of the muscular and/or tendinous insertion from the fulcrum point, that is, from the mandibular joint (Gans & Bock, 1965; Alexander, 1983; Rieppel, 1978). A third parameter of importance is the height of the coronoid process, which becomes more critical the more acute the angle of insertion (DeMar & Barghusen, 1972).

The greatest torque is transmitted to the lower jaw by vertically inserting adductor musculature. With a skull as flat as that of *Simosaurus,* vertically positioned muscle fibers would have a short absolute length and hence a very restricted excursion range within a tolerable range of the length/tension ratio (see Rieppel, 1984, 1985, for further discussion). The relative degree of passive stretching in-

TABLE 7. Measurements (in millimeters) of the tibia of *Simosaurus gaillardoti*.

Specimen number	Measurements			
	Length	Lateral width	Minimal width	Medial width
SMNS 14733	ca. 90	33.5	ca. 22	ca. 30.5
SMNS 15978	90.7	29.5	17.5	29.5
SMNS uncatalogued	90	29	18	28

curred by a jaw adductor muscle fiber upon jaw opening depends on the insertional angle and is maximal with a vertical orientation of the fiber relative to the long axis of the lower jaw (Rieppel, 1978). Vertically oriented jaw adductor muscle fibers would not only be the shortest in absolute terms (due to the flat skull) but would also incur the greatest degree of relative stretching upon jaw opening. The force a muscle may generate upon contraction depends on the degree of passive stretching prior to contraction (Gans & Bock, 1965; Alexander, 1983). Muscle force decreases with an increasing degree of passive stretching, according to the length/tension ratio, which depends on the degree of overlap of actin and myosin filaments within each sarcomere. The absolute excursion range of a muscle fiber therefore increases with increasing absolute length, since passive stretching will be spread across a larger number of individual sarcomeres, each remaining within a tolerable range of the length/tension ratio. However, all simple relations of muscle fiber action and jaw closure will be complicated by the complex jaw adductor muscle architecture generally encountered in reptiles (Gans & De Vree, 1987; Gans et al., 1985).

The large upper temporal fenestrae of *Simosaurus* indicate a large physiological cross-section of the jaw adductor musculature, but most fibers appear to have been positioned at an oblique angle relative to the long axis of the lower jaw (Rieppel, 1989a). The lateral ledge on the surangular indicates a well-developed m. adductor mandibulae externus superficialis, which would have originated from the lower surface of the posterior part of the upper temporal fossa and from the anterior surface of the posteroventrally slanting quadrate, and which would have inserted into the lateral surface of the surangular. Accordingly, these fibers would have slanted from an anteroventrally positioned insertion to a posterodorsally positioned point of origin. The same orientation of muscle fibers has to be assumed for deeper layers of the jaw adductor musculature originating from the posterior temporal region and inserting into the central insertional tendon and adductor fossa of the lower jaw. The mechanical advantage of these fibers increases with increasing degree of jaw closure. Aside from the adductive component, these fibers would exert a retractive force on the lower jaw ramus, which increases with increasing degree of jaw opening.

Muscle fibers originating from the broad anterior corner of the upper temporal fossa would have to slant in a posteroventral direction to insert into the central insertional tendon fastened to the lower jaw ramus behind the posteriorly extended tooth row. Aside from the adductive component, these

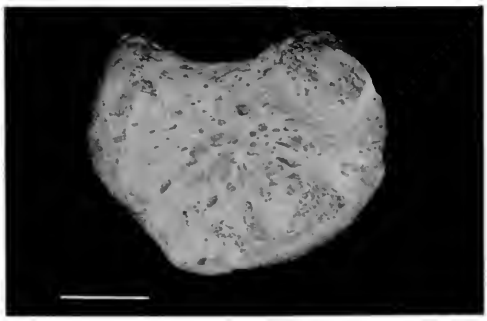

FIG. 34. Astragalus of *Simosaurus gaillardoti* (SMNS 14733, #123 of Huene, 1952). Scale bar = 10 mm.

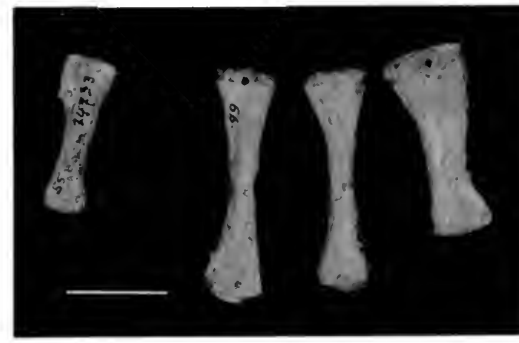

FIG. 35. Metatarsal series of *Simosaurus gaillardoti* (SMNS 14733). Scale bar = 20 mm.

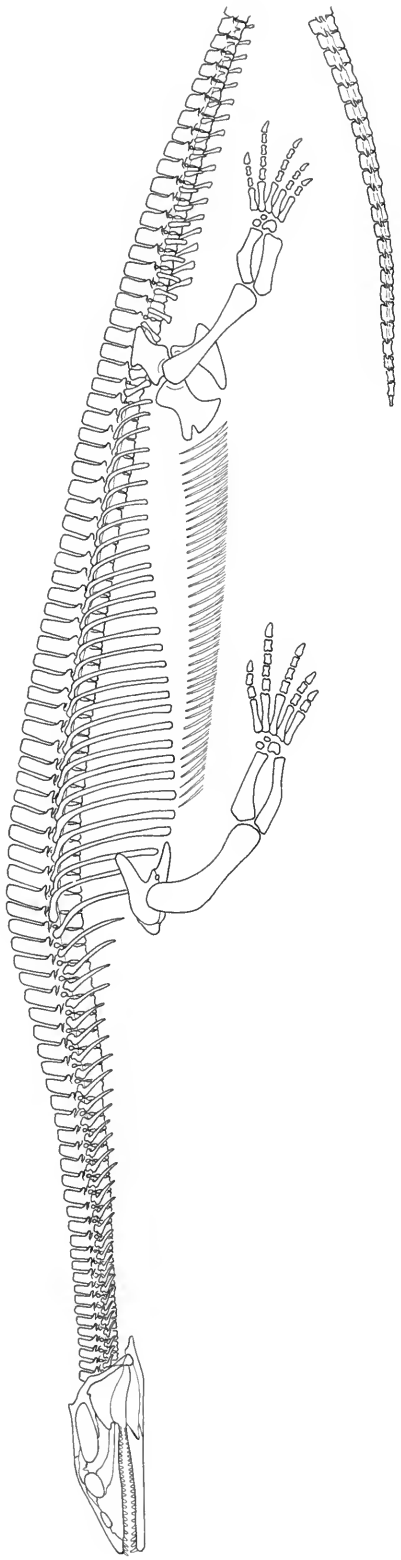

fibers would exert a strong anterior pull, as would the pterygoideus muscle, which was strongly developed with a large anterior (dorsal) portion originating on the dorsal surface of the palate behind the orbit. The mechanical advantage of these muscle portions with respect to jaw adduction increases with increasing degree of jaw opening. The anterior pull of the anterior adductor muscle fibers and of the pterygoideus muscle would increase with increasing degree of jaw closure. The morphology of the lower jaw joint (see the description above) appears to reflect these mechanical correlates, in that the lower jaw is locked against the quadrate to counteract the anterior pull from the pterygoideus muscle and anterior portions of the external jaw adductor muscle, which may have been only partially compensated for by the retractive component generated by the posterior jaw adductor muscle fibers.

It appears, therefore, that the pterygoideus muscle as well as anterior portions of the adductor musculature were able to effect a strong and rapid jaw closure in *Simosaurus*. A strong pterygoideus musculature, as indicated by the development of an anterior (dorsal) portion in *Simosaurus,* would be particularly critical to achieving rapid jaw closure against hydrodynamic drag (Taylor, 1987, p. 176). Any crushing effect with the jaws near to closure would have to be effected by the posterior portions of the jaw adductor musculature with fibers pulling in a posterodorsal direction, and whose retractive force component may be compensated by isometric contraction of the antagonistic anterior adductor fibers and pterygoideus muscle portions. The only means to increase the crushing force on the tooth row generated by the posterodorsally slanting posterior adductor fibers is by increasing the height of the coronoid process (DeMar & Barghusen, 1972; Rieppel, 1985), but this process is entirely absent in *Simosaurus*.

It may be noted at this juncture that Olson (1961) presented a biomechanical model of the evolution of tetrapod jaw mechanics, which are postulated to have changed from a kinetic inertial system favoring rapid initial jaw closure in anthracosaurian amphibians to the static pressure system favoring strong adductive forces with the jaws near to closure in reptiles. Olson (1961) also suggested that secondarily aquatic reptiles tend to revert to a kinetic inertial system. As argued on an earlier

←

FIG. 36. Reconstruction of the skeleton of *Simosaurus gaillardoti* (approx. 7.5% of natural size).

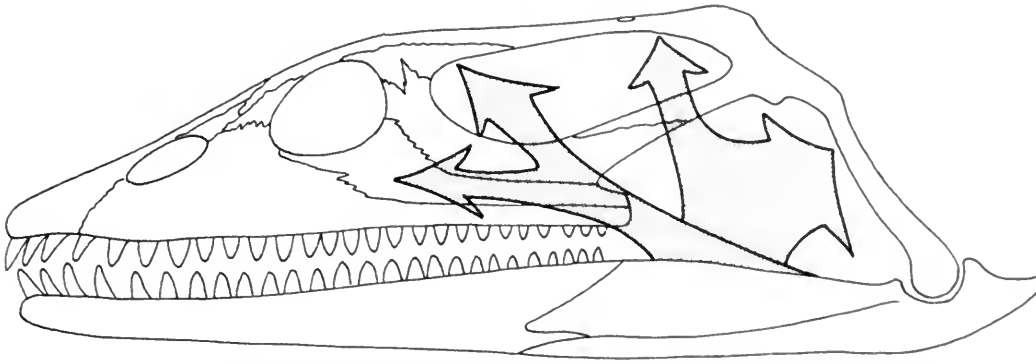

FIG. 37. The dual jaw adductor system of *Simosaurus*. For further discussion, see text.

occasion (Rieppel, 1989a), this model of the evolution of jaw mechanics in secondarily aquatic reptiles seems too simple, since *Simosaurus* shows a dual system (Fig. 37), with an anterior group of muscles favoring rapid jaw closure ("kinetic inertial fibers") and a posterior group of fibers favoring adduction with the jaws near to closure ("static pressure fibers"). A similar dual system was reconstructed by Taylor (1992) for the large plesiosaur *Rhomaleosaurus* from the Lower Jurassic of England and may, indeed, be characteristic of eusauropterygians in general.

Simosaurus lacks the longirostrine skull with jaws bearing long, slender, and laterally directed teeth as are observed in the piscivorous *Nothosaurus* species. *Simosaurus* also lacks the high coronoid process and the deep posterior temporal region observed in the lower jaw and skull of the obviously durophagous placodonts. The latter also show strongly procumbent and chisel-shaped anterior teeth in the upper and lower jaw, which were presumably used to pick up hard-shelled sessile prey such as bivalves from the substrate and which, again, are absent in *Simosaurus*. On the other hand, *Simosaurus* appears to have been able to perform a strong and quick snapping bite, followed by a moderate crushing action with the jaws near to closure. Such a pattern of jaw mechanics might be expected in a predator of moderately hard-shelled prey such as hard-scaled fishes (of "holostean" grade) or, perhaps, ammonoids (*Ceratites*).

The orientation of the intervertebral articulations indicates that lateral undulation may have played a reduced role in the locomotion of *Simosaurus*. The standard zygapophyseal articulations are strengthened not only by an additional zygosphene–zygantrum articulation, but also by the differentiation of additional infrapre- and infrapostzygapophyses in the trunk, in the sacrum, and at least in the proximal tail region. The pre- and postzygapophyses as well as the infrapre- and infrapostzygapophyses show a distinct tendency toward dorsolateral inclination of the articular surface, increasing along an anteroposterior gradient in the vertebral column. A tendency toward dorsolateral inclination of the prezygapophyses (ventrolateral inclination of postzygapophyses) is also observed in the vertebral column of *Placodus*, again increasing along an anteroposterior gradient, but the same structural trend is not observed in the vertebral column of *Nothosaurus*. Accordingly, paraxial propulsion is also assumed to have been the predominant mode of locomotion in placodonts, especially in those taxa characterized by the development of dermal armor such as *Cyamodus* (Pinna & Nosotti, 1989; see summary in Storrs, 1993b). In plesiosaurs, zygapophyseal articulations between vertebrae are strongly inclined (Brown, 1981), such that the width across the zygapophyses is less than centrum width throughout the vertebral column (Storrs, 1993a, character 48). The morphology of intervertebral articulations in plesiosaurs correlates with a shift from axial propulsion to paraxial propulsion, also reflected by the shortening of trunk and tail and modification of the limbs to form paddles (Storrs, 1993b). In *Simosaurus*, an initial shift to paraxial locomotion may be reflected by the changing orientation of vertebral zygapophyses and the dorsoventrally flattened trunk. Interlocking of pre- and postzygapophyses and infrapre- and infrapostzygapophyses with almost vertically oriented articular surfaces effectively reduces the potential for lateral undulation in the posterior part of the axial skeleton, whereas the neck and anterior trunk regions with more horizontally oriented pre- and postzyg-

apophyses would preserve their potential for extensive lateral bending during prey capture. The flat skull would tend to minimize drag as the head was swept laterally in pursuit of prey (Taylor, 1987, p. 190).

Principal thrust in forward locomotion seems to have been generated by the forelimbs of *Simosaurus* rather than through lateral undulation. The stylo- and zeugopodial elements of the forelimbs are much more strongly developed than those of the hindlimbs in the two associated skeletons available (ontogenetic variation of limb proportions remains unknown for *Simosaurus*). The strong reduction of the dorsal blade of the scapula would seem to prevent the upstroke of the front limb from becoming a major component of the propulsion-generating limb movement. *Simosaurus,* therefore, had not developed full capabilities of underwater flight. The strongly developed ventral parts of the pectoral girdle correlate with a well-developed deltopectoral crest on the humerus and indicate that the downstroke of the front limb may have been the principal thrust-producing movement. This would result in a type of locomotion intermediate between true underwater flight and rowing, corresponding to the otariid model developed by Godfrey (1984) for plesiosaurs (see also Storrs, 1991, 1993b); Carroll and Gaskill (1985) postulated a similar type of locomotion for the pachypleurosaur *Neusticosaurus edwardsii,* and Storrs (1991, 1993b) for *Corosaurus.* In *Simosaurus* SMNS 14733, the ratio of humerus length/femur length is 1.28; the corresponding ratio ranges from 1.13 to 1.84 in *Neusticosaurus edwardsii.*

Functional morphological correlates in the skeleton of *Simosaurus* result in the reconstruction of its mode of life as an animal of the shallow open water, roaming the sea at moderate speed in the search for free-swimming fish and, perhaps, mollusk prey such as ammonoids (*Ceratites*). Such conclusions contrast with S. Schmidt's (1988) reconstruction of *Simosaurus* as a primarily terrestrial animal.

Phylogenetic Analysis

Phylogeny reconstruction will be based on a number of "paradigm" terminal taxa, selected according to sufficient current knowledge of their skeletal morphology to be useful for phylogenetic analysis. This procedure is justified with reference to the fact that missing data may influence cladistic analysis in rather unpredictable ways (Platnick et al., 1991; see also Appendix I). However, as more terminal taxa become better known in the future and are added to the analysis of cladistic interrelationships of the Sauropterygia, the results presented in this study may change.

The Pachypleurosauroidea is generally treated as a monophyletic taxon, sister-group to the Eusauropterygia (plus Placodontia *sensu* Storrs, 1991, 1993a; see also Rieppel, 1987, 1993a). The monophyly of the Pachypleurosauroidea is, however, rather weakly supported (by the probable absence of the ectopterygoid and the complex morphology of the retroarticular process; Rieppel, 1989a) and may be called into question by current revisionary work focusing on a redescription of the pachypleurosaurs from the lower Muschelkalk (Rieppel, 1993d) and the redescription of the Chinese material of *Keichousaurus* by Lin Kebang (Ph.D. thesis in progress). It is for these reasons that the well-known genera *Dactylosaurus* (Sues & Carroll, 1985; and pers. obs. on the holotype of *Dactylosaurus schroederi* Nopcsa, 1928), *Serpianosaurus* (Rieppel, 1989a), and *Neusticosaurus* (Carroll & Gaskill, 1985; Sander, 1989) are chosen to represent the pachypleurosaurs. *Serpianosaurus* and *Neusticosaurus* are here coded as a single clade (terminal taxon) based on earlier evidence of monophyly (e.g., extreme reduction of the upper temporal fossa, gastral rib morphology; Rieppel, 1987, 1993b).

The Nothosauridae (*sensu* Rieppel, 1984) comprise the genera *Lariosaurus, Ceresiosaurus, Nothosaurus,* and *Paranothosaurus.* Of these, the genera *Nothosaurus* and *Lariosaurus* will be used as terminal taxa. *Nothosaurus* is known from abundant cranial and postcranial material deposited in public repositories (see Appendix II). The genus *Lariosaurus* is currently under revision (Rieppel & Tschanz, work in progress) and remains controversial until this work is completed (Tschanz, 1989; Kuhn-Schnyder, 1990; Storrs, 1993a). The holotype of *Lariosaurus balsami* was destroyed during World War II, and the "Munich specimen" (BSP AS I 802) was designated the neotype by Kuhn-Schnyder (1987). Another well-preserved and complete specimen of *Lariosaurus* is the "Frankfurt specimen" (SMF R-13), purchased by E. Rüppell in 1850 and described by Boulenger (1898). The specimen comes from Perledo, the type locality for the genus, and together with the "Munich specimen" it forms the basis for inclusion of *Lariosaurus* in the present analysis. *Paranothosaurus* is probably a junior synonym of *Nothosaurus* (Rieppel & Wild, 1994). The genus *Ceresiosaurus* is known from Peyer's (1931a) published work; this

material has since been reprepared, and new material has been collected. The material of *Ceresiosaurus* currently available requires redescription before it can be entered into phylogenetic analysis, but it is not available for study at the present time.

Additional terminal taxa used in this study are the genera *Cymatosaurus* and *Pistosaurus*. Data for *Pistosaurus* result from personal inspection of the only surviving skull of *Pistosaurus longaevus* (see Edinger, 1935, for a history of the specimens of *Pistosaurus*); the postcranial skeleton of *Pistosaurus* was described by Sues (1987a). *Cymatosaurus* is one of the most problematical taxa used in this analysis, because of the very incomplete knowledge of its postcranial skeleton. However, two isolated humeri are included in this study (see Appendix II) that were identified as those of *Cymatosaurus*. The reason is that both elements are very distinctive, and both come from lower Muschelkalk deposits that have yielded *Dactylosaurus* and/or *Anarosaurus, Nothosaurus,* and *Cymatosaurus* but no other taxon. Data for *Corosaurus* are taken from Storrs (1991) and FMNH specimens.

Placodus will be used as a representative genus for the Placodontia, on the basis of an ongoing revision of its osteology and taxonomy. *Paraplacodus,* purportedly the most plesiomorphic placodont with respect to some characters (i.e., dentition; Peyer, 1931b, 1935), requires redescription of a fairly complete specimen (Kuhn-Schnyder, 1942) before it can reliably be used in phylogeny reconstruction. Some important characters in the skull of *Paraplacodus* have been recorded by Zanon (1989, and pers. obs.).

The phylogenetic analysis of sauropterygian interrelationships presented here relies heavily on the work of Gauthier, Kluge, and Rowe (1988) on amniote relationships. Their data matrix for amniotes forms the core of the present analysis, after deletion of all those characters informative with respect to or within the Synapsida only. The remaining list of characters was further augmented by the addition of characters taken from Evans (1988) and Storrs (1991, 1993a) and by characters that emerged from personal inspection of the sauropterygian material referred to in Appendix II. Due to the addition of new characters and redefinition of old ones, the numbering of the characters given below no longer corresponds to character numbers in Gauthier, Kluge, and Rowe (1988), Evans (1988), Storrs (1991, 1993a), or Rieppel (1993a). Character codings of archosauromorph taxa are mostly the same as in Gauthier, Kluge, and Rowe (1988) except for the Protorosauria (for which terminal taxon they were unable to recover diagnostic characters; Gauthier, Kluge, & Rowe, 1988, p. 205). Their Protorosauria is here replaced by the Prolacertiformes (see discussion in Evans, 1988, p. 227), and the prolacertiform characters are taken from Wild (1973), Gow (1975), Chatterjee (1980), Evans (1988), and Rieppel (1989b). *Claudiosaurus* (Carroll, 1981) was added to their list of taxa, and Lepidosauromorpha were broken down into potential subgroups, viz., Younginiformes, Kuehneosauridae, Rhynchocephalia (*Gephyrosaurus* and Sphenodontida; Gauthier, Estes, & de Queiroz, 1988), and Squamata. If different from Gauthier, Kluge, and Rowe (1988) and Evans (1988), character codings are based on the following published descriptions:

Captorhinidae: Heaton (1979), Heaton and Reisz (1980, 1986)

Testudines: Gaffney (1979b, 1990)

Araeoscelidia: Vaughn (1955), Reisz (1981), Reisz et al. (1984)

Younginiformes: Gow (1975), Carroll (1981), Currie (1981, 1982)

Kuehneosauridae: Robinson (1962), Colbert (1970)

Rhynchocephalia: Robinson (1973), Evans (1980, 1981), Fraser (1982, 1988a,b), Fraser and Walkden (1984), Whiteside (1986)

Squamata: Gauthier, Estes, and de Queiroz (1988), and pers. obs.

Rhynchosauria: Chatterjee (1974), Benton (1983)

Choristodera: Sigogneau-Russell (1979, 1981), Sigogneau-Russell and Russell (1978)

Trilophosaurus: Gregory (1944)

Definition of Characters

1. Premaxillae small (0) or large (1), forming most of snout in front of external nares.

The character translates into posteriorly positioned ("retracted") external nares.

2. Premaxilla without (0) or with (1) postnarial process, excluding maxilla from posterior margin of external naris.

3. Snout unconstricted (0) or constricted (1).

Constriction of the rostrum at the level of the anterolateral margin of the external naris where the premaxilla meets the maxilla is characteristic of longirostrine sauropterygians such as the Nothosauridae (*sensu* Rieppel, 1994a, including *Nothosaurus* and *Lariosaurus*) and *Cymatosaurus*. The character also occurs in *Placodus,* but it is absent

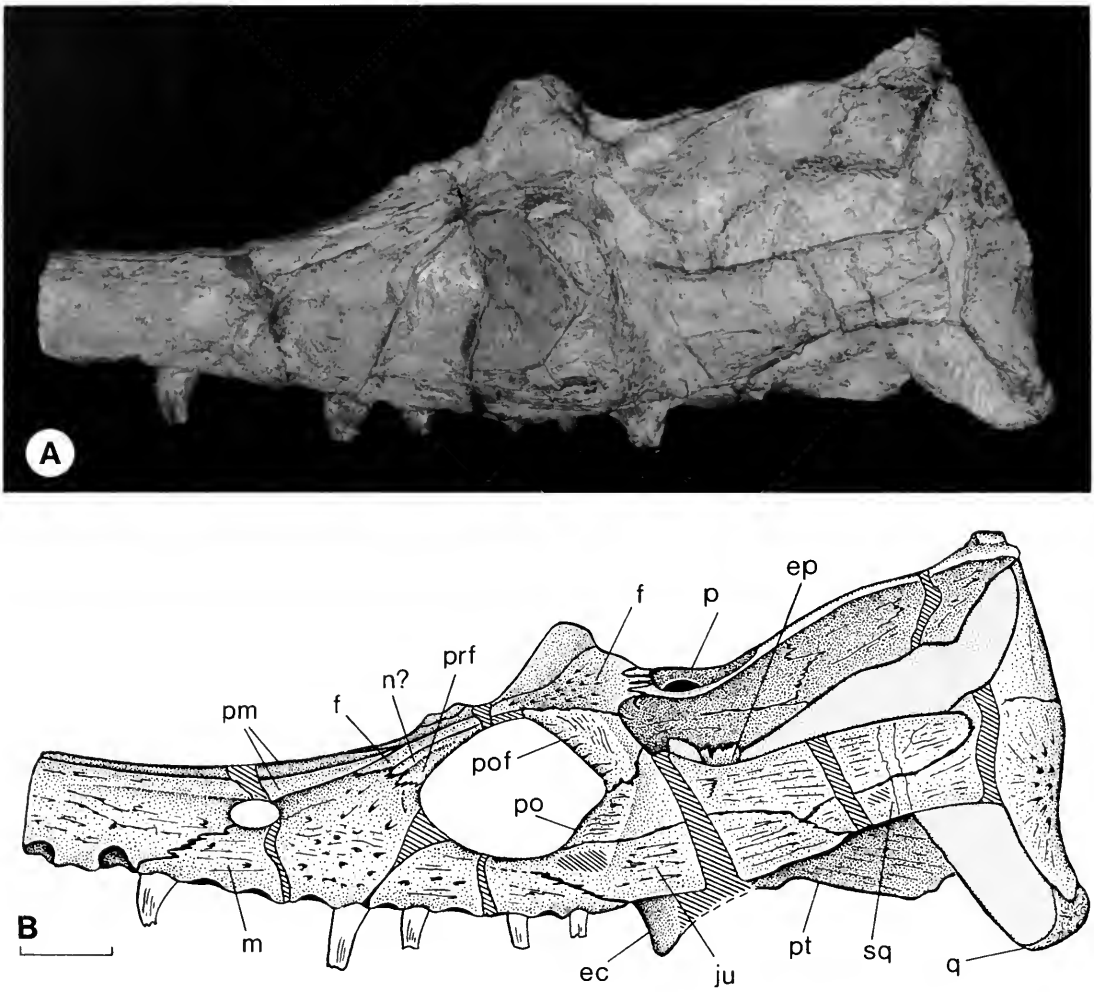

FIG. 38. Skull of *Pistosaurus longaevus* (the "second" specimen of Meyer, 1847–1855, Pl. 22, Fig. 1; Oberfränkisches Erdgeschichtliches Museum, Bayreuth, BT uncatalogued). **A,** Oblique dorsolateral view; **B,** lateral view, partially restored. Abbreviations: ec, ectopterygoid; ep, epipterygoid; f, frontal; ju, jugal; m, maxilla; n, nasal; p, parietal; pm, premaxilla; po, postorbital; pof, postfrontal; prf, prefrontal; pt, pterygoid, q, quadrate; sq, squamosal. Scale bar = 20 mm.

in the pachypleurosaur genera *Dactylosaurus, Serpianosaurus,* and *Neusticosaurus. Simosaurus* shows no conspicuous constriction of the broad and relatively short snout at the level of the premaxillary–maxillary suture, although a weak embayment can be seen in relatively small skulls (*Simosaurus* "*guilielmi*"). This may reflect initial development of snout constriction or secondary loss of that character. Snout constriction is coded as absent (0) for *Simosaurus* in order to avoid influence on pattern reconstruction by a priori hypotheses of character transformation. *Pistosaurus* has a longirostrine skull with a tapering and pointed snout but without distinct rostral constriction.

4. Nasals shorter (0) or longer (1) than frontal(s).

5. Nasals entering posterior margin of external naris (0) or reduced (absent) with no contact with the margin of the external naris (1).

Reduction of the nasals is characteristic of *Cymatosaurus.* Much reduced nasals have been described for *Pistosaurus* (Koken, 1893; Edinger, 1935; Sues, 1987a), but unequivocal identification of the nasal bones on the only available specimen of *Pistosaurus longaevus* is difficult (Fig. 38). The reduced nasals may have been better exposed on a second skull (*Pistosaurus* "*grandaevus*" of Meyer, 1847–1855), which is now lost.

6. Nasals meet in dorsomedial suture (0) or are separated from one another by nasal processes of the premaxillae extending back to the frontal bone(s) (1).

This character is difficult to assess because of extreme variability. Both conditions occur in the pachypleurosaur genus *Neusticosaurus*, which shows the nasal processes of the premaxillae always extending back to meet the frontal in ventral view. The nasals meet in a dorsomedial suture when they are broad enough to cover the premaxillary processes in dorsal view. In *Dactylosaurus* the nasals meet in the dorsal midline of the skull, but character variation cannot be assessed in this genus due to the lack of specimens. Within the Nothosauridae, the best known skulls are those of *Nothosaurus*. The nasals meet in a dorsomedial suture in all well-preserved skulls, but one specimen of *Nothosaurus* (cf. *N. mirabilis*, SMNS 10977) shows the nasal process of the premaxilla meeting the frontal. The character is coded as polymorphic for that genus. Reduction of the nasals in *Cymatosaurus* and *Pistosaurus* results in an invariable contact of the premaxilla with the frontal: characters 5 and 6 are interdependent in these two genera. In *Placodus* the nasals are fused and broadly separate the premaxillae from the frontals (Sues, 1987b).

7. The lacrimal is present and enters the external naris (0) or remains excluded from the external naris by a contact of maxilla and nasal (1), or the lacrimal is absent (2). The character is coded as unordered.

8. The prefrontal and postfrontal are separated by the frontal along the dorsal margin of the orbit (0), or a contact of prefrontal and postfrontal excludes the frontal from the dorsal margin of the orbit (1).

9. Preorbital and postorbital region of skull of subequal length (0), preorbital region distinctly longer than postorbital region (1), or postorbital region distinctly longer (2). The character is coded as unordered.

The elongated postorbital region of the skull is one of the few characters supporting Storrs's (1991, 1993a) conclusion that the Placodontia is the sister-group of the Eusauropterygia (Rieppel, 1993a). In pachypleurosaurs, the postorbital skull is distinctly shorter than the preorbital skull. In *Placodus*, the postorbital region of the skull is not as markedly elongated as it is in the Eusauropterygia included in this study, yet it still ranges from 115% (BT 13, original of Sues, 1987b) to 120% (in the holotype of "*Placodus hypsiceps*"; Meyer, 1863) of the preorbital skull. In the Cyamodontoidea (*Cyamodus*), the postorbital region is distinctly elongated, and *Placodus* is coded accordingly in this analysis. In the brevirostrine eusauropterygian *Simosaurus* (SMNS 13060), the postorbital region is about 150% (if measured to the mandibular condyles of the quadrate; approximately 135% if measured to the posterior margin of the squamosal) of the preorbital skull. In *Nothosaurus mirabilis*, the nothosaur with the relatively longest rostrum, the postorbital region of the skull still amounts to 145% of the preorbital skull length (measurements based on the complete skull of BM[NH] 42829; 142% in the somewhat less well preserved specimen of Meyer, 1847–1855, Pl. 2, Figs. 1–2; postorbital region measured from posterior margin of orbit to posterior end of squamosal).

10. Upper temporal fossa absent (0), present and subequal or larger than the orbit (1), or present but distinctly smaller than orbit (2). The character is coded as unordered.

Absence of an upper temporal fossa is the plesiomorphic condition; its presence is diagnostic of the Diapsida (Evans, 1988; Gauthier, Kluge, & Rowe, 1988). If present, the plesiomorphic size of the upper temporal fossa is roughly comparable to that of the orbit or somewhat smaller (1). In the pachypleurosaurs, the upper temporal fossa is very distinctly smaller than the orbit, although its relative size still varies: the upper temporal fossa is relatively larger in *Dactylosaurus* (Sues & Carroll, 1985) than in the *Serpianosaurus–Neusticosaurus* clade (Carroll & Gaskill, 1985; Rieppel, 1989a; Sander, 1989). The significant increase in the size of the upper temporal fossa in relation to the size of the orbit in *Placodus* and in the Eusauropterygia is one of the characters supporting Storrs's (1991, 1993a) conclusion that *Placodus* is the sister-group of the Eusauropterygia (Rieppel, 1993a). However, enlargement of the upper temporal fossa in these taxa is logically correlated with elongation of the postorbital region of the skull (character 9; see discussion above) and therefore is not coded separately in this study.

11. Frontal(s) paired (0) or fused (1) in the adult.

12. Frontal(s) without (0) or with (1) distinct posterolateral processes.

13. The frontal does not enter the margin of the upper temporal fossa (0) or narrowly enters the anteromedial margin of the upper temporal fossa (1).

The frontal is excluded from the anteromedial margin of the upper temporal fossa in *Cymatosaurus* cf. *C. silesiacus* (SMNS 10977; see also Schrammen, 1899), but the frontal bone enters the

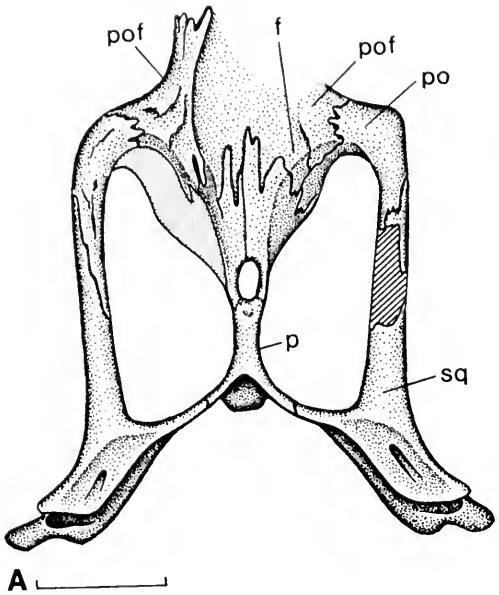

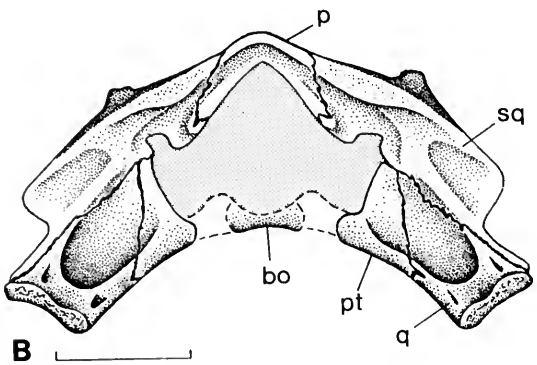

FIG. 39. Incomplete skull of *Cymatosaurus* sp. (BGR uncatalogued, lower Muschelkalk, Sacrau, Gogolin [Poland]. **A,** Dorsal view; **B,** occipital view. Abbreviations: bo, basioccipital; f, frontal; p, parietal; po, postorbital; pof, postfrontal; prf, prefrontal; pt, pterygoid, q, quadrate; sq, squamosal. Scale bar = 20 mm.

anteromedial margin of the upper temporal fossa in *Cymatosaurus friedericianus* (Fritsch, 1894, and pers. obs.; see also Schrammen, 1899) and in an unidentified partial skull of *Cymatosaurus* kept at the Bundesanstalt für Geowissenschaften und Rohstoffe, Berlin (Fig. 39). The character is coded as polymorphic for *Cymatosaurus*. The frontal also narrowly enters the anteromedial margin of the upper temporal fossa in *Pistosaurus*.

14. Parietal(s) paired (0) or fused (1) in adult.

15. Pineal foramen at the middle of the skull table (0), displaced posteriorly (1), displaced anteriorly (2), or absent (3). The character is coded as unordered.

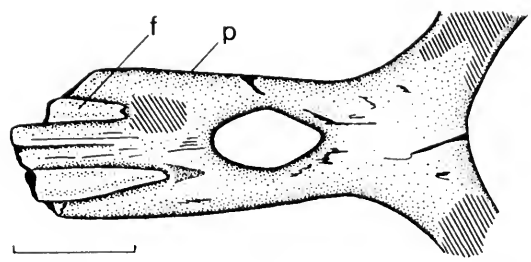

FIG. 40. Parietal skull table of cf. *Cymatosaurus* (BRG uncatalogued, lower Muschelkalk [*Pecten*- and *Dadocrinus*-beds], Gogolin [Poland]). Abbreviations: f, frontal; p, parietal. Scale bar = 20 mm.

The plesiomorphic condition of this character is the pineal foramen centered in the middle of the parietal skull table. Among sauropterygians, this condition is observed in pachypleurosaurs and in *Cymatosaurus*. In some taxa, including *Placodus* (BSP 1968.I.75, where the frontal enters the anterior margin of the foramen) and *Pistosaurus,* the pineal foramen is displaced anteriorly. In other Eusauropterygia, the pineal foramen is displaced to a posterior position in the parietal skull table.

16. Parietal skull table broad (0), strongly constricted (1), or forming a sagittal crest (2). The character is coded as unordered.

Constriction of the parietal skull table results in larger upper temporal fossae and provides a greater area of origin for the deep jaw adductor musculature. The pachypleurosaurs retain a broad parietal skull table, as does *Placodus*. *Cymatosaurus* usually shows a constricted parietal, although one (isolated) parietal retains a relatively broad skull table (Fig. 40). At this time, *Cymatosaurus* is coded polymorphic for this character, although future revisionary work may prove the broad parietal to be characteristic of *Eurysaurus* (currently treated as a junior synonym of *Cymatosaurus,* but see *Eurysaurus schafferi* Arthaber, 1924). *Simosaurus* and *Nothosaurus* show a markedly constricted parietal skull table, as does *Pistosaurus*.

In sauropterygians with a strongly constricted parietal skull table, the area for origin of deep jaw adductor muscles may be further increased by the development of a sagittal crest on the posterior part of the parietal. The character is polymorphic within the genus *Nothosaurus* (*Nothosaurus edingerae*; Schultze, 1970; Rieppel & Wild, 1994) and a sagittal crest is well developed in *Pistosaurus*.

17. Postparietals present (0) or absent (1).

18. Tabulars present (0) or absent (1).

19. Supratemporals present (0) or absent (1).

20. The jugal extends anteriorly along the ventral margin of the orbit (0), is restricted to a position behind the orbit but enters the latter's posterior margin (1), or is restricted to a position behind the orbit without reaching the latter's posterior margin (2). The character is coded as unordered.

In the *Serpianosaurus–Neusticosaurus* clade, the jugal is a slender and curved element defining the posteroventral and ventral margin of the orbit, meeting the prefrontal anteriorly in most if not all specimens. A similar configuration of the jugal may be assumed for *Dactylosaurus,* where the character remains unknown. In *Placodus,* the jugal forms the ventral margin of the orbit and extends anteriorly beyond the level of the anterior margin of the orbit, an autapomorphic feature of the genus (Fig. 41). In *Simosaurus,* the main body of the jugal lies behind the orbit, but a slender process continues anteriorly to define the lower margin of the orbit. In *Nothosaurus,* the jugal remains restricted to a position behind the orbit, without entering the latter's posterior margin in most specimens. There is, however, a partial skull of *Nothosaurus* (SMNS 56838) that shows a narrow entry of the jugal into the posterior margin of the orbit. The genus is, therefore, coded polymorphic (1 and 2) for this character at this time, although a slight possibility exists that the generic identity of this skull may have to be revised in the future (the jugal has been said to enter the back of the orbit in a small (juvenile?) specimen of *Ceresiosaurus* [K. Tschanz, pers. comm.], and the presence of *Ceresiosaurus* in the German Triassic [Lettenkeuper] may be indicated by an ulna [see below]). The relation of the jugal to the orbit in *Lariosaurus* remains controversial, due to the fact that none of the material is well enough preserved to allow the unequivocal identification of the character. In *Cymatosaurus* (SMNS 10977), the jugal bone defines the posteroventral margin of the orbit and extends anteriorly up to a level shortly behind the midpoint of the orbit (the genus is coded 1). In *Pistosaurus,* the anterior process of the jugal is hard to distinguish from the posterior part of the maxilla but seems to define the ventral margin of the orbit (coded 0).

21. The jugal extends backward no farther than to the middle of the cheek region (0) or nearly to the posterior end of the skull (1).

In pachypleurosaurs, the jugal remains broadly separated from the squamosal, the plesiomorphic condition also observed in other diapsids (with the exception of some squamates). The jugal also remains separate from the squamosal in *Placodus*

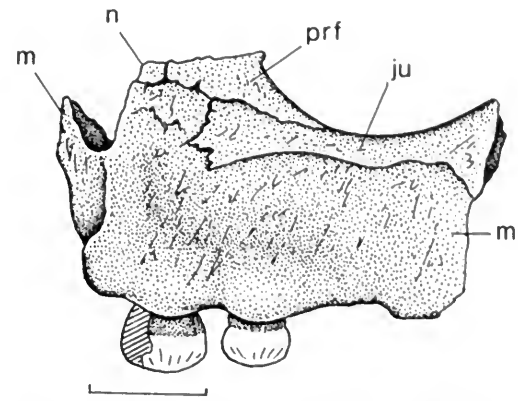

FIG. 41. Skull fragment of *Placodus gigas* (SMF 4162, upper Muschelkalk, Bayreuth). Abbreviations: ju, jugal; m, maxilla; n, nasal; prf, prefrontal. Scale bar = 20 mm.

(Sues, 1987b), *Cymatosaurus,* and *Simosaurus,* although the latter genus shows the posterior extension of the maxilla and jugal discussed as character 46. In *Pistosaurus,* the jugal meets the squamosal along the ventral margin of the cheek (upper temporal arch). In *Nothosaurus,* the posterior extension of the maxilla and jugal results in a close approximation of the posterior tip of the jugal and the anterior tip of the squamosal, but whether a contact is established by the two bones remains unknown due to the problematical preservation of the material. The presence of a contact between squamosal and jugal is therefore not entered as a separate character in the phylogenetic analysis.

22. Lower temporal fossa absent (0), present and closed ventrally (1), or present but open ventrally (2). Since the presence of a ventrally open lower temporal fenestra logically implies loss of the lower temporal bar, and hence the previous presence of a ventrally closed temporal fenestra, this character is coded as ordered.

Some controversy surrounded the interpretation of the lower cheek region in sauropterygians, that is, whether the cheek had become emarginated ventrally or a lower temporal arch had been lost (Kuhn-Schnyder, 1962, 1967). Cladistic analysis initially did not resolve the question (Rieppel, 1989a; Zanon, 1989), but a more recent investigation (Rieppel, 1993b) showed the assumption of loss of a lower temporal arch to be more parsimonious than the assumption of ventral emargination of the cheek. Since presence of the lower temporal arch (character 1) must logically precede loss of the lower temporal arch (character 2), this character is coded as ordered, but reversible (for a discussion of a secondary development of the

lower temporal arch, see Whiteside, 1986, and Fraser, 1988).

Placodus is exceptional among the taxa here discussed because it shows an upper but no lower temporal fossa; the latter is thought to have been closed secondarily (Sues, 1987). The jugal meets the quadratojugal (if present) along the lower margin of the cheek (as is also the case in the Cyamodontoidea). *Paraplacodus,* on the other hand, shows a deeply excavated cheek region with a curved jugal defining the posterior margin of the orbit and without a posterior process, suggesting the loss of a lower temporal arch (Zanon, 1989; Pinna, 1989, and pers. obs.), and a deep excavation of the lower cheek region is also characteristic of at least some Cyamodontoidea (e.g., *Placochelys*; Jaekel, 1907, and pers. obs.). The hypothesis of secondary closure of the cheek region in *Placodus* is thus accepted.

23. Squamosal descends to (0) or remains broadly separated from (1) ventral margin of skull. See discussion of character 34.

24. Quadratojugal present (0) or absent (1).

The quadratojugal is present in pachypleurosaurs, where it is situated in front of the ventrally descending process of the squamosal, which covers the quadrate laterally. The presence of a small quadratojugal in *Simosaurus* was first reported by Schultze (1970), but the squamosal still extends far down on the lateral surface of the quadrate. Rieppel (1994a) described a quadratojugal in acid-prepared braincase material of *Nothosaurus,* but this report may be erroneous, the suture supposedly delineating the quadratojugal resulting from erosion of the bone surface. No quadratojugal is present in the well-preserved and well-prepared specimens of *Nothosaurus* described by Schröder (1914; see Appendix II), where the squamosal extends far down toward the ventral margin of the skull. The same is true of *Cymatosaurus* (Fig. 39B) and *Pistosaurus* (Fig. 38), two genera in which the quadratojugal is absent. Sues (1987b) described a large quadratojugal in *Placodus,* restricting the squamosal to a dorsal position in the posterior temporal region of the skull, but its delineation from the squamosal is controversial (cf. Broili, 1912; Pinna, 1989; Sues found a faint suture delineating the squamosal from the quadratojugal in BT 13 but not in the SMF specimens; pers. comm.). Personal observation of BT 13 and SMNS 18644 and of the holotype of *Placodus hypsiceps* Meyer, 1863 (a junior synonym of *Placodus gigas*), in my view supports Broili's (1912) conclusion that a quadratojugal may be absent, that is, fused to the squamosal in *Placodus.* However, since a large quadratojugal is present in the Cyamodontoidea (*Cyamodus kuhnschnyderi,* Nosotti & Pinna, 1993a, and pers. obs.; *Placochelys placodonta,* Jaekel, 1907, and pers. obs.), the reconstruction of the skull of *Placodus* given by Sues (1987b) is here provisionally accepted, and *Placodus* coded 1 for character 23 and 0 for character 24 (quadratojugal present but fused to squamosal). Restriction of the squamosal of *Placodus* to a dorsal position on the posterior temporal region of the skull (due to the presence of a large quadratojugal) follows from both Sues's (1987b) and Pinna's (1989) reconstructions.

25. Quadratojugal with (0) or without (1) anterior process.

The character is partially correlated with characters 21 and 22 defined above. Absence of the quadratojugal logically correlates with the absence of an anterior process of that bone. However, a complete lower temporal arch may be formed by the jugal alone, the posterior process of the jugal extending all along the lower margin of the lower temporal fenestra to meet the quadratojugal in a posterior position as the latter lost the anterior ramus.

26. Occiput with paroccipital process forming the lower margin of the posttemporal fossa and extending laterally (0), paroccipital processes trending posteriorly (1), or occiput platelike with no distinct paroccipital process and with strongly reduced posttemporal fossae (2). The character is coded as unordered.

In pachypleurosaurs, *Simosaurus, Nothosaurus* (Fig. 42A), and *Lariosaurus,* the occiput is platelike and the posttemporal fossae much reduced or absent. Closure of the occiput is effected by the occipital exposure of the parietal and squamosal bones as well as by an expansion of the occipital exposure of the opisthotic and exoccipital bones. The occiput of *Cymatosaurus* and *Pistosaurus* is still insufficiently known at this time. In *Placodus* (as well as in the Cyamodontoidea), well-defined paroccipital processes extend posterolaterally (Fig. 42B).

27. Mandibular articulations approximately at level with occipital condyle (0) or displaced to a level distinctly behind occipital condyle (1), or positioned anterior to the occipital condyle (2). The character is coded as unordered.

This character is coded as polymorphic for the genus *Nothosaurus,* taking into account the deeply excavated occiput in *Nothosaurus juvenilis* (Rieppel, 1994b). A posterior displacement of the mandibular joints generally results in a deeply excavated occiput with posterolaterally trending par-

occipital processes; hence, this character would seem to be partially correlated with character 32. However, the mandibular joints are level with the occipital condyle in *Placodus,* where the paroccipital processes are trending posterolaterally.

28. Exoccipitals do (0) or do not (1) meet dorsal to the basioccipital condyle.

The exoccipital and basioccipital are completely fused in *Captorhinus,* such that the contribution of the exoccipital to the occipital condyle cannot be determined. In turtles, the exoccipitals usually participate in the formation of the occipital condyle (Gaffney, 1979b, p. 114). In diapsid reptiles, the occipital condyle is generally formed by the basioccipital only, and the exoccipitals remain separated above the occipital condyle. This is also the condition characteristic for the Eosauropterygia and placodonts (except for an autapomorphous contact of the exoccipitals above the occipital condyle in *Cyamodus*).

29. Quadrate with straight posterior margin (0) or quadrate shaft deeply excavated (concave) posteriorly (1).

The posterior excavation of the shaft of the quadrate is indicative of the presence of a large tympanum and hence of an impedance-matching middle ear, as was present in pachypleurosaurs (Rieppel, 1989a). In *Placodus,* the quadrate is deeply excavated posteriorly, and there is no reason to believe that a tympanum was absent, although the relative size of the tympanum was reduced in adaptation to aquatic habits. If a tympanum was present in *Simosaurus,* it would have been much reduced and housed in a dorsal recess formed by the squamosal bone (see discussion above, and Kuhn-Schnyder, 1961; Rieppel, 1989a). There is no posterior excavation of the quadrate in *Simosaurus,* nor in *Nothosaurus, Cymatosaurus,* and *Pistosaurus,* which all seem to have lacked a tympanum.

30. Quadrate covered by squamosal and quadratojugal in lateral view (0), or quadrate exposed in lateral view (1).

This character is easily understood in a comparison of the plesiomorphic condition (*Captorhinus, Petrolacosaurus, Youngina*) and the apomorphic condition (lizard). Assignment of character states is less easy in other taxa such as *Placodus* and eosauropterygians. The quadrate is covered in lateral view in *Placodus* (by the squamosal and, possibly, the quadratojugal) and in *Pistosaurus* (by the squamosal only). In pachypleurosaurs, *Simosaurus, Cymatosaurus,* and nothosaurs, the quadrate is exposed in lateral view to some degree, at least, but this seems to result from a narrowing of the lateral edge of the descending process of the squamosal and, if present, of the quadratojugal. Morphologically, the squamosal and, if present, the quadratojugal descend to a level narrowly above the mandibular condyle of the quadrate, such that the latter is coded as being laterally covered in these groups.

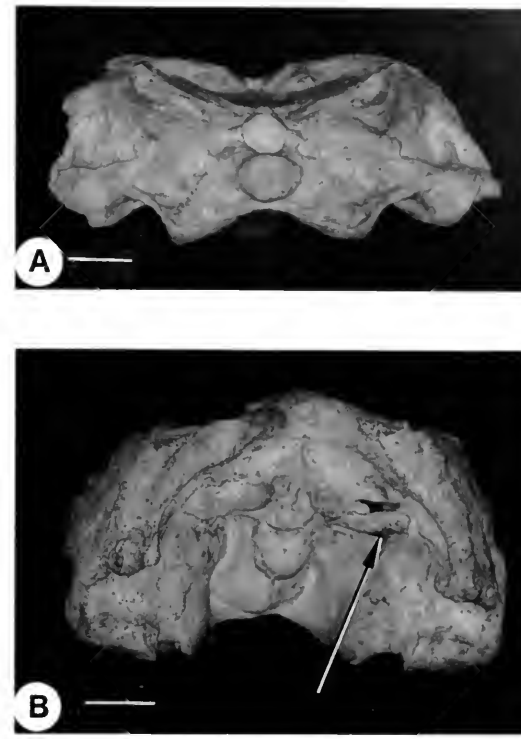

FIG. 42. **A,** Skull of *Nothosaurus mirabilis* (SMNS 56286, upper Muschelkalk, Berlichingen a.d. Jagst) in occipital view; **B,** skull of *Placodus gigas* (SMF R-360, upper Muschelkalk, Bayreuth; original of Broili, 1912, p. 147) in occipital view. The arrow points to the paroccipital process of *Placodus.* Scale bar = 20 mm.

31. Lateral conch on quadrate absent (0) or present (1).

32. Palate kinetic (0) or akinetic (1).

This is a complex character that involves a suite of structures that relate the dermal palate to the base of the braincase in a palatobasal articulation. The plesiomorphic condition is characterized by some separation of the pterygoids in front of the palatobasal articulation. The pterygoids articulate with basicranial basipterygoid processes in a synovial joint. The basipterygoid processes form by ossifications of the basitrabecular processes which develop as lateral projections from the posterior end of the trabeculae cranii just in front of the point of fusion of the trabeculae with the acrochordal cartilage. The acrochordal cartilage is

sometimes considered to be part of the basicranial plate (Bellairs & Kamal, 1981), and it is positioned behind the hypophysis. As a consequence, the palatobasal articulation lies lateral to the sella turcica, a depression in the floor of the braincase that received the hypophysis in the fully developed skull.

An akinetic palate is characterized by the fusion of the pterygoids to the basicranium, which obliterates the basitrabecular process during ontogeny (Rieppel, 1977) as well as the interpterygoid fossa. The development of an akinetic palate would thus seem to logically correlate with the absence (loss) of the basipterygoid processes. However, Sues (1987b) described large "basipterygoid processes" in *Placodus* in combination with an akinetic palate. These processes lie behind the level of the sella turcica, and even if one takes into account the shortening of the posterior basicranium that characterizes the skull of *Placodus,* it is hard to see how basitrabecular processes may have contributed to the formation of the "basipterygoid processes" described by Sues (1987b). These processes emerge from the ventral surface of the basicranium immediately in front of the occipital condyle, and whereas there is some contribution of the basisphenoid to the anterior aspect of these processes, they seem to derive mainly from the basioccipital (Zanon, 1989; Nosotti & Pinna, 1993b). This interpretation is supported by inspection of the cyamodontoid *Placochelys placodonta* (MB R.1765), where basioccipital tubera are distinct and the basioccipital remains separate from the basisphenoid.

33. Basioccipital tubera free (0) or in complex relation to the pterygoid, as they extend ventrally (1) or laterally (2). The character is coded as unordered. This character was first recognized by Zanon (1989) and will be redefined here.

The plesiomorphic condition is the presence of posterolateral projections on the basioccipital (the spheno-occipital tubercle of Oelrich, 1956) serving the insertion of the longus colli muscle. In eosauropterygians and *Placodus,* the ventral surface of the basisphenoid and basioccipital are largely covered by the posteriorly expanded pterygoids that meet all along the midline in the formation of an akinetic palate (a partial exposure of the posterior braincase floor constitutes a character reversal in *Pistosaurus*; Sues, 1987a). On topological grounds, the "basipterygoid processes" of *Placodus* described by Sues represent enlarged basioccipital tubera supporting the posterior (quadrate) ramus of the pterygoid. Some of the flexor musculature of the head may still have inserted into their posterior surface. In *Simosaurus* and *Nothosaurus,* basioccipital tubera are again present but no longer located ventral to the occipital condyle. Instead, they extend lateral to the occipital condyle, enclosing between them and the pterygoid the eustachian foramen (Rieppel, 1994a), which may be closed in some specimens of *Nothosaurus.* Although the topological relations of the basioccipital tubera are different as compared to *Placodus,* they still establish a complex relation to the quadrate ramus of the pterygoid. The occiput of pachypleurosaurs, *Cymatosaurus,* and *Pistosaurus* is not well enough known to identify the character state for these taxa.

34. Suborbital fenestra (infraorbital foramen of Oelrich, 1956) absent (0) or present (1).

Sues (1987b) described a suborbital depression in the palate of *Placodus,* which he considered homologous to the suborbital fenestra of other diapsids. A distinct cleft is seen between ectopterygoid, palatine, and maxilla in the skull of *Placodus* (Fig. 43), and a similar cleft is observed in *Placochelys placodonta* (MB R.1765). The infraorbital cleft is well developed in a fragmentary skull of *Placodus* (SMNS 18641), which shows, however, that the foramen has no connection to the floor of the orbit. A suborbital fenestra was reported for *Paraplacodus* by Zanon (1989), but personal inspection of the material showed nothing but a tooth pushed upward and located in the posterolateral corner of the orbit. *Placodus* was accordingly coded both for the presence and absence of the suborbital fenestra in the cladistic analysis, with no effect on tree topology. Since *Placodus* (and other sauropterygians) are diapsids, a reduction of the suborbital fenestra must be assumed. The suborbital fenestra is absent in pachypleurosaurs as well as in all other Eusauropterygia included in this analysis.

Turtles present a particular problem with respect to this character. Gaffney (1972) described a foramen palatinum posterius in the palate of turtles which has not generally been hypothesized to be homologous with the suborbital fenestra in diapsids. During early stages of ossification of the palate, however, the foramen palatinum posterius appears in the same topological position as does the suborbital fenestra (Rieppel, 1993e), and a homology of these foramina has recently been proposed in a review of amniote phylogeny by Laurin and Reisz (1994). Again, turtles were coded for the presence and absence of this character.

Of all combinations of alternative coding of this character in turtles and *Placodus,* only one had

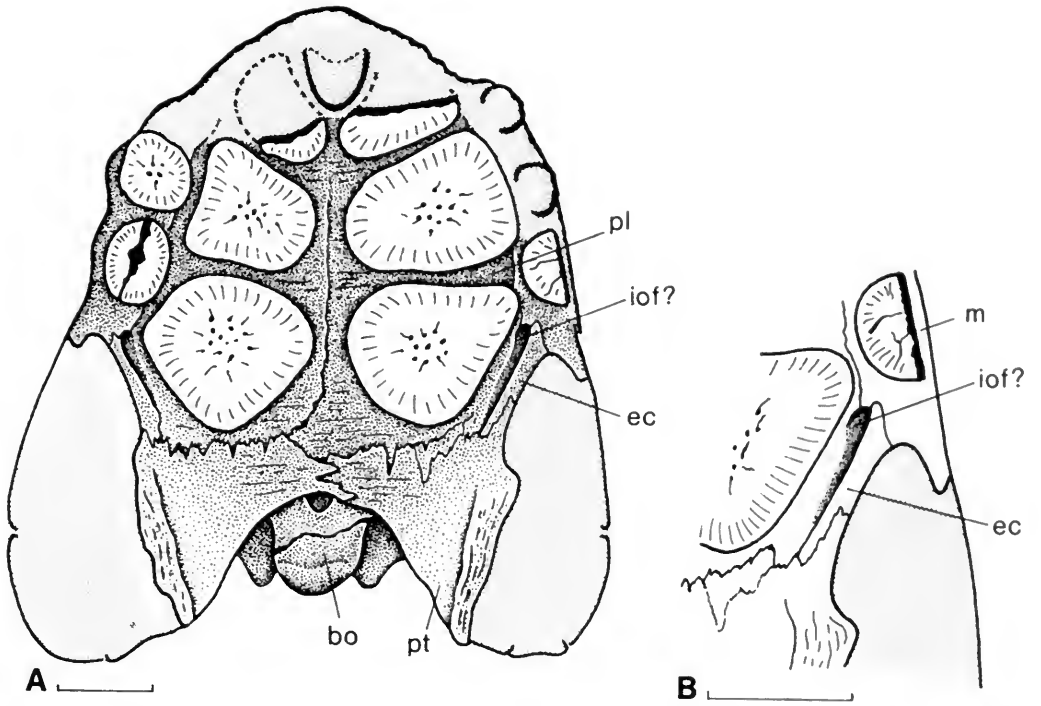

FIG. 43. **A,** Skull of *Placodus gigas* (SMF R-359, upper Muschelkalk, Bayreuth) in ventral view; **B,** magnified view of the infraorbital fenestra of Sues (1987b). Abbreviations: ec, ectopterygoid; iof, infraorbital foramen; m, maxilla; pl, palatine. Scale bar = 20 mm.

any impact on the tree, and that was coding the infraorbital fenestra absent in turtles but present in *Placodus*. The tree preserved its topology (see discussion below), but its length increased by one step (using DELTRAN optimization), as the loss of the infraorbital fenestra was treated as convergence in turtles and Eosauropterygia.

35. Pterygoid flanges well developed (0) or strongly reduced (1).

The plesiomorphic condition is a dermal palate with well-developed transverse flanges formed by the pterygoid and ectopterygoid. These define the anterior margin of the suborbital fenestra and serve as the site of origin of a strong pterygoideus muscle (Carroll, 1969). *Placodus* retains well-developed pterygoid flanges, as does *Corosaurus* (Storrs, 1991, p. 18), *Cymatosaurus,* and *Pistosaurus* among the Eusauropterygia under consideration. Pterygoid flanges are very reduced or virtually absent in pachypleurosaurs as well as in *Simosaurus, Nothosaurus,* and *Lariosaurus.*

36. Premaxillae enter internal naris (0) or are excluded (1).

This character may, to some degree, be interdependent with the elongation of the snout in longirostrine sauropterygians but is less ambiguously defined than snout elongation. Although characterized by a distinct rostrum set off from the preorbital skull by a rostral constriction, *Placodus* can hardly be viewed as a longirostrine skull in comparison, for example, to (some) *Nothosaurus, Cymatosaurus,* and *Pistosaurus.* Yet the premaxillae are excluded from the internal naris in *Placodus* (the confluent internal nares are autapomorphic for *Placodus* at the level of the present analysis), but not in the brevirostrine *Simosaurus,* nor in the *Serpianosaurus–Neusticosaurus* clade (Carroll & Gaskill, 1985; Sander, 1989).

37. Ectopterygoid present (0) or absent (1).

This character is entered here as a synapomorphy (loss of ectopterygoid) of *Dactylosaurus* and the *Serpianosaurus–Neusticosaurus* clade, although it is admitted that empirical evidence for the absence (loss) of the ectopterygoid in pachypleurosaurs is weak because of the difficult nature of the material. However, the ectopterygoid is a rather distinct element in the palate of *Simosaurus* and *Nothosaurus,* so that the expectation would

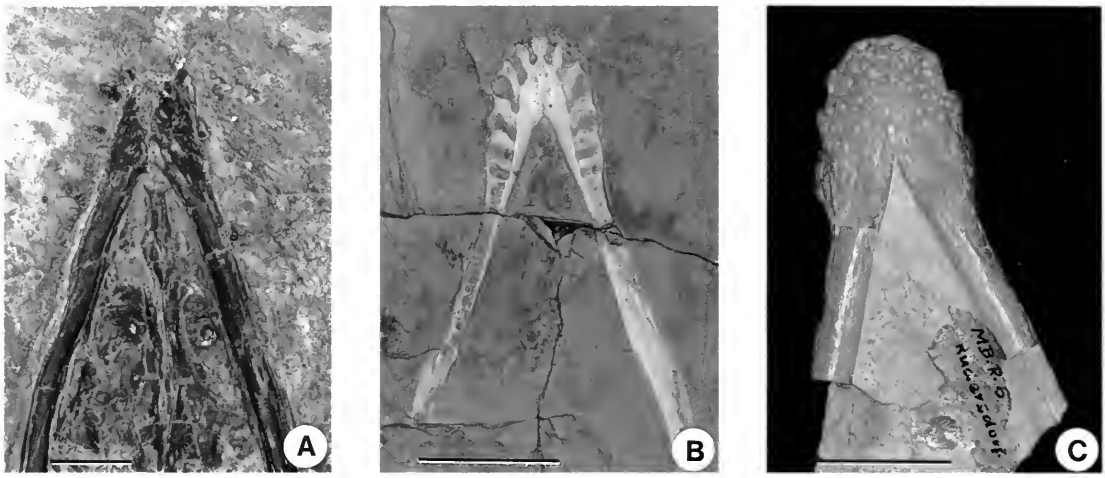

FIG. 44. **A,** Mandibular symphysis of *Lariosaurus* (SMF R-13, upper Ladinian, Perledo), ventral view; **B,** mandibular symphysis of *Cymatosaurus* (BGR uncatalogued, lower Muschelkalk [*Pecten*- and *Dadocrinus*-beds], Gogolin [Poland]); **C,** mandibular symphysis of *Nothosaurus* (MB R.6, lower Muschelkalk, Rüdersdorf; original of Schuster & Bloch, 1925).

be that at least one or two among the hundreds of specimens of the *Serpianosaurus–Neusticosaurus* clade would have documented its presence.

38. Retroarticular process of lower jaw absent (0) or present (1).

39. Distinct coronoid process of lower jaw absent (0) or present (1).

The coronoid process is distinct in *Placodus* but absent in pachypleurosaurs, *Simosaurus, Nothosaurus,* and *Lariosaurus.* The lower jaws of *Cymatosaurus* and *Pistosaurus* remain incompletely known and unknown, respectively. Characters related to the presence or absence of a coronoid process are the presence of a posterior coronoid process of the dentary bone and the presence or absence of the lateral exposure of the coronoid bone. *Placodus* shows a very limited lateral exposure of the coronoid bone, most of the coronoid process being formed by the dentary (Drevermann, 1933; Huene, 1936). In eosauropterygians with no coronoid process, the coronoid bone is not exposed in the lateral view of the lower jaw.

40. Mandibular symphysis short (0) or elongated (1).

An elongated (deep) mandibular symphysis is a derived character supporting Storrs's (1991, 1993a) conclusion that the Placondontia is the sister-group of the Eusauropterygia. In the plesiomorphic condition, the mandibular symphysis is short, as is true for the pachypleurosaur genera here considered (there is one alleged pachypleurosaur, *Anarosaurus multidentatus* Huene, 1958, with an extended symphysis, but its affinity is, in fact, with *Cymatosaurus* [Rieppel, 1995]). The mandibular symphysis is not expanded in *Simosaurus,* but it is to a variable degree in the genera *Nothosaurus, Lariosaurus,* and *Cymatosaurus* (Fig. 44). The lower jaw of *Pistosaurus* remains unknown.

Elongation of the mandibular symphysis may be correlated with a distinct pattern of tooth replacement. Whereas the maxillary, dentary, and palatine teeth of *Placodus* show a distinct vertical replacement, the replacement teeth on the premaxilla and on the mandibular symphysis show significant lateral (anterior) migration through the jaw bones during the replacement cycle (Fig. 45). A lateral (anterior) migration of premaxillary and symphyseal replacement teeth is also distinct in *Nothosaurus* (Edmund, 1960, 1969) and *Cymatosaurus* (Fig. 44B), and at least for *Nothosaurus* there is also evidence for a lateral migration of the lateral maxillary and dentary replacement teeth (Fig. 46). A lateral migration of the replacement teeth has also been described for *Simosaurus* (Edmund, 1960, using the figures in Huene, 1921), a claim that conflicts with Jaekel's (1905, 1907) description of vertical tooth replacement in this genus. Personal observations indicate lateral (anterior) migration of anterior replacement teeth and vertical tooth replacement in lateral teeth of *Simosaurus.* However, patterns of tooth replacement throughout the Sauropterygia require further study before the significance of this character can be assessed.

FIG. 45. Lower jaw of *Placodus gigas* (BSP AS VII 1209, upper Muschelkalk, Bayreuth) in dorsal view. Note the replacement pit exposed on the left symphyseal surface. Scale bar = 20 mm.

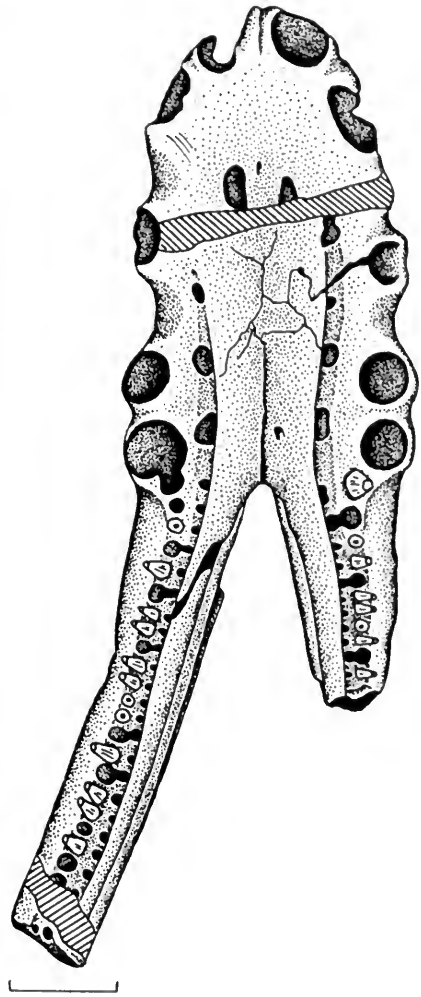

FIG. 46. Mandibular symphysis of *Nothosaurus mirabilis* (SMNS 59817, upper Muschelkalk, Hegnabrunn) in dorsal view. Note the replacement pits medial to the functional tooth positions. Scale bar = 20 mm.

There is an important difference in the mandibular symphysis of *Placodus* versus the eusauropterygians considered here. A substantial segment of the mandibular symphysis of *Placodus* is formed by the splenial (Drevermann, 1933), which remains excluded from the symphysis in *Nothosaurus* (Fig. 46), *Lariosaurus,* and *Cymatosaurus.*

41. Splenial bone enters the mandibular symphysis (0) or remains excluded therefrom (1).

42. Teeth set in shallow or deep sockets (0) or superficially attached to bone (1).

43. Anterior (premaxillary and dentary) teeth upright (0) or strongly procumbent (1).

Chisel-shaped anterior teeth of *Placodus* are strongly procumbent, as are the anterior premaxillary and dentary fangs of the Eusauropterygia (including *Lariosaurus*; Mazin, 1985) included in this study.

44. Premaxillary and anterior dentary fangs absent (0) or present (1).

In *Lariosaurus* and *Nothosaurus,* the (usually five) premaxillary and (usually five) anterior dentary teeth are enlarged and fang-like. The large alveoli of the fourth and fifth tooth on the dentary are reflected in a broad posterior part of the symphysis, set off from the remaining lower jaw ramus by a distinct constriction (Fig. 44C). Such a constriction at the posterior part of the symphysis is not observed in *Cymatosaurus* (Fig. 44B), but the premaxillary and anterior dentary teeth are distinctly enlarged. The character remains unknown for *Pistosaurus.* In *Corosaurus,* only the anterior dentary teeth are enlarged, but not the anterior premaxillary teeth (Storrs, 1991).

45. One or two caniniform teeth present (0) or absent (1) on maxilla.

46. The maxillary tooth row is restricted to a level in front of the posterior margin of the orbit (0), or it extends backward to a level below the anterior corner of the upper temporal fossa (1), or it extends backward to a level below the middle part of the upper temporal fossa (2). The character is coded as unordered.

The plesiomorphic condition is a maxillary tooth row extending posteriorly to a level somewhere in front of the posterior margin of the orbit, as seen in pachypleurosaurs and *Placodus*. In *Simosaurus, Nothosaurus, Lariosaurus,* and *Corosaurus* (Storrs, 1991), the maxilla, and with it the maxillary tooth row, is extended backward. In *Lariosaurus* and *Corosaurus* (Storrs, 1991), this continues to a level below the anterior corner of the upper temporal fossa (see also Mazin, 1985; Tintori & Renesto, 1990), and in *Simosaurus* and *Nothosaurus* to a level below the middle part of the upper temporal fossa. The posterior extension of the tooth row beyond the orbit is correlated with the development of the dual jaw adductor system discussed above.

47. Teeth on pterygoid flange present (0) or absent (1).

48. Vertebrae notochordal (0) or non-notochordal (1).

49. Vertebrae amphicoelous (0), platycoelous (1), or other (2). The character is coded as unordered.

Haas (1966) reported a derived ossification pattern in the centra of "nothosaurs" and "placodonts," characterized by what he called "terminal plugs." These observations recall the ossification pattern in limb bones of sauropterygians, in which "terminal plugs" had been identified as epiphyses by Lydekker (1889, p. 149), an interpretation rejected by Moodie (1908). Unfortunately, the nature of this ossification pattern and its taxonomic distribution among amniotes is not well enough known at this time to use the character in phylogenetic analysis.

50. Dorsal intercentra present (0) or absent (1).

51. Cervical intercentra present (0) or absent (1).

52. Cervical centra rounded (0) or keeled (1) ventrally.

53. Zygosphene–zygantrum articulation absent (0) or present (1).

A zygosphene–zygantrum articulation, as observed in *Nothosaurus, Simosaurus,* and *Pistosaurus* (Sanz, 1983), for example, consists of a bipartite anterior process located at the base of the neural arch above the prezygapophyses (the zygosphene), which fits into a notch at the base of the neural arch of the preceding vertebra, again located above the postzygapophyses. *Placodus* shows a hyposphene–hypantrum articulation: the hyposphene is a projection from the base of the neural spine, located below the postzygapophyses, that fits into a socket at the base of the neural arch of the succeeding vertebra, again located below the prezygapophyses (Fig. 47). On topological grounds, the zygosphene–zygantrum articulation cannot be compared to the hyposphene–hypantrum articulation. *Placodus* is accordingly coded with the zygosphene–zygantrum articulation absent (the hyposphene–hypantrum articulation is an autapomorphy of *Placodus* among the genera included in this analysis). In pachypleurosaurs, the projection is from between the prezygapophyses, and the socket is between the postzygapophyses of the preceding vertebra. Accordingly, pachypleurosaurs are coded as sharing the presence of a zygosphene–zygantrum articulation (see also Kuhn-Schnyder, 1959; Carroll & Gaskill, 1985).

54. Sutural facets receiving the pedicels of the neural arch on the dorsal surface of the centrum in the dorsal region are narrow (0) or expanded into a cruciform or "butterfly-shaped" platform (1).

In the presacral region, the neurocentral suture runs between the centrum and the neural arch below the rib articulation (diapophysis), but through the rib articulation in the sacrum and caudal region. The neurocentral suture commonly fuses during ontogeny, particularly in terrestrial animals, but where it remains open the pedicel of the neural arch is received on the dorsal surface of the centrum in a contact that does not exceed the transverse diameter of the centrum to a significant degree.

The neurocentral suture remains open in sauropterygians (as in many marine reptiles). As a consequence, the neural arch frequently dissociates from the centrum in pachypleurosaurs, *Simosaurus,* and *Nothosaurus* in the cervical and dorsal region of the vertebral column. This dissociation reveals, in these taxa, a broadened facet formed by the dorsal surface of the centrum to receive the pedicels of the neural arch (Figs. 16, 48–49). This facet has lateroventrally inclined lateral lappets in the cervical region but becomes fully horizontal within the dorsal region, where it exceeds the width of the body of the centrum as seen in ventral view. *Pistosaurus* shows the same apomorphic contact of the centrum and neural arch

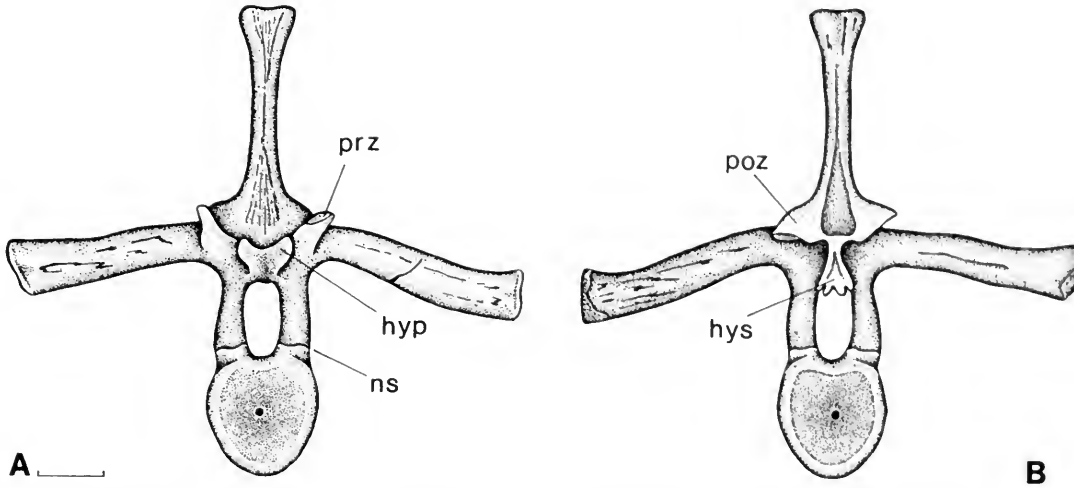

FIG. 47. Isolated dorsal vertebra of a placodont (?*Cyamodus*, SMNS 59825, upper Muschelkalk, Hegnabrunn), showing the hyposphene–hypantrum articulation. **A**, Anterior view; **B**, posterior view. Abbreviations: hyp, hypantrum; hys, hyposphene; ns, neurocentral suture; poz, postzygapophysis; prz, prezygapophysis. Scale bar = 20 mm.

in dorsal vertebrae, except that in this taxon the contact area on the centrum bears distinct sockets on either side of the neural canal for the reception of peglike projections from the neural arch (Fig. 49B). The vertebral column of *Cymatosaurus* remains unknown. Outside the Eosauropterygia, the same lateral flaring of the neural arch facets on the centrum is observed, as far as is known, in choristoderes (Sigogneau-Russell, 1981), but it is absent in *Hovasaurus* (an aquatic younginiform; Currie, 1981) and *Palaeopleurosaurus* (an aquatic rhynchocephalian; Carroll, 1985).

In *Placodus*, the neural arch separates less easily from the centrum in the cervical and dorsal vertebral column, although the neurocentral suture can still be identified. In cases where a dissociation of the elements has occurred during fossilization, the centrum can be seen to form narrow ridges on either side of the neural canal for the reception of the narrow pedicels of the neural arches. That the pedicels of the neural arch are received on ridges rather than in grooves on the centrum may be correlated with the derived shape of the neural canal in this taxon, which is unusually high and narrow. Whereas *Placodus* may not exactly represent the plesiomorphic condition with respect to this character (but could be autapomorphic), it certainly lacks the specialized contact seen in pachypleurosaurs and in the eusauropterygians included in this study.

55. Transverse processes of neural arches of the dorsal region relatively short (0) or distinctly elongated (1).

56. Cervical ribs without (0) or with (1) a distinct free anterior process.

In pachypleurosaurs, *Nothosaurus*, and *Pistosaurus* (Sues, 1987a), the anterior tip of the cervical ribs is drawn out into a free process. Such is not the case in *Simosaurus*, whose cervical ribs show a broad "shoulder" but no distinct process, but for the reasons discussed above, the absence of the anterior process might well be due to breakage. The character is coded as unknown for *Simosaurus*. A free anterior process is present on the cervical ribs of *Placodus*.

57. Dorsal ribs without (0) or with (1) pachyostosis.

Rib pachyostosis is a character sometimes difficult to establish, because it may show gradual variation and may also be subject to ontogenetic variation. Rib pachyostosis is present in *Neusticosaurus* (coded as polymorphic for the *Serpianosaurus–Neusticosaurus* clade), and it is also present in *Lariosaurus*.

58. The number of sacral ribs is two (0), three (1), or four or more (2). The character is coded as unordered.

The plesiomorphic character is two sacral ribs. Such has been reported to be the case in *Keichousaurus*, a pachypleurosaur from China (Lin Kebang, confirmed by Sues, 1987a), but in the pachypleurosaurs entered in this analysis (*Dactylosaurus*,

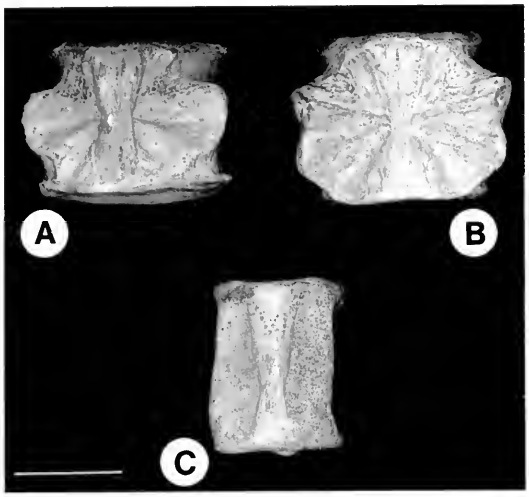

FIG. 48. **A,** Isolated dorsal centrum of *Simosaurus* (SMNS 54763, upper Muschelkalk, Crailsheim) in dorsal view; **B,** isolated dorsal centrum of *Nothosaurus* (SMNS 59820, upper Muschelkalk, Bindlach near Bayreuth) in dorsal view; **C,** isolated dorsal centrum of *Placodus* (SMNS 59826, upper Muschelkalk, Hegnabrunn) in dorsal view. Scale bar = 20 mm.

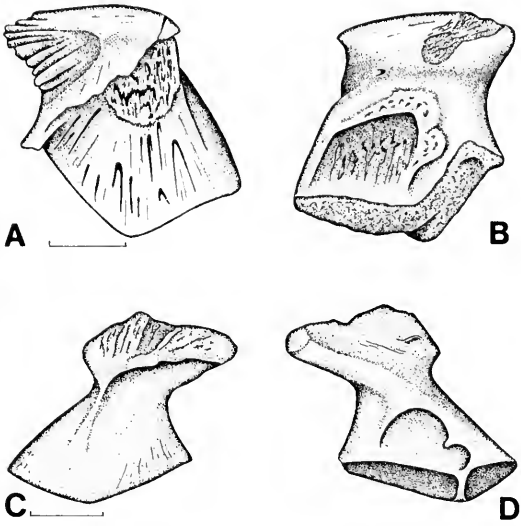

FIG. 50. **A, B,** Right ilium of *Nothosaurus* (SMNS 59821, upper Muschelkalk [Trochitenkalk], ?Bindlach near Bayreuth) in lateral (**A**) and medial (**B**) views; **C, D,** left ilium of *Placodus gigas* (SMF 1035, cast of Drevermann's [1933] specimen) in lateral (**C**) and medial (**D**) views. Scale bar = 20 mm.

Serpianosaurus–Neusticosaurus clade), three sacral ribs is the typical number. As argued above, three functional sacral ribs were present in *Simosaurus* and *Nothosaurus* (Schröder, 1914), and the same is true of *Placodus* (Drevermann, 1933), which shows the same basic morphology of the ilium (Fig. 50) as do *Simosaurus* and *Nothosaurus*. *Lariosaurus* is reported to have five sacral ribs (Peyer, 1933–1934; Tintori & Renesto, 1990). The number of sacral ribs cannot be established in SMF R-13, and it is four with the possible "sacralization" of a lumbar rib in BSP AS I 802. Revisionary work in progress will establish the number of functional sacral ribs in *Lariosaurus* (probably four in the adult; see Tintori & Renesto, 1990, Pl. 1, and BSP AS I 802) as well as any variation, but a number higher than three would be autapomorphic for *Lariosaurus* in the present analysis and hence is uninformative. The number of sacral ribs remains unknown for *Cymatosaurus* and *Pistosaurus*. Outside the Eosauropterygia and the placodonts, three sacral ribs are observed in choristoderes (Sigogneau-Russell, 1981).

59. Sacral ribs with (0) or without (1) distinct expansion of distal head.

As described above, the sacral ribs of *Simosau-*

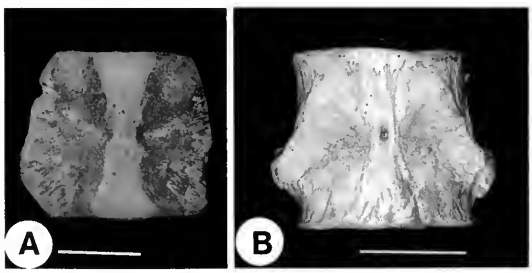

FIG. 49. **A,** Isolated dorsal centrum from an unidentified pachypleurosaur (MHI uncatalogued, lower Muschelkalk [lower Dolomites], Neidenfels) in dorsal view (scale bar = 5 mm); **B,** isolated dorsal centrum of *Pistosaurus* (MHI 1278, upper Muschelkalk, Neidenfels) in dorsal view (scale bar = 20 mm).

FIG. 51. Pelvic region in the holotype of *Nothosaurus* "*raabi*" Schröder, 1914 (MB I.007-18, lower Muschelkalk, Rüdersdorf). Scale bar = 20 mm.

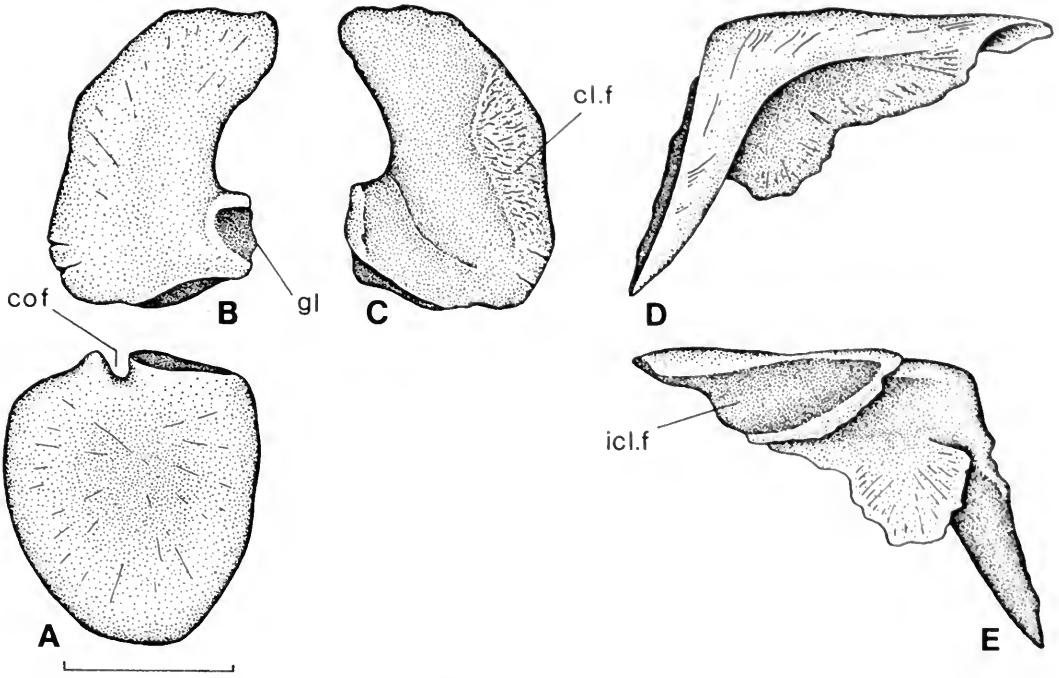

FIG. 52. Pectoral girdle of *Placodus gigas* (SMF 1035, cast of Drevermann's [1933] specimen). **A**, Left coracoid in lateral (ventral) view; **B**, left scapula in lateral view; **C**, left scapula in medial view; **D**, left clavicle in dorsal view; **E**, left clavicle in medial view. Abbreviations: cl.f, clavicular facet on medial surface of scapula; cof, coracoid foramen; gl, glenoid; icl.f, interclavicular facet on left clavicle. Scale bar = 50 mm.

rus are characterized by a distinct expansion of their distal head, and the same is true of the sacral ribs of *Placodus*, where the third functional sacral rib is again the most massive one. In pachypleurosaurs, the distal expansion of sacral ribs is not pronounced, the articular head scarcely or not at all set off from the shaft of the rib. The same is true of *Nothosaurus* (Fig. 51) and of *Lariosaurus* (Peyer, 1934–1935; Tintori & Renesto, 1990). Sacral rib morphology remains unknown for *Cymatosaurus* and *Pistosaurus*.

60. Cleithrum present (0) or absent (1).

61. Clavicles broad (0) or narrow (1) medially.

62. Clavicles positioned dorsally (0) or anteroventrally (1) to the interclavicle.

The anteroventral position of the clavicles with respect to the interclavicle was first recognized as a eosauropterygian synapomorphy by Carroll and Gaskill (1985), and it is shared by *Placodus* (Drevermann, 1933), as well as by choristoderes (Sigogneau-Russell, 1981).

63. Clavicles do not meet in front of the interclavicle (0) or meet in an interdigitating anteromedial suture (1).

In pachypleurosaurs, *Simosaurus*, *Nothosaurus*, and *Lariosaurus*, the clavicles meet in an interdigitating suture in front of the interclavicle. In *Placodus* (Fig. 52), the clavicles reach closely to the ventral midline with their tapering anteromedial tip but fail to meet each other. Drevermann's (1933) reconstruction of the dermal pectoral girdle shows the lack of an anteromedial suture between the clavicles, a conclusion supported by the rounded anteromedial tips of the interclavicles. An anteromedial suture between the two clavicles is also absent in *Corosaurus* (Storrs, 1991).

64. Clavicles without (0) or with (1) anterolaterally expanded corners.

The clavicle of *Dactylosaurus* shows an anterolateral expansion of the clavicle into a horizontal shelf of bone defining a pronounced anterolateral corner. The same character is seen in the clavicles of *Simosaurus* and *Nothosaurus* (Fig. 53). An anterolateral expansion of the clavicle is absent in the *Serpianosaurus–Neusticosaurus* clade as well as in *Placodus* (Fig. 52). The character appears to be present in *Lariosaurus* but obscured by pachyostosis of the clavicle. The character is here coded

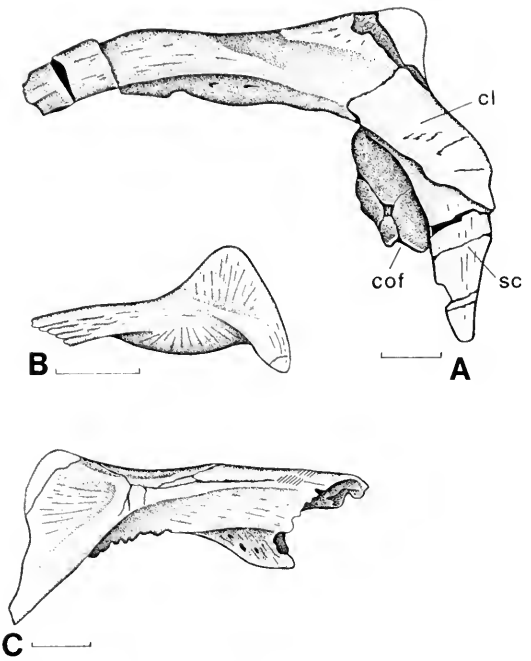

FIG. 53. The clavicle in *Nothosaurus* sp. **A,** Right clavicle and scapula (BM[NH] 38669, Lettenkeuper?, Hoheneck) in dorsal view; **B,** right clavicle (MB R.728, lower Muschelkalk, Upper Silesia) in dorsal view; **C,** left clavicle (SMNS 59822, upper Muschelkalk, Hegnabrunn) in dorsal view. Abbreviations: cl, clavicle; cof, coracoid foramen; sc, scapula. Scale bar = 20 mm.

as unknown for *Lariosaurus,* pending further revision of the genus.

65. Clavicle applied to the anterior (lateral) (0) or to the medial (1) surface of scapula.

The reverse relation of the clavicle and scapula was first recognized as a eosauropterygian synapomorphy by Carroll and Gaskill (1985), and it is shared by *Placodus* (Drevermann, 1933). However, the detailed relationship of the clavicle to the scapula differs in pachypleurosaurs, *Simosaurus, Nothosaurus, Lariosaurus,* and *Pistosaurus* (Sues, 1987a) as compared to *Placodus,* in correlation with a different morphology of the scapula. In the eosauropterygian genera, the scapula has a broad ventral (glenoid) portion that extends into a narrow and short posterodorsal process. The clavicle is applied to the anterior aspect of the dorsal process, with an extension onto the medial surface of the scapula (Fig. 54). In *Placodus,* the articulation of the clavicle is restricted to the medial side of the anterior part of the scapula, which forms a high and narrow blade (Fig. 52C).

66. Interclavicle rhomboidal (0) or T-shaped (1).

67. Posterior process on (T-shaped) interclavicle elongate (0), short (1), or rudimentary or absent (2). The character is partially correlated with character 66 (the absence of a posterior stem presupposes the presence of a T-shaped interclavicle) and is coded as unordered.

An elongated posterior stem is the plesiomorphic condition for a T-shaped interclavicle. The interclavicle of *Dactylosaurus* is not known in detail, but a much abbreviated posterior stem may be present in the *Serpianosaurus–Neusticosaurus* clade (Rieppel, 1989a, Fig. 8h). It is, however, completely absent in the vast majority of the specimens and, if present, is very rudimentary. A similarly much reduced posterior stem of the interclavicle may occur in the pachypleurosaur *Keichousaurus* (Lin Kebang, pers. comm., and CM 91.92.1). The character is coded as unknown for *Dactylosaurus* and polymorphic (2 and 3) for the *Serpianosaurus–Neusticosaurus* clade. *Simosaurus* retains a distinct yet relatively short posterior stem of the interclavicle. Huene (1952, Fig. 62) figured a large interclavicle with a long posterior stem from the Grenzbonebed of the upper Muschelkalk separating the Muschelkalk from the Keuper, but whether or not this element is to be referred to *Simosaurus* remains questionable. Mention may be made at this junction of an isolated interclavicle (Figs. 55A–B) of distinctly larger size than seems otherwise typical for *Simosaurus,* retaining the base of a distinct posterior process. Because the taxonomic status of these elements remains unclear at the present time, *Simosaurus* is coded for a short posterior stem of the interclavicle (1) as documented by the articulated skeleton (SMNS 14733; Huene, 1952). *Nothosaurus* was described as having no posterior stem on the interclavicle by Koken (1893), and the same is true for an as yet undescribed specimen of *Nothosaurus* from the upper Muschelkalk (Fig. 55C). There are, however, two isolated interclavicles with pointed posterior tips, one of which (Fig. 55D) is associated with parts of the clavicles that establish a broad anteromedial contact. The other (Fig. 56) retains a facet on its anterior margin indicating an anteromedial contact of the clavicles. On this basis, these elements are referred to *Nothosaurus,* and the genus accordingly coded for a rudimentary or absent posterior stem (2 and 3).

Placodus (Drevermann, 1933) retains a short but distinct posterior stem on the interclavicle. The interclavicle of *Cymatosaurus* and *Pistosaurus* remains unknown.

68. Scapula broad (0) or narrow (1) above glenoid.

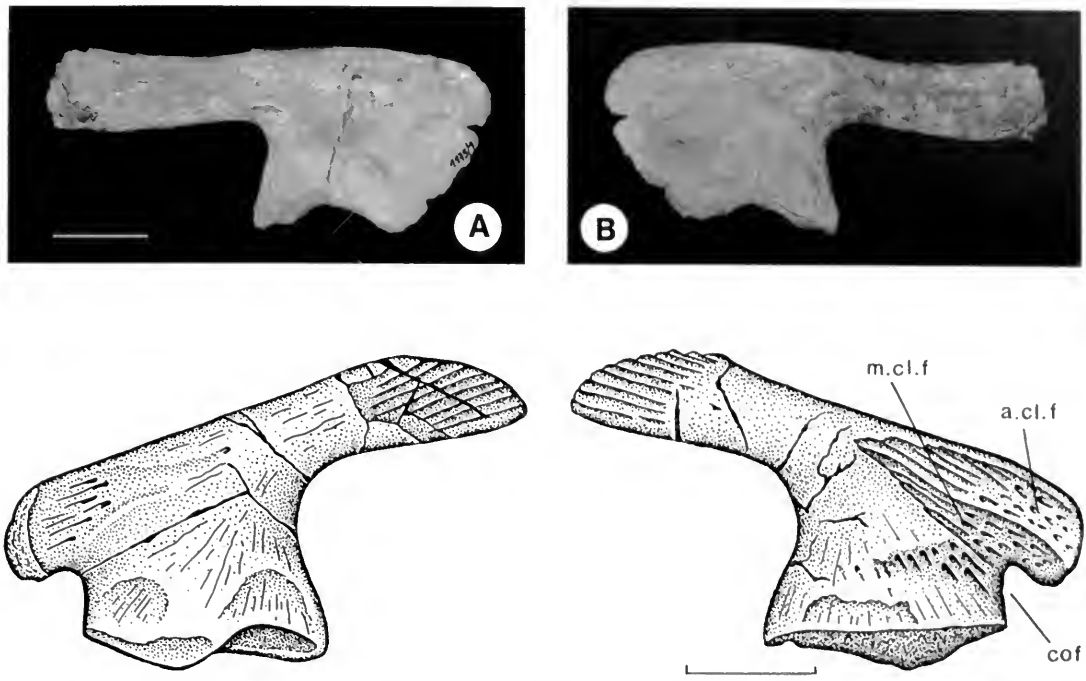

FIG. 54. Scapula of *Nothosaurus*. **A, B,** Right scapula (MHI 1175/1, upper Muschelkalk [Discoceratitenschichten], Wittighausen) in lateral (**A**) and medial (**B**) views; **C, D,** left scapula (MHI 1277, upper Muschelkalk [*Dorsoplanus* biozone], Gottwollshausen) in lateral (**C**) and medial (**D**) views. Abbreviations: a.cl.f, anterior clavicular facet on left scapula; cof, coracoid foramen; m.cl.f., medial clavicular facet on left scapula. Scale bar = 20 mm.

69. Supraglenoid buttress present (0) or absent (1).

70. One (0) or two (1) coracoid ossifications.

71. Coracoid foramen enclosed by coracoid ossification (0) or between coracoid and scapula (1).

In the plesiomorphic condition, the coracoid foramen is enclosed within the coracoid ossification (Romer, 1956; between coracoid and scapula in *Proganochelys*, Gaffney, 1990). In the Eosauropterygia, as well as in *Placodus*, the coracoid foramen is represented by a notch in the coracoid, closed by the adjacent notch in the scapula. The coracoid foramen is present in *Dactylosaurus* (and *Keichousaurus*; pers. obs.).

72. Pectoral fenestration absent (0) or present (1).

Storrs (1991) defined the pectoral fenestration as a synapomorphy of the Sauropterygia. The pectoral fenestra is the open space located between the dermal pectoral girdle anteriorly and the coracoids posteriorly. In all sauropterygians, the coracoids meet in the ventral midline, except for *Placodus* (Drevermann, 1933). Storrs (1991) concluded that this must be due to an autapomorphic reduction of the coracoid plates in *Placodus*, and his practice to code presence of the pectoral fenestration in the latter genus is followed in this study.

73. Limbs short and stout (0) or long and slender (1).

74. Humerus rather straight (0) or angulated ("curved") (1).

The "curved humerus" has long been cited as a "nothosaurian" character. The sauropterygian humerus appears "curved" in adult individuals due to a distinct angulation along its anterior margin (related to the deltopectoral crest on its ventral surface) and an evenly concave posterior margin. Curvature of the humerus is one of the characters used to support Storrs's (1991, 1993a) hypothesis that the Placodontia is the sister-group to the Eusauropterygia.

An angulated humerus is characteristic of adult *Dactylosaurus* (sex y; Rieppel, 1993b, Fig. 8) and adult representatives of the *Serpianosaurus–Neusticosaurus* clade (sex y; Carroll & Gaskill, 1985; Rieppel, 1989a; Sander, 1989), as well as of *Simosaurus, Nothosaurus, Lariosaurus,* and *Placodus*. The humerus of *Pistosaurus* is weakly angulated (Sues, 1987a), whereas that of *Cymatosaurus* (SMNS 58463) is not angulated (Fig. 57). A com-

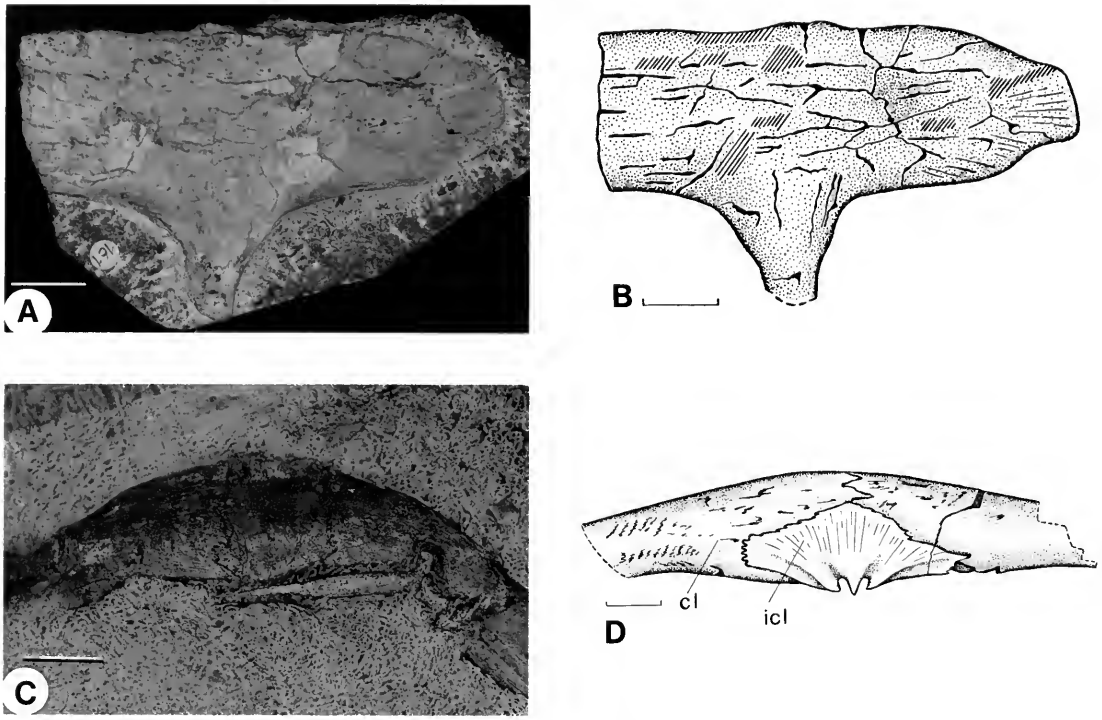

FIG. 55. **A, B,** Isolated interclavicle, probably of *Simosaurus* (SMNS 59823, upper Muschelkalk [*spinosus* biozone], Hegnabrunn); **C,** anterior dermal pectoral girdle of *Nothosaurus* (SMNS 56618, upper Muschelkalk [upper *nodosus* biozone], Berlichingen) showing the absence of a posterior stem on the interclavicle; **D,** fragment of the dermal pectoral girdle of an unidentified sauropterygian (MB R.328, upper Muschelkalk, Bayreuth) in dorsal view. Abbreviations: cl, clavicle; icl, interclavicle. Scale bar = 20 mm.

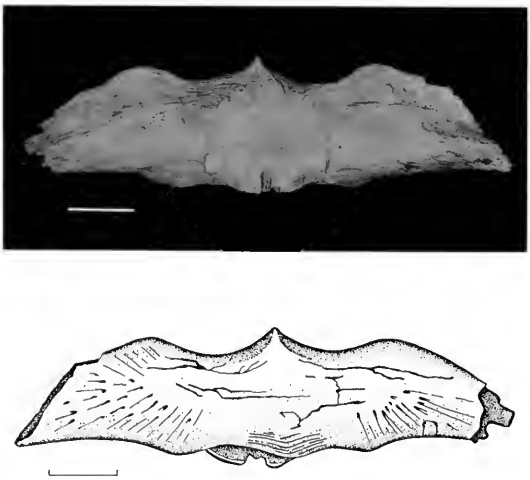

FIG. 56. Isolated interclavicle of an unidentified sauropterygian, probably *Placodus* (SMNS 59824, upper Muschelkalk [*robustus* biozone], Bindlach near Bayreuth). Anterior is at the bottom. Scale bar = 20 mm.

parison of humeri of *Dactylosaurus, Neusticosaurus,* and *Nothosaurus* (Fig. 58) shows very close similarities in the general shape of the bone, which indicates that humerus angulation ("curvature") is not a character restricted to the placodonts and Eusauropterygia.

The "curved" humerus is interdependent with the general tendency, within the Sauropterygia, to have a forelimb that is of a more robust construction than the hindlimb. Storrs (1991, 1993a) coded this character separately, although "forelimb more robust than hindlimb" is a trait difficult to define, because of both gradual variation between taxa and ontogenetic variation within taxa. The character cannot be expressed as a simple length relation of humerus/femur. Whereas the humerus shows, in general, strongly positive allometric growth within the Sauropterygia (with a relatively small humerus in juveniles), the genus *Anarosaurus* (not included in this study) shows an exceptionally long femur (see Rieppel, 1993b, for comparative data), which still is much more slender than the humerus; in *Lariosaurus* SMF R-13, the

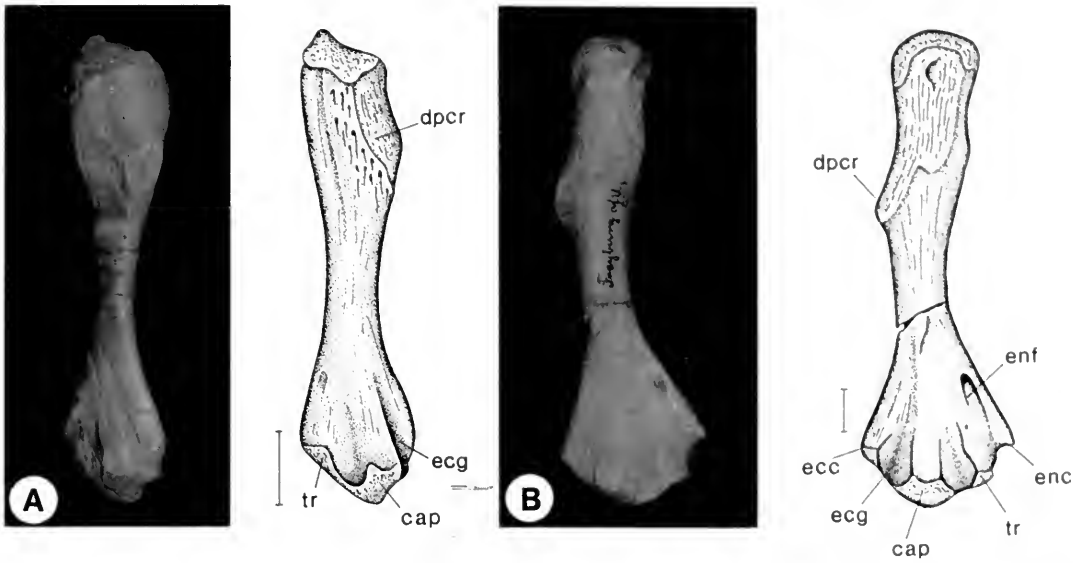

FIG. 57. Humerus of *Cymatosaurus* sp. **A,** SMNS 58463, lower Muschelkalk, Winterswijk; **B,** Martin-Luther University Halle, uncatalogued, lower Muschelkalk (Schaumkalk), Freyburg/Unstrut. Abbreviations: cap, capitellum; dpcr, deltopectoral crest; ecc, ectepicondyle; ecg, ectepicondylar groove; enc, entepicondyle; enf, entepicondylar foramen; tr, trochlea. Scale bar = 10 mm.

femur again is distinctly longer but less robust than the humerus. The other extreme is provided by genera such as *Ceresiosaurus* (Peyer, 1931a) with a forelimb that, in the adult at least, is much more robust than the hindlimb. The zeugopodial elements of the forelimb are longer than the same elements of the hindlimb in *Simosaurus* (this relation is variable in the *Serpianosaurus–Neusticosaurus* clade; tibia and fibula are unknown in *Dactylosaurus*), but such is not also the case in *Nothosaurus* (MB I.007.18, *N. "raabi"* of Schröder, 1914). If any zeugopodial element is distinctly enlarged, it is the ulna (accounted for by character 87), but in *Lariosaurus* (SMF R-13) the tibia is longer yet not as broad as the ulna (the fibula is incompletely exposed in this specimen). If the numbers of carpal and tarsal ossifications differ in sauropterygians, the larger number is always found in the carpus, but this relation is also true of non-sauropterygians with a hindlimb much more strongly developed than the forelimb. If hyperphalangy occurs in sauropterygians (*Keichousaurus, Lariosaurus, Ceresiosaurus*), it occurs in the manus, but, among the taxa considered in this analysis, hyperphalangy of the manus is an autapomorphy of *Lariosaurus* and hence uninformative. For the reasons detailed above, neither the increased robustness of the forelimbs nor the relative length of the hindlimb will be coded as a separate character in this analysis (Storrs, 1991, 1993a).

75. Humerus with prominent (0) or reduced (1) epicondyles.

The entepicondyle and ectepicondyle of the humerus are generally reduced in the Eosauropterygia and in *Placodus*. Within that group, the epicondyles are, however, comparatively well developed in *Dactylosaurus* (adult sex y; Rieppel, 1993b) and in *Cymatosaurus*.

76. The ectepicondylar groove is open and notched anteriorly (0), open without anterior notch (1), or closed (2) (i.e., ectepicondylar foramen present). The character is coded as unordered.

The plesiomorphic character is an ectepicondylar groove that sets off the ectepicondyle from the humeral shaft, thereby creating a more or less distinct notch at the distal end of the humerus. The plesiomorphic condition is well exemplified by an isolated humerus from the lowermost Muschelkalk (lower Gogolin beds) of Gogolin (Poland) described by Huene (1944) (Fig. 58A). The ectepicondylar notch is distinct in eosauropterygians with a distinct ectepicondyle (in *Dactylosaurus*, occasionally in the *Serpianosaurus–Neusticosaurus* clade [adult sex y], and in *Cymatosaurus*), but it is absent in the humeri of *Simosaurus* and *Pistosaurus*. An ectepicondylar notch is occasionally present in small humeri of *Nothosaurus* (BM[NH]

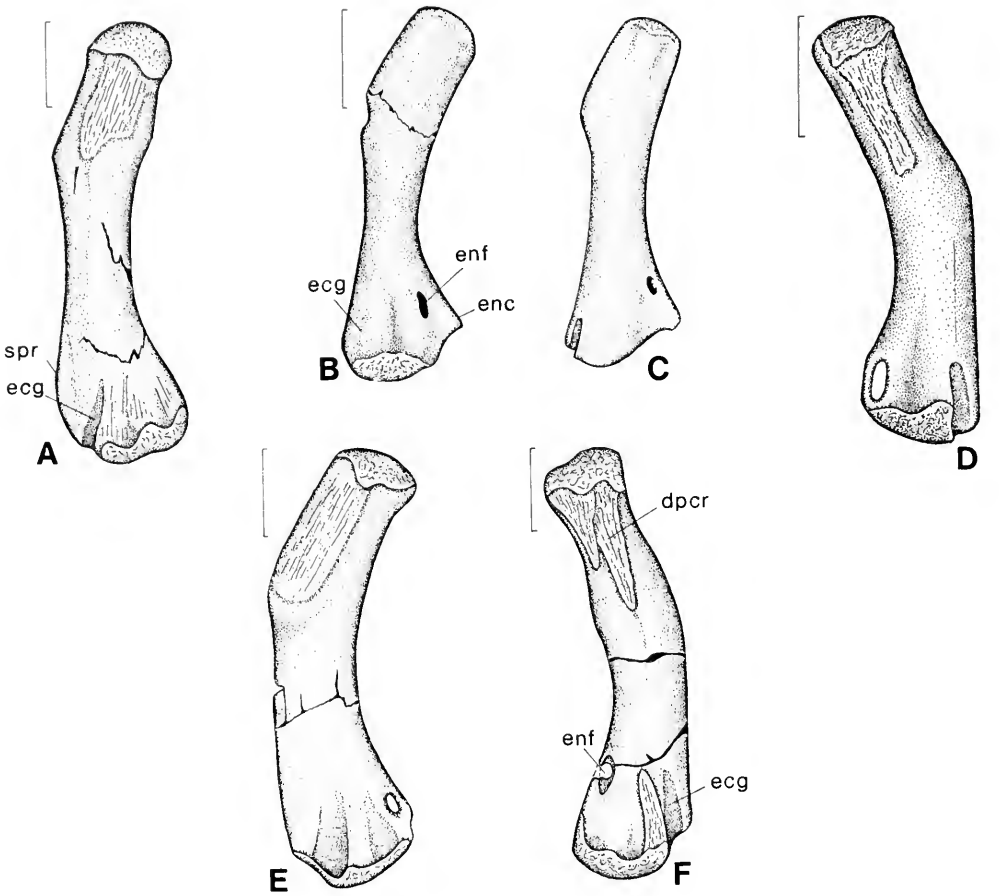

FIG. 58. Humeri of Sauropterygia. **A,** Unidentified sauropterygian (SMNS 16253, lower Muschelkalk, Gogolin [Poland]; original of Huene, 1944); **B,** *Dactylosaurus schroederi* (SMF R-4097a, lower Muschelkalk, Kamien Gorny Slaski [Poland], drawing of cast), right humerus in ventral view; **C,** *Dactylosaurus schroederi* (SMF R-4097a, lower Muschelkalk, Kamien Gorny Slaski [Poland], drawing of cast), left humerus in dorsal view; **D,** *Nothosaurus* "*raabi*" (holotype, MB I.007-18, lower Muschelkalk, Rüdersdorf); **E,** *Nothosaurus* sp. (Martin-Luther University Halle, uncatalogued, lower Muschelkalk, Halle); **F,** *Nothosaurus* sp. (BM[NH] 40052, Muschelkalk, Nürnberg; original of Lydekker, 1889, Pt. II, Fig. 84). Abbreviations: dpcr, deltopectoral crest; ecg, ectepicondylar groove; enc, entepicondyle; enf, entepicondylar foramen; spr, supinator ridge. Scale bar = 5 mm in B and C, 20 mm in A, D, E, and F.

R-40052; Lydekker, 1889, p. 296, Fig. 84) but absent in larger specimens (Fig. 59B). It is unknown whether this reflects ontogenetic or taxonomic variation, or both.

Placodus presents a particular problem because the distal end of the humerus described by Drevermann (1933) as showing an ectepicondylar foramen is, in fact, an incomplete humerus of *Nothosaurus*. The humerus of *Placodus* lacks an ectepicondylar foramen, but it shows a distinct ectepicondylar notch (Figs. 59A, 60).

77. Entepicondylar foramen present (0) or absent (1).

An entepicondylar foramen is generally present in the pachypleurosaurs, the plesiomorphic condition. As described above, the entepicondylar foramen is absent in *Simosaurus,* as well as in *Pistosaurus* (Sues, 1987a), but the foramen is present in *Nothosaurus* and *Cymatosaurus.* Disregarding the nothosaur humerus attributed to *Placodus* by Drevermann (1933), the entepicondylar foramen is also absent in *Placodus.*

78. Radius shorter than ulna (0), or longer than ulna (1), or approximately of the same length (2). The character is coded as unordered.

With an ossified olecranon, the ulna is usually longer than the radius, the plesiomorphic condition. In sauropterygians, the olecranon does not ossify, which reduces the relative length of the (ossified) ulna. Equal length of radius and ulna is

FIG. 59. **A,** Humerus of *Placodus gigas* (SMNS 59827, upper Muschelkalk [*spinosus–nodosus* biozone], Hegnabrunn), **B,** humerus of *Nothosaurus* sp. (SMNS 16250b, upper Muschelkalk, Bindlach near Bayreuth).

one of the characters supporting Storrs's (1991, 1993a) conclusion that the Placodontia is the sister-group of the Eusauropterygia (Rieppel, 1993a).

The radius is longer than the ulna in *Dactylosaurus* (the radius/ulna ratio is 1.14 in Nopcsa's [1928] specimen), a condition that is also found in *Neusticosaurus* (Carroll & Gaskill, 1985, Table 3; Sander, 1989, Table 4). In *Serpianosaurus,* the radius is only slightly longer than the ulna, or the two bones are equal in length. In *Simosaurus,* the radius and ulna are equal in length. In *Nothosaurus* (MB I.007.18, *N.* "*raabi*" of Schröder, 1914), the radius/ulna ratio is 1.02, that is, practically equal in length, as they also are in *Pistosaurus* (Sues, 1987a). Radius and ulna are incompletely preserved in the skeleton of *Placodus* described by Drevermann (1933), but the two bones are very similar in length in *Paraplacodus* (Peyer, 1935).

In Sauropterygia with an unossified olecranon, the proximal head of the ulna is generally expanded, although to a variable degree. Within pachypleurosaurs, the proximal head of the ulna is not distinctly broadened except for *Keichousaurus,* in which the entire ulna is greatly broadened (Young, 1958, and pers. obs.). The ulna of *Kei-*

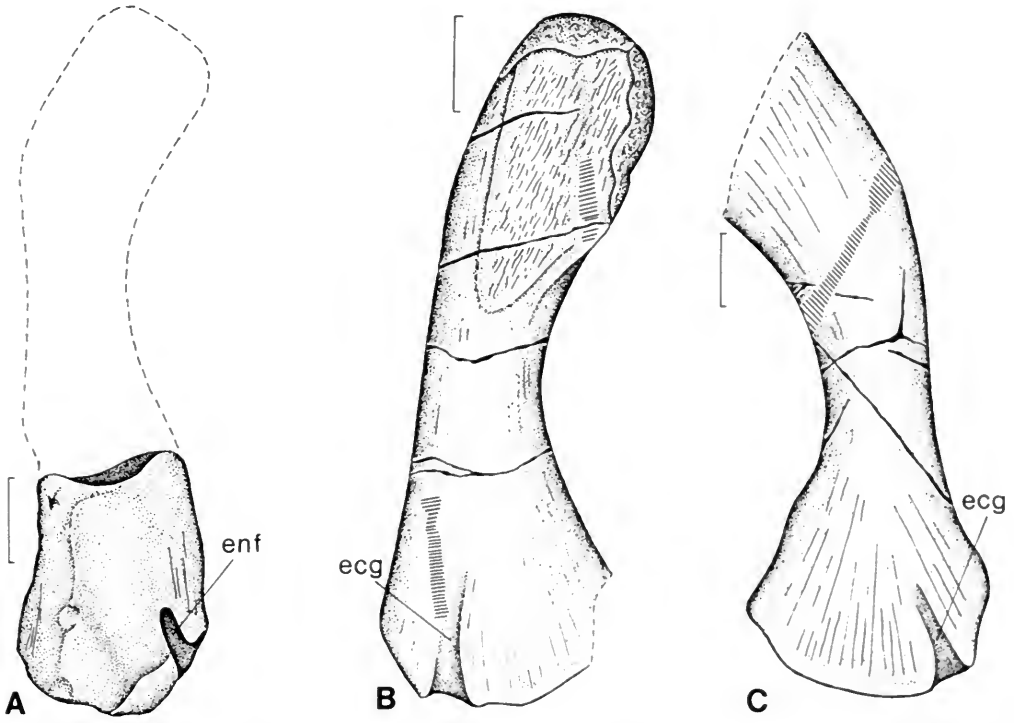

FIG. 60. **A,** Distal end of the humerus of *Nothosaurus* sp., attributed to *Placodus* by Drevermann (1933; SMF 1035); **B,** humerus of *Placodus gigas* (SMNS 59827, upper Muschelkalk [*spinosus–nodosus* biozone], Hegnabrunn); **C,** humerus of *Placodus* (MHI 776, upper Muschelkalk [Discoceratitenschichten] Grombach). Abbreviations: ecg, ectepicondylar groove; enf, entepicondylar foramen. Scale bar = 20 mm.

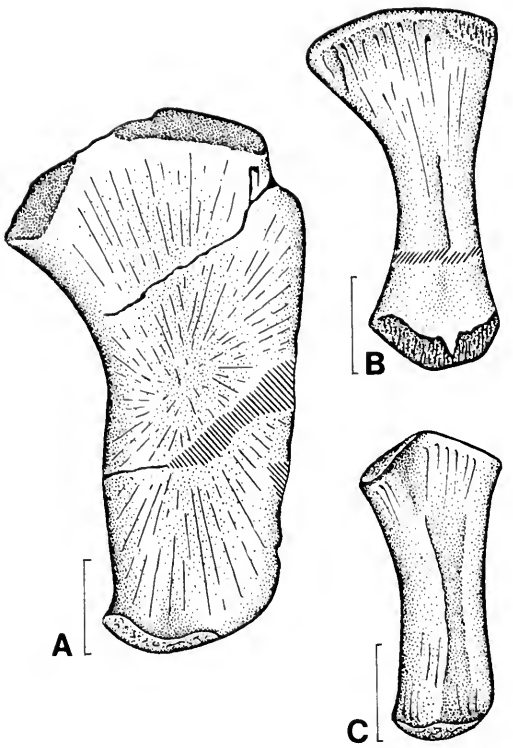

FIG. 61. Isolated ulnae of unidentified sauropterygians (referred to *Nothosaurus* sp. in the SMNS collections). **A,** SMNS 7175, upper Lettenkeuper, Hoheneck; **B,** SMNS 1892, Lettenkeuper, Hoheneck; **C,** SMNS 56686, upper Muschelkalk, Sommerhausen near Würzburg. Scale bar = 20 mm.

chousaurus is, in fact, very reminiscent of the ulna in *Lariosaurus*; however, the shape of the ulna varies quite extensively among the specimens currently referred to *Lariosaurus,* which is the reason why Peyer (1933–1934) chose to diagnose *Lariosaurus* by a much expanded proximal head of the ulna (among other characters). His character definition is accepted here. For the specimens currently referred to *Lariosaurus,* the ratio of the ulna length/proximal width ranges from 1.4 to 2.1, with SMF R-13 showing a ratio of 1.65. In *Simosaurus* SMNS 14733, the ratio is 2.89; for *Nothosaurus* (MB I.007.18, *N.* "*raabi*" of Schröder, 1914), the ratio is 2.23. Based on Sues (1987a, Fig. 4A), the ratio is 2.4 in *Pistosaurus.* For *Placodus,* the ratio is unknown, but the preserved proximal part of the ulna does not appear strongly expanded either. A number of isolated ulnae have been referred to *Nothosaurus* (SMNS 7175, SMNS 1892, SMNS 5668) that document a certain variability of shape of that element (Fig. 61), but one specimen (SMNS 7175) seems much broader than would be expected in *Nothosaurus* and shows a ratio of ulna length/proximal width of 1.82. However, this particular element may well be referable to *Ceresiosaurus* (rather than *Nothosaurus*), a genus currently viewed as sister-taxon of *Lariosaurus* (Tschanz, 1989; Storrs, 1993a). With the terminal taxa used in this study, the widening of the ulna in *Keichousaurus* and in *Lariosaurus* has no resolving power, and the character is not entered into the data matrix.

79. Iliac blade well developed (0), reduced (1), or absent (2).

The plesiomorphic condition is a well-developed iliac blade ascending in a posterodorsal direction and carrying an anterior spina praeacetabuli (Siebenrock, 1894). The posterior extent of the iliac blade relative to the posterior margin of the ischium is variable and depends not only on the relative size of the iliac blade but also on its orientation (horizontal or slanting in a posterodorsal direction). *Placodus* and the Eusauropterygia included in this study (the ilium is incomplete, but the iliac blade appears elongate and not reduced in *Pistosaurus* [Sues, 1987a] and unknown in *Cymatosaurus*) share a similar morphology of the ilium characterized by an iliac blade of reduced size, which retains a spina praeacetabuli. Pachypleurosaurs, however, have effectively lost the iliac blade; the ilium retains only a narrow process extending upward from the broadened acetabular portion. There is no indication of an iliac blade in *Lariosaurus,* which again retains a narrow dorsal process of the ilium only.

80. Pubis without (0) or with (1) distinctly notched (concave) ventral (medial) margin.

Simosaurus and *Nothosaurus* show a notch or concavity in the ventral (medial) margin of the pubis. This contrasts with the evenly convex ventral (medial) margin of the pubis in pachypleurosaurs. A concavity is also absent on the ventral (medial) margin of the pubis in *Placodus* (due to reduction of the pubis?). The character is here treated as presently unknown for *Lariosaurus.* The same is true for the pubis of *Cymatosaurus* and *Pistosaurus.*

81. Thyroid fenestra absent (0) or present (1).

In the plesiomorphic condition, pubis and ischium form a closed plate. In the derived condition, a large fenestra thyroidea develops between pubis and ischium, which is present in pachypleurosaurs, *Simosaurus,* and *Nothosaurus.* Due to the incomplete knowledge of the ventral elements of the pelvic girdle in *Pistosaurus* (Sues, 1987a), the character is coded as unknown for that genus. The

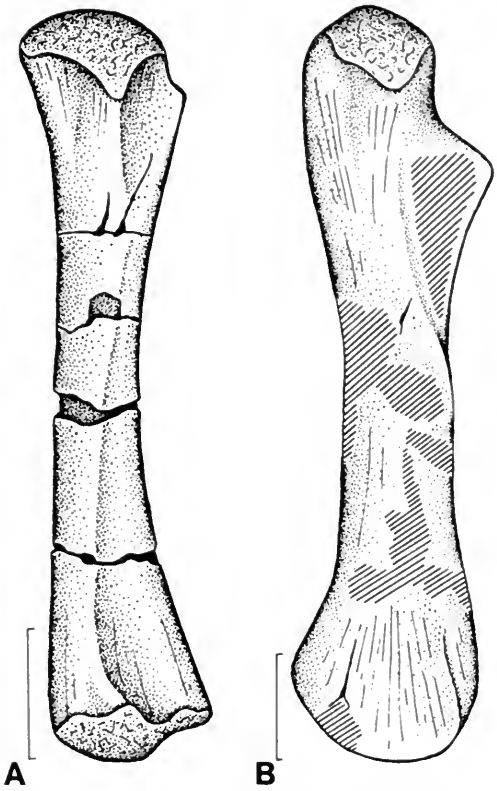

FIG. 62. **A,** Femur of *Nothosaurus* sp. (BM[NH] 40053, Muschelkalk, Nürnberg); **B,** femur of *Placodus gigas* (SMNS uncatalogued, coll. M. Wild #1798, upper Muschelkalk, Bindlach near Bayreuth). Scale bar = 20 mm.

same is true for *Cymatosaurus*. A small fenestra, closed ventrally (medially) by a contact of the pubis with the ischium, is present in *Placodus*, and a convincing argument has been made that this represents a reduced thyroid fenestra (Sues, 1987b; Storrs, 1991).

82. Acetabulum oval (0) or circular (1).

83. Femoral shaft stout and straight (0) or slender and sigmoidally curved (1).

In the Sauropterygia, the femur is generally slender and may either be straight or show some slight sigmoidal curvature. A slender and more or less straight femur is coded 1.

84. Intertrochanteric fossa well defined (0) or reduced (1), or rudimentary or absent (2).

A well-developed trochanter separated from the shaft of the femur by a well-developed intertrochanteric fossa is the plesiomorphic condition. A reduced intertrochanteric fossa is retained in *Placodus* (Fig. 62), where the trochanter is well set off from the shaft of the femur. In pachypleurosaurs,

FIG. 63. Proximal head of the femur. **A,** *Simosaurus gaillardoti* (SMNS 14733, #81 of Huene, 1952); **B,** *Nothosaurus* sp. (SMNS 59829, upper Muschelkalk, Bindlach near Bayreuth); **C,** *Cyamodus* (SMNS 59828, upper Muschelkalk, Hegnabrunn). Scale bar = 20 mm.

Simosaurus, Nothosaurus, and *Pistosaurus* (Sues, 1987a), the trochanter is represented by a more or less distinct thickening on the ventral surface of the proximal end of the femur, which results in a triangular cross-section of the bone at that level. The intertrochanteric fossa is rudimentary or absent (Fig. 63). The femur of *Cymatosaurus* is unknown. A well-developed trochanter is present in *Corosaurus,* separated from the shaft by a distinct intertrochanteric fossa (Storrs, 1991).

85. Distal femoral condyles prominent (0) or not projecting markedly beyond shaft (1).

86. Anterior femoral condyle relative to posterior condyle larger and extending further distally (0) or smaller and of subequal extent distally (1).

87. The perforating artery passes between astragalus and calcaneum (0) or between the distal heads of tibia and fibula proximal to the astragalus (1).

This character is discussed in detail by Rieppel (1993c). The plesiomorphic condition (for this level of analysis) is represented by a tarsus in which the astragalus and calcaneum meet in a suture that is pierced by a foramen though which passes the perforating artery. In turtles and lepidosauriforms, the perforating artery passes proximal to the astragalus and calcaneum (which may fuse during ontogeny) through the spatium interosseum between the distal ends of the tibia and fibula. In the Sauropterygia, secondarily aquatic habits have resulted in skeletal reductions, the astragalus and calcaneum commonly appearing as separate rounded ossifications in the proximal tarsus. The position of the astragalus at the distal end of the spatium interosseum, together with the marked

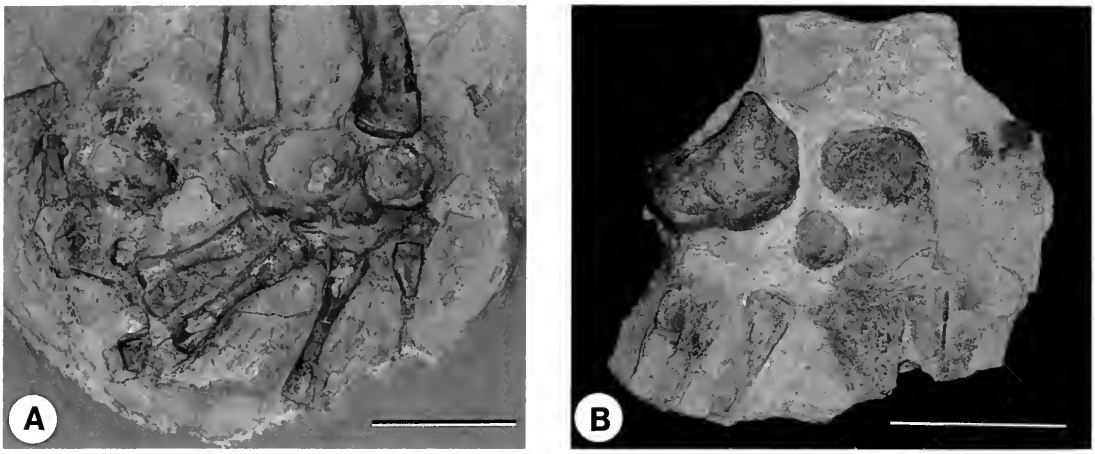

FIG. 64. Tarsus of *Nothosaurus* "*raabi*" Schröder, 1914. **A**, Holotype (MB I.007-18, lower Muschelkalk, Rüdersdorf); **B**, SMF R-4546, lower Muschelkalk, Oberdorla, Thüringen.

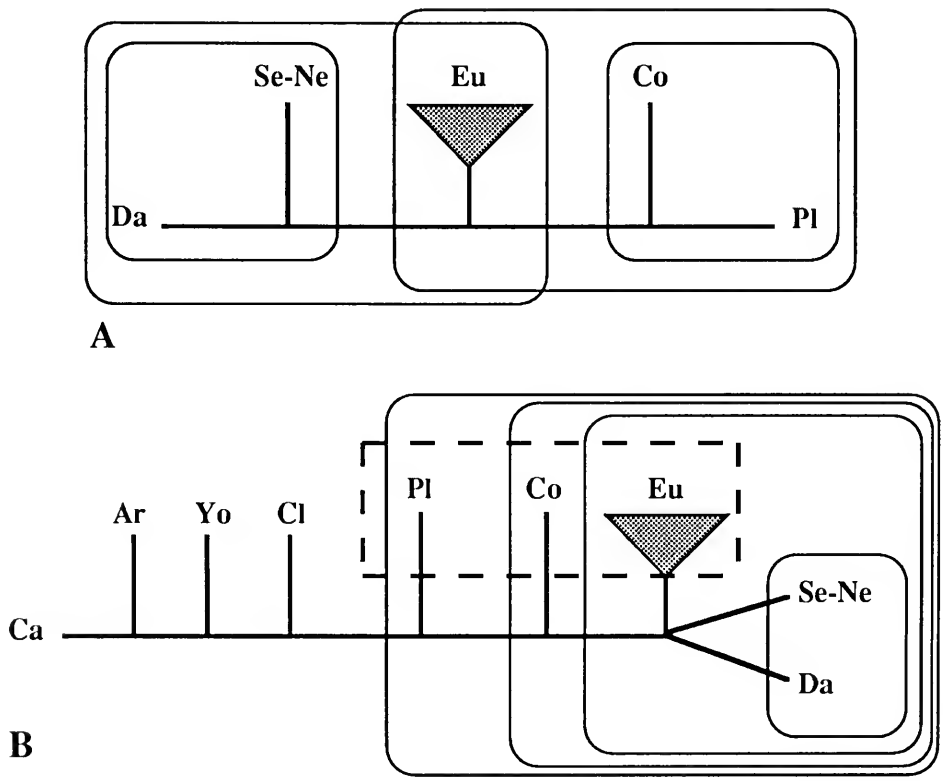

FIG. 65. **A**, Strict consensus tree of nine equally parsimonious unrooted networks (TL = 85, CI = 0.694, RC = 0.421) for ingroup taxa only; **B**, strict consensus tree of six equally parsimonious unrooted networks (TL = 167, CI = 0.707, RC = 0.535) for ingroup taxa plus the four taxa used as outgroups by Storrs (1991, 1993a). Abbreviations: Ar, Araeoscelidia; Ca, Captorhinidae; Cl, *Claudiosaurus*; Co, *Corosaurus*; Da, *Dactylosaurus*; Eu, Eusauropterygia; Pl, *Placodus*; Se-Ne, *Serpianosaurus–Neusticosaurus* clade. The Nothosauriformes are circled with a dashed line. For further discussion, see text.

TABLE 8. Data matrix for the taxa included in the cladistic analysis. For discussions on changing character codings, see text.

	1	1	2	3	4	5	6	7	8	9	10
1	Ancestor	0	0	0	0	0	0	0	0	0	0
2	Captorhinidae	0	0	0	0	0	0	0	0	0	0
3	Testudines	0	0	0	0	0	0	1	0&1	0&2	0
4	Araeoscelidia	0	0	0	0	0	0	0	0	1	1
5	Younginiformes	0	0	0	0	0	0	1	0	1	1
6	Kuehneosauridae	0	0	0	0	0	0	1	0	0	1
7	Rhynchocephalia	0	0	0	0	0	0	1&2	0	0	1
8	Squamata	0	0	0	0	0	0	1&2	0&1	0&1&2	1
9	Rhynchosauria	1	1	0	0	0	0	1	0	0	1
10	Prolacertiformes	1	1	0	1	0	0	1	0	1	1
11	Trilophosaurus	1	2	0	0	0	0	?	1	1	1
12	Choristodera	1	1	0	1	0	0	1	0	2	1
13	Archosauriformes	1	1	0	1	0	0	1	0	0&1	1
14	Claudiosaurus	0	0	0	0	0	0	1	0	1	1
15	Dactylosaurus	1	0	0	0	0	0	2	0	1	2
16	Serpiano-Neustico	1	0	0	0	0	0&1	2	0	1	2
17	Simosaurus	1	0	0	0	0	1	2	0	2	1
18	Nothosaurus	1	0	1	0	0	0&1	2	0	2	1
19	Lariosaurus	1	0	1	0	0	?	2	0	2	1
20	Corosaurus	1	0	0	0	0	0	2	0	2	1
21	Cymatosaurus	1	0	1	0	1	1	2	1	2	1
22	Pistosaurus	1	0	0	0	1	1	2	0	1	1
23	Placodus	1	0	1	1	0	0	2	1	2	1
24	Pareiasauria	0	0	0	0	0	0	0	1	0	0
25	Procolophonidae	0	0	0	0	1	0	1	0	0	0
26	Palaeagama	0	?	0	0	0	0	?	0	1	1
27	Paliguana	0	?	0	0	0	0	?	0	1	1
28	Saurosternon	?	?	?	?	?	?	?	?	?	?
29	Coelurosauravus	1	0	0	1	0	0	?	?	0	1

concavity on its proximal margin (Fig. 64; see also Romer, 1956, Fig. 189D, for the tarsus of *Lariosaurus*), is here taken as evidence that the perforating artery passed proximal to the astragalus between the distal heads of tibia and fibula (on the same basis, a proximal course of the perforating artery is assumed for rhynchosaurs; Chatterjee, 1974).

88. Calcaneal tuber absent (0) or present (1).

89. Foot short and broad (0) or long and slender (1).

90. Distal tarsal 1 present (0) or absent (1).

91. Distal tarsal 5 present (0) or absent (1).

92. Total number of tarsal ossifications four or more (0), three (1), or two (2). The character is coded as unordered.

As far as is known at this time, the maximum number of tarsal ossifications recorded in pachypleurosaurs and the Eusauropterygia is four (*Lariosaurus* SMF R-13, with distal tarsals 4 and 3 ossified in the left pes; whether *Simosaurus* also retained four tarsal ossifications is questionable). Three tarsal ossifications (astragalus, calcaneum, and distal tarsal 4) are present in *Nothosaurus* (MB I.997.18; *N.* "*raabi*" of Schröder, 1914), and *Simosaurus* may have shared the same number. The tarsal ossifications of *Dactylosaurus* are unknown. In the *Serpianosaurus–Neusticosaurus* clade, the number of tarsal ossifications drops to two (astragalus and calcaneum), and two tarsal ossifications are thought to be present in *Placodus* (Drevermann, 1933; the same number of tarsal

TABLE 8. Data matrix for the taxa included in the cladistic analysis (*continued*).

	2	11	12	13	14	15	16	17	18	19	20
1	Ancestor	0	0	0	0	0	0	0	0	0	0
2	Captorhinidae	0	0	?	0	0&2	0	0	1	0	0
3	Testudines	0	0	?	0	3	0	1	1	0&1	0
4	Araeoscelidia	0	1	0	0	0	0	0	0	0	0
5	Younginiformes	0	1	0	0	0	0	0	0&1	0	0
6	Kuehneosauridae	0	1	0	0	2	0	1	1	1	0
7	Rhynchocephalia	0&1	0&1	0	0&1	0&2	0&1	1	1	0&1	0&1
8	Squamata	0&1	0	0	0&1	0&2&3	0&1	1	1	0&1	0&1
9	Rhynchosauria	0	0	0	1	3	2	1	1	1	0
10	Prolacertiformes	0	0&1	0	0&1	2&3	0	1	1	0&1	0
11	Trilophosaurus	0	0	1	0	3	2	1	1	?	0
12	Choristodera	0	0	0	0	3	1	1	1	1	0
13	Archosauriformes	0&1	0&1	0&1	0&1	0&3	0&1	1	1	0&1	0
14	Claudiosaurus	0	1	0	0	0	0	1	1	1	0
15	Dactylosaurus	0	1	0	0	0	0	1	1	1	?
16	Serpiano-Neustico	0	1	0	0	0	0	1	1	1	0
17	Simosaurus	1	0	0	1	1	1	1	1	1	0
18	Nothosaurus	1	1	0	1	1	1&2	1	1	1	1&2
19	Lariosaurus	1	1	0	1	1	1	1	1	1	?
20	Corosaurus	0	1	0	0	0	1	1	1	1	2
21	Cymatosaurus	0	1	0&1	1	0	0&1	1	1	1	1
22	Pistosaurus	1	1	1	1	2	2	1	1	1	0
23	Placodus	0	1	0	0	2	0	1	1	1	0
24	Pareiasauria	0	0	?	1	2	0	0	1	0	0
25	Procolophonidae	0	1	?	0	2	0	1	1	0	0
26	Palaeagama	0	0	0	0	0	0	1	1	0	0
27	Paliguana	0	0	0	0	0	0	0	0	?	0
28	Saurosternon	?	?	?	?	?	?	?	?	?	?
29	Coelurosauravus	0	0	0	0	?	0	1	1	0	1

ossifications has been reported for *Paraplacodus*, Kuhn-Schnyder, 1942).

93. Metatarsal 5 long and slender (0) or distinctly shorter than the other metatarsals and with a broad base (1).

94. Metatarsal 5 straight (0) or "hooked" (1).

The data discussed above (characters 1 through 94) as coded in the data matrix (Table 8) were analyzed using the software package PAUP version 3.1.1, developed by David L. Swofford (Swofford, 1990; Swofford & Begle, 1993). The principal goal of the present analysis is the test of two alternative hypotheses of sauropterygian interrelationships, that is, the monophyly of the Nothosauriformes (Storrs, 1991, 1993a; nesting placodonts within the Sauropterygia) versus the monophyly of the "Euryapsida" (Rieppel, 1989a; Zanon, 1989; grouping placodonts as sister-taxon of the Eosauropterygia). The test will be based on local (ingroup without or with an all-zero ancestor) and global (ingroup plus multiple outgroups) parsimony.

In a first step, an unrooted network was constructed for the ingroup only, which is here considered to comprise the taxa *Corosaurus, Cymatosaurus, Dactylosaurus, Lariosaurus, Nothosaurus, Pistosaurus, Serpianosaurus–Neusticosaurus, Simosaurus,* and *Placodus.* Deleting all other taxa from the analysis causes a number of characters to become constant and/or uninformative; these were ignored in the analysis (characters 1–2, 4, 7, 12, 17–19, 21–23, 25, 28, 30–34, 38, 41–42, 47–48, 50–56, 58, 60, 62, 65, 68–74, 81–83, 85–91,

TABLE 8. Data matrix for the taxa included in the cladistic analysis (*continued*).

	3	21	22	23	24	25	26	27	28	29	30
1	Ancestor	0	0	0	0	0	0	0	0	0	0
2	Captorhinidae	0	0	0	0	0	0	0	?	0	0
3	Testudines	0	0	1	0	0	0	0&2	0	1	1
4	Araeoscelidia	0	0&1	0	0	0	0	0	1	0	0
5	Younginiformes	0	1	0	0	0	0	0	1	1	1
6	Kuehneosauridae	0	2	1	1	1	0	0	1	1	1
7	Rhynchocephalia	1	1&2	0	0	1	0&1	0	1	1	1
8	Squamata	0	2	1	1	?	0	0&1&2	0&1	1	1
9	Rhynchosauria	1	1	1	0	0	1	0	0	1	1
10	Prolacertiformes	0&1	2	1	0&1	1	1	0	1	1	1
11	Trilophosaurus	?	0	?	0	?	1	2	?	1	1
12	Choristodera	0	1	1	0&1	0	1	1	1	1	1
13	Archosauriformes	1	1	1	0	0	0&1	0&1&2	1	1	1
14	Claudiosaurus	0	2	0	0	1	0	0	?	0	0
15	Dactylosaurus	0	2	0	0	1	2	0	?	1	1
16	Serpiano-Neustico	0	2	0	0	1	2	0	?	1	1
17	Simosaurus	0	2	0	0	1	2	1	1	0	1
18	Nothosaurus	0	2	0	1	?	2	0&1	1	0	1
19	Lariosaurus	0	2	0	?	?	2	0	?	0	1
20	Corosaurus	0	2	0	?	?	1	1	1	0	1
21	Cymatosaurus	0	2	0	1	?	?	1	?	0	1
22	Pistosaurus	0	2	0	1	?	?	1	?	0	1
23	Placodus	0	2	0	0	0	1	0	1	1	1
24	Pareiasauria	0	0	1	0	0	0	2	0	0	0
25	Procolophonidae	0	0	1	0	0	0	2	0&1	1	0
26	Palaeagama	0	2	1	1	?	0	?	?	1	1
27	Paliguana	0	2	1	?	?	0	?	?	1	1
28	Saurosternon	?	?	?	?	?	?	?	?	?	?
29	Coelurosauravus	0	2	0	0	1	?	?	?	1	1

and 93–94). With the branch-and-bound algorithm implemented (addition sequence: stepwise), nine equally most parsimonious reconstructions (MPRs) were obtained, a network with a tree length (TL) of 85 steps, a consistency index (CI) of 0.694, and a rescaled consistency index (RC) of 0.421. Lack of resolution is restricted to the Eusauropterygian taxa. The strict consensus tree of those nine MPRs (Fig. 65A) is equivocal with respect to the potential grouping of *Placodus* versus pachypleurosaur taxa within a monophyletic group comprising the Eusauropterygia.

Rooting the ingroup network by implementation of an all-zero ancestor polarizes the characters as discussed in the character definitions given above and specifies sister-group relationships contradicting the concept of the Nothosauriformes (Storrs, 1991, 1993a, placing the Placondontia as sister-group of the Eusauropterygia). Instead, *Placodus* falls out as sister-taxon of all other Sauropterygia (Fig. 66), here referred to as Eosauropterygia. Using the ingroup taxa only as before, but rooting the tree by implementation of the assumption of an all-zero ancestor, again renders numerous characters constant and/or uninformative; these characters were ignored in the analysis: 1–2, 4, 7, 17–19, 21–23, 28, 30–34, 38, 42, 47, 50–52, 55–56, 58, 60, 62, 65, 69–73, 81–83, 85–91, and 93–94. With the branch-and-bound algorithm implemented (addition sequence: stepwise), six equally MPRs were obtained, with a TL of 110 steps, a CI of 0.673, and an RC of 0.391.

TABLE 8. Data matrix for the taxa included in the cladistic analysis (*continued*).

		4 31	32	33	34	35	36	37	38	39	40
1	Ancestor	0	0	0	0	0	0	0	0	0	0
2	Captorhinidae	0	0	0	0	0	0	1	0	0	0
3	Testudines	0	0&1	0	1	0	0&1	1	0&1	0	0
4	Araeoscelidia	0	0	0	1	0	0	0	0	0	0
5	Younginiformes	0	0	0	1	0	0	0	1	1	0
6	Kuehneosauridae	1	0	0	1	0	?	?	1	0	0
7	Rhynchocephalia	0&1	0	0	1	0	0	0	1	1	0
8	Squamata	1	0	0	1	0	0&1	0	1	1	0
9	Rhynchosauria	0	0	0	1	0	1	0	1	1	0
10	Prolacertiformes	0	0	0	1	0	0	0	1	0&1	0
11	Trilophosaurus	0	0	0	1	0	0	0	1	1	0
12	Choristodera	0	?	0	1	0	1	0	1	0	0
13	Archosauriformes	0	0&1	0	1	0	0&1	0&1	1	0&1	0
14	Claudiosaurus	0	0	0	1	1	0	0	0	0	0
15	Dactylosaurus	0	1	?	0	1	0	1	1	0	0
16	Serpiano-Neustico	0	1	?	0	1	0	1	1	0	0
17	Simosaurus	0	1	2	0	1	0	0	1	0	0
18	Nothosaurus	0	1	2	0	1	1	0	1	0	1
19	Lariosaurus	0	1	?	0	1	?	0	1	0	1
20	Corosaurus	0	1	2	0	0	?	?	1	1	1
21	Cymatosaurus	0	1	?	0	0	1	0	1	?	1
22	Pistosaurus	0	1	?	0	0	?	0	1	?	?
23	Placodus	0	1	1	0	0	1	0	1	1	1
24	Pareiasauria	0	1	0	1	0	0	0	1	0	0
25	Procolophonidae	0	0	0	1	0	0	0	1	1	0
26	Palaeagama	0	0	?	?	?	?	?	?	?	?
27	Paliguana	0	0	?	?	?	?	?	1	?	?
28	Saurosternon	?	?	?	?	?	?	?	?	?	?
29	Coelurosauravus	0	?	?	?	?	?	?	1	0	0

All six MPRs support the position of *Placodus* as sister-taxon of all other sauropterygians (Eosauropterygia), the position of *Corosaurus* as sister-taxon of all other Eosauropterygia, the monophyly of pachypleurosaurs and their position as sister-group of the Eusauropterygia, and the monophyly of the Eusauropterygia. Support is 100% for the position of *Simosaurus* as sister-taxon of a monophyletic clade that includes *Cymatosaurus, Nothosaurus, Lariosaurus,* and *Pistosaurus.* The relative relationships among those latter four genera remain unresolved (but see Rieppel, 1994a).

The implementation of DELTRAN character optimization will minimize the number of synapomorphies diagnostic at any node that will subsequently be lost again within that same clade. For that reason, it will generally indicate synapomorphous characters (character states) at a level of minimal inclusiveness (rather than maximal inclusiveness as ACCTRAN character optimization would). Character optimization strategies do not influence tree topologies, and the enumeration of synapomorphies below will generally be based on the implementation of DELTRAN character optimization. Monophyly of the Sauropterygia, including *Placodus* and the Eosauropterygia, is supported by 9(2), 10(1), 12(1), 26(1), 43(1), 45(1), 66(1), 67(1), 74(1), 75(1), 78(2), 79(1), 84(1), and 92(2). Rooting the tree by

TABLE 8. Data matrix for the taxa included in the cladistic analysis (*continued*).

5		41	42	43	44	45	46	47	48	49	50
1	Ancestor	0	0	0	0	0	0	0	0	0	0
2	Captorhinidae	0	0	0	?	0	0	0	0	0	0
3	Testudines	1	?	?	?	?	?	0	0&1	0&2	1
4	Araeoscelidia	1	0	0	0	0	0	0	0	0	0
5	Younginiformes	?	0	0	0	1	0	0	0	0	0
6	Kuehneosauridae	?	0	0	0	1	0	1	1	0	1
7	Rhynchocephalia	1	1	0	0	1	0	1	0&1	0	0&1
8	Squamata	1	1	0	0	1	0	1	1	0&2	1
9	Rhynchosauria	0	0	?	0	1	0	1	1	0	0
10	Prolacertiformes	1	0	0	0	1	0	0&1	1	0&2	0&1
11	Trilophosaurus	?	0	?	0	1	0	1	1	1&2	0
12	Choristodera	1	0	0	0	1	0	0	1	1	1
13	Archosauriformes	1	0	0	0	1	0	0&1	1	0&1&2	0&1
14	Claudiosaurus	1	0	0	0	1	0	0	?	0	0
15	Dactylosaurus	?	0	0	0	1	0	1	1	0	1
16	Serpiano-Neustico	?	0	0	0	1	0	1	1	0	1
17	Simosaurus	1	0	1	0	1	2	1	1	1	1
18	Nothosaurus	1	0	1	1	0	2	1	1	1	1
19	Lariosaurus	?	0	1	1	0	1	1	1	1	1
20	Corosaurus	?	0	1	?	1	1	1	1	0	1
21	Cymatosaurus	1	0	1	1	0	0	1	1	?	1
22	Pistosaurus	?	0	1	?	0	0	1	1	1	1
23	Placodus	0	0	1	0	1	0	1	0	0	1
24	Pareiasauria	0	0	0	0	1	0	0	0	0	0
25	Procolophonidae	1	0	0	0	1	0	1	0	0	0
26	Palaeagama	?	1	?	0	1	0	?	?	0	0
27	Paliguana	?	?	?	0	1	0	?	?	?	?
28	Saurosternon	?	?	?	?	?	?	?	?	0	0
29	Coelurosauravus	?	1	0	0	1	0	?	?	0	1

implementation of an all-zero ancestor will group the taxa strictly on the presence of characters, but, as will become obvious with the introduction of outgroups, some of the characters listed as synapomorphies of the Eosauropterygia are, in fact, diagnostic at a more inclusive level within the Diapsida. Within the Sauropterygia, *Corosaurus* and the other Eosauropterygia are united by characters absent in *Placodus*: 48(1), 53(1), 64(1), and 68(1). Eosauropterygia other than *Corosaurus* are united by the following characters: 25(1), 26(2), 35(1), 54(1), 63(1), and 84(2).

Because most of the characters listed above are informative in the reconstruction of phylogenetic interrelationships among diapsids other than the Sauropterygia, the two competing hypotheses of monophyly of Nothosauriformes (Storrs, 1991, 1993a) versus "Euryapsida" (Rieppel, 1989a; Zanon, 1989; treating placodonts as sister-group of the Eosauropterygia) were tested by the introduction of the outgroup taxa used by Storrs (1991, 1993a), viz., Captorhinidae, Araeoscelidia, Younginiformes, and *Claudiosaurus*. The strict consensus tree for six equally parsimonious unrooted networks (Fig. 65B; TL = 167 steps; CI = 0.707; RC = 0.535) indicates the impossibility of the Nothosauriformes becoming a monophyletic assemblage, no matter where the root is placed. Rooting the ingroup (as defined above, and assumed to be

TABLE 8. Data matrix for the taxa included in the cladistic analysis (*continued*).

	6	51	52	53	54	55	56	57	58	59	60
1	Ancestor	0	0	0	0	0	0	0	0	0	0
2	Captorhinidae	0	0	0	?	0	0	0	0	0	?
3	Testudines	0&1	1	0	0	0	0	0	0	0	1
4	Araeoscelidia	0	1	0	?	0	0	0	0	0	0
5	Younginiformes	0	1	0	0	0	0	0	0	0	0&1
6	Kuehneosauridae	1	1	0	?	1	?	0	0	0	?
7	Rhynchocephalia	0	1	1	0	0	0	0	0	0	1
8	Squamata	0	1	0&1	0	0	0	0	0	0	1
9	Rhynchosauria	0	1	0	?	0	0	0	0	0	1
10	Prolacertiformes	0&1	1	0	?	0	1	0	0	0	1
11	Trilophosaurus	0	1	0	?	0	1	0	0	0	1
12	Choristodera	0	1	0	1	0	1	0	1	0	1
13	Archosauriformes	0&1	1	0	0	1	1	0	0&2	0	1
14	Claudiosaurus	0	1	0	?	0	1	0	0	0	1
15	Dactylosaurus	1	1	1	1	0	1	0	1	1	1
16	Serpiano-Neustico	1	1	1	1	0	1	0&1	1	1	1
17	Simosaurus	1	1	1	1	0	?	0	1	0	1
18	Nothosaurus	1	1	1	1	0	1	0	1	1	1
19	Lariosaurus	1	1	?	?	0	1	1	2	1	1
20	Corosaurus	1	1	1	?	0	?	0	1	0	1
21	Cymatosaurus	1	1	?	?	0	?	?	?	?	1
22	Pistosaurus	1	1	1	1	0	1	0	?	?	1
23	Placodus	1	1	0	0	1	1	0	1	0	1
24	Pareiasauria	0	0	0	0	0	0	0	0	1	0
25	Procolophonidae	0	1	0	0	0	0	0	0	1	1
26	Palaeagama	?	?	?	0	0	0	0	0	1	?
27	Paliguana	?	?	?	?	?	?	?	?	?	?
28	Saurosternon	?	?	1	0	0	?	0	?	?	1
29	Coelurosauravus	1	?	0	0	0	0	0	0	?	?

monophyletic) on the four outgroup taxa used by Storrs (1991, 1993a; the outgroup composed of these taxa was assumed to be paraphyletic) and deleting all other (potential outgroup) taxa from the analysis rendered characters constant and/or uninformative that were accordingly ignored in the analysis: 2, 4, 21, 23, 28, 31, 42, 52, 55, 88, and 93–94. Character 22 is the only multistate character treated as ordered; *Placodus* was coded for the absence of the infraorbital fenestra (see discussion of character 34). With the branch-and-bound algorithm implemented (addition sequence: stepwise), six equally MPRs were obtained, with a TL of 167 steps, a CI of 0.707, and an RC of 0.535. The tree topologies for the ingroup are identical to those described for the previous run, the only conflict of resolution being expressed by a polytomy in the strict consensus tree involving *Cymatosaurus, Nothosaurus, Lariosaurus,* and *Pistosaurus* (Fig. 66). All nodes, including the monophyletic *Cymatosaurus–Nothosaurus–Lariosaurus–Pistosaurus* clade, are supported by all six trees. The tree is interesting in that it shows *Claudiosaurus* rather than Younginiformes as sister-taxon of the Eosauropterygia plus *Placodus* (the same result was obtained by Storrs [1991, 1993a], but not by Rieppel [1993a]). The tree differs from the results of Storrs (1991, 1993a) in the position of *Placodus* as sister-taxon of the Eosauropterygia and in the position of *Corosaurus* as sister-taxon

TABLE 8. Data matrix for the taxa included in the cladistic analysis (*continued*).

	7	61	62	63	64	65	66	67	68	69	70
1	Ancestor	0	0	0	0	0	0	0	0	0	0
2	Captorhinidae	0	0	0	0	0	0	?	0	0	1
3	Testudines	0	0	0	0	0	1	0	0	?	0
4	Araeoscelidia	0	0	0	0	0	1	0	0	0	1
5	Younginiformes	1	0	0	0	0	0&1	0	0	1	0
6	Kuehneosauridae	?	?	?	?	?	?	?	1	1	0
7	Rhynchocephalia	1	0	0	0	0	1	0	0	1	0
8	Squamata	0&1	0	0	0	0	1	0&1	0	1	0
9	Rhynchosauria	1	0	0	0	0	1	0	0	1	0
10	Prolacertiformes	1	0	0	0	0	0	?	0	1	0
11	Trilophosaurus	1	0	0	0	0	1	0	0	1	0
12	Choristodera	1	1	0	0	0	1	0	0	1	0
13	Archosauriformes	1	0	0	0	0	1	0	0	1	0
14	Claudiosaurus	1	0	0	0	0	1	0	0	1	0
15	Dactylosaurus	0	1	1	1	1	?	?	1	1	0
16	Serpiano-Neustico	0	1	1	0	1	0&1	2	1	1	0
17	Simosaurus	0	1	1	1	1	1	1	1	1	0
18	Nothosaurus	0	1	1	1	1	0&1	2	1	1	0
19	Lariosaurus	0	1	1	?	1	?	?	1	1	0
20	Corosaurus	1	1	0	1	1	1	1	1	1	0
21	Cymatosaurus	?	?	?	?	?	?	?	?	1	0
22	Pistosaurus	?	?	?	?	?	?	?	1	1	0
23	Placodus	1	1	0	0	1	1	1	0	1	0
24	Pareiasauria	0	0	0	0	0	1	0	1	?	1
25	Procolophonidae	0	0	0	0	0	1	0	1	?	1
26	Palaeagama	1	?	?	?	?	1	0	?	?	?
27	Paliguana	?	?	?	?	?	?	?	?	?	?
28	Saurosternon	1	1	0	0	?	1	0	0	1	0
29	Coelurosauravus	?	?	?	?	?	?	?	?	?	?

of all remaining Eosauropterygia, as described above already. With DELTRAN character optimization implemented, the Younginiformes, *Claudiosaurus,* and the Sauropterygia are grouped together by the following characters: 7(1), 22(1), 45(1), 61(1), 69(1), 70(0), 82(1), 83(1), 84(1), and 86(1). *Claudiosaurus* and the Sauropterygia are grouped together by the following characters: 17(1), 19(1), 22(2), 56(1), 60(1), 75(1), and 85(1). Synapomorphies of the Sauropterygia finally are as follows: 1(1), 7(2), 9(2), 26(1), 30(1), 32(1), 34(0), 38(1), 40(1), 43(1), 47(1), 50(1), 51(1), 58(1), 62(1), 65(1), 67(1), 71(1), 72(1), 74(1), 78(2), 79(1), 81(1), 89(0), 90(1), 91(1), and 92(2) (character 34[0] is an eosauropterygian synapomorphy if *Placodus* is coded for the presence of the infraorbital foramen). The Eosauropterygia are grouped to the exclusion of *Placodus* by the following characters: 33(2), 48(1), 53(1), 64(1), and 68(1). (Characters 33 and 34 are uninformative if the ingroup taxa alone are considered; see above.) Characters that unite all other Eosauropterygia to the exclusion of *Corosaurus* are the following: 25(1), 26(2), 35(1), 54(1), 61(0), 63(1), 84(2), and 87(1) (note that character 87[1] is coded as unknown for *Placodus* and *Corosaurus*). Eusauropterygian synapomorphies are as follows: 6(1), 11(1), 14(1), 15(1), 16(1), 27(1), 49(1), 76(1), and 92(1); the *Cymatosaurus–Nothosaurus–Lariosaurus–Pistosaurus* clade groups to the exclusion of *Simosaurus* on the basis of the

TABLE 8. Data matrix for the taxa included in the cladistic analysis (*continued*).

8		71	72	73	74	75	76	77	78	79	80
1	Ancestor	0	0	0	0	0	0	0	0	0	0
2	Captorhinidae	0	0	0	0	0	0	0	0	0	0
3	Testudines	1	0	0	0	0&1	0&2	1	0	1&2	0
4	Araeoscelidia	0	0	1	0	0	0	0	0	0	0
5	Younginiformes	0	0	1	0	0	0&2	0	0&1	0	0
6	Kuehneosauridae	0	0	1	0	0	2	1	2	0	0
7	Rhynchocephalia	0	0	1	0	0	2	0	0	0	0
8	Squamata	0	0	1	0	0	0&2	1	0	0	0
9	Rhynchosauria	0&1	0	1	0	0	0	1	0	0	0
10	Prolacertiformes	0	0	1	0	0	0	1	1&2	0	0
11	Trilophosaurus	0	0	1	0	0	0	1	0	0	0
12	Choristodera	0	0	1	0	0	0&2	1	2	0	0
13	Archosauriformes	0&1	0	1	0	0&1	0	1	0	0	0
14	Claudiosaurus	0	0	0	0	1	1	0	0	0	0
15	Dactylosaurus	1	1	0	1	0	0	0	1	2	0
16	Serpiano-Neustico	1	1	0	1	1	0&1	0	1&2	2	0
17	Simosaurus	1	1	0	1	1	1	1	2	1	1
18	Nothosaurus	1	1	0	1	1	0&1	0	2	1	1
19	Lariosaurus	1	1	0	1	1	1	0	2	2	0
20	Corosaurus	1	1	0	1	1	0	0	2	1	0
21	Cymatosaurus	?	?	0	0	0	0	0	?	?	?
22	Pistosaurus	?	?	0	1	1	1	1	2	0	?
23	Placodus	1	1	0	1	1	0	1	2	1	0
24	Pareiasauria	0	0	0	0	0	2	0	0	0	0
25	Procolophonidae	0	0	0	0	0	?	0	0	0	0
26	Palaeagama	?	0	1	0	0	0	0	?	0	0
27	Paliguana	?	?	?	?	?	?	?	?	?	?
28	Saurosternon	0	0	1	0	0	0	0	2	0	0
29	Coelurosauravus	?	?	1	0	0	0	0	0	0	0

following: 3(1), 24(1), 36(1), 40(1), 44(1), 45(0), and 59(1).

The ultimate test of sauropterygian interrelationships involves the assessment of global parsimony over all taxa included in the data matrix (Table 8) (see Appendix I for taxa 24–29). For non-sauropterygian taxa, large parts of that matrix are based on characters taken from Gauthier, Kluge, and Rowe (1988) and Evans (1988), yet some of the codings were changed according to the published descriptions quoted at the beginning of this section. The data matrix was therefore tested for diapsid interrelationships by the deletion of all sauropterygian (*Placodus* plus Eosauropterygia) taxa. This procedure renders characters constant and/or uninformative that were accordingly ignored in the analysis: 3, 5, 6, 33, 35, 40, 43–44, 46, 52, 54, 57–59, 62–65, 67–68, 72, 74, 79–80, and 92. With the branch-and-bound search option implemented, two equally parsimonious unrooted networks were found with a TL of 214 steps, a CI of 0.799, and an RC of 0.510. Lack of resolution was restricted to archosauromorph taxa. Turtles (coded 34[0]—see Appendix I) were found to be adjacent to the Lepidosauriformes (Lepidosauromorpha). Rooting the network on an all-zero ancestor produced (branch-and-bound search option implemented) two equally parsimonious trees with a TL of 218 steps, a CI of 0.789, and an RC of 0.545. The strict consensus tree is ((Captorhinidae,

TABLE 8. Data matrix for the taxa included in the cladistic analysis (*continued*).

9		81	82	83	84	85	86	87	88	89	90
1	Ancestor	0	0	0	0	0	0	0	0	0	0
2	Captorhinidae	0	0	0	0	0	0	0	0	0	0
3	Testudines	1	0	0	0	1	1	1	0	0	0&1
4	Araeoscelidia	0	0	0	0	0	0	0	0	1	0
5	Younginiformes	0	1	1	1	0	1	0	0	1	0
6	Kuehneosauridae	1	1	1	1	0	1	?	?	?	?
7	Rhynchocephalia	1	1	1	1	0	1	1	0	1	0&1
8	Squamata	1	1	1	1	0	1	1	0	1	1
9	Rhynchosauria	0	1	1	1	0	1	1	1	1	0
10	Prolacertiformes	0&1	1	1	1	0	1	0	0&1	1	0&1
11	Trilophosaurus	0	1	1	1	0	1	0	1	1	0
12	Choristodera	0	1	1	1	1	1	?	1	1	0
13	Archosauriformes	0	1	1	1&2	0&1	1	0	1	1	0&1
14	Claudiosaurus	0	1	1	1	1	1	0	0	1	0
15	Dactylosaurus	1	1	?	?	?	?	?	?	?	?
16	Serpiano-Neustico	1	1	1	2	1	1	1	0	0	1
17	Simosaurus	1	1	1	2	1	1	1	0	0	1
18	Nothosaurus	1	1	1	2	1	1	1	0	0	1
19	Lariosaurus	1	1	1	2	1	1	1	0	0	1
20	Corosaurus	1	1	1	1	1	1	?	0	?	?
21	Cymatosaurus	?	?	?	?	?	1	?	?	?	?
22	Pistosaurus	?	?	1	?	?	?	?	?	?	?
23	Placodus	1	1	1	1	1	1	?	0	0	1
24	Pareiasauria	0	1	0	0	0	0	0	0	0	0
25	Procolophonidae	0	0	0	0	0	0	0	0	0	0
26	Palaeagama	?	1	1	0	1	1	0	0	1	?
27	Paliguana	?	?	?	?	?	?	?	?	?	?
28	Saurosternon	0	1	1	0	1	1	0	0	1	0
29	Coelurosauravus	0	?	1	?	1	0	0	0	1	0

(((((Testudines, (Kuehneosauridae, (Rhynchocephalia, Squamata))), ((Rhynchosauria, Trilophosaurus), (Prolacertiformes, Choristodera), Archosauriformes)), Younginiformes), Claudiosaurus), Araeoscelidia)), Ancestor). Under the implementation of DELTRAN character optimization, turtles share with diapsid reptiles the following synapomorphies: 41(1), 52(1), and 66(1) (the homology of the interclavicle with the entoplastron is discussed in Rieppel, 1993e). Neodiapsid synapomorphies shared by turtles are as follows: 7(1), 18(1), 29(1), 30(1), 38(1) (turtles were coded polymorphic for this character), 60(1), and 93(1). Saurian synapomorphies shared by turtles are as follows: 15(3), 17(1), 19(1) (polymorphic for turtles), 23(1), 48(1) (polymorphic for turtles), 77(1), 91(1), and 94(1). Lepidosauriform synapomorphies shared by turtles are the following: 9(1) (polymorphic for turtles), 50(1), 81(1), and 87(1).

Global parsimony reconstruction over the data matrix presented in Table 8, including 22 ingroup taxa (see Fig. 68), raises the number of taxa beyond the limits of exact searches (exhaustive or branch-and-bound). A heuristic search was therefore conducted to obtain an unrooted network linking the 22 ingroup taxa (turtles and *Placodus* coded 34[0]—see Appendix I). Character 22 was coded as ordered, and all other multistate characters as unordered (character 52 was uninformative and ignored). The search employed random stepwise

TABLE 8. Data matrix for the taxa included in the cladistic analysis (*continued*).

10		91	92	93	94
1	Ancestor	0	0	0	0
2	Captorhinidae	0	0	0	0
3	Testudines	1	0	1	1
4	Araeoscelidia	0	0	0	0
5	Younginiformes	0	0	1	0
6	Kuehneosauridae	?	?	?	?
7	Rhynchocephalia	1	0	1	1
8	Squamata	1	0	1	1
9	Rhynchosauria	1	0	1	1
10	Prolacertiformes	1	0	1	0&1
11	Trilophosaurus	1	0	1	1
12	Choristodera	1	0	1	1
13	Archosauriformes	1	0	1	1
14	Claudiosaurus	0	0	0	0
15	Dactylosaurus	?	?	?	?
16	Serpiano-Neustico	1	2	0	0
17	Simosaurus	1	1	0	0
18	Nothosaurus	1	1	0	0
19	Lariosaurus	1	0	0	0
20	Corosaurus	?	?	?	?
21	Cymatosaurus	?	?	?	?
22	Pistosaurus	?	?	?	?
23	Placodus	1	2	0	0
24	Pareiasauria	1	0	0	0
25	Procolophonidae	1	0	0	0
26	Palaeagama	?	?	1	0
27	Paliguana	?	?	?	?
28	Saurosternon	0	0	1	0
29	Coelurosauravus	0	0	0	0

addition, and branch swapping (on minimal trees only) was effected by tree bisection and reconnection. Ten replications yielded a total of 36 equally parsimonious unrooted trees with a TL of 347 steps, a CI of 0.654, and an RC of 0.464. Lack of resolution was restricted to three crown-groups, that is, among archosauromorph taxa, among Lepidosauriformes (Kuehneosauridae, Rhynchocephalia, and Squamata), and among the Eusauropterygia (*Cymatosaurus–Nothosaurus–Lariosaurus–Pistosaurus* clade). Assessment of global parsimony over all taxa considered in an unrooted network does not alter the interrelationships of the Sauropterygia as discussed above (Fig. 65B). Since the topology of the unrooted network is identical to the rooted tree (Fig. 68), character discussion will be limited to the rooted tree.

The tree for the 22 ingroup taxa (all characters informative) was rooted on an all-zero ancestor, assuming monophyly of the Reptilia (*sensu* Gauthier, Kluge, & Rowe, 1988). Character 22 was coded as ordered, and all other multistate characters as unordered (all characters informative). The heuristic search employed random stepwise addition, and branch swapping (on minimal trees only) was effected by tree bisection and reconnection. One hundred replications yielded a total of 36 equally parsimonious trees with a TL of 351 steps, a CI of 0.650, and an RC of 0.471 (coding *Placodus* 34[1] and turtles 34[0] increases TL by

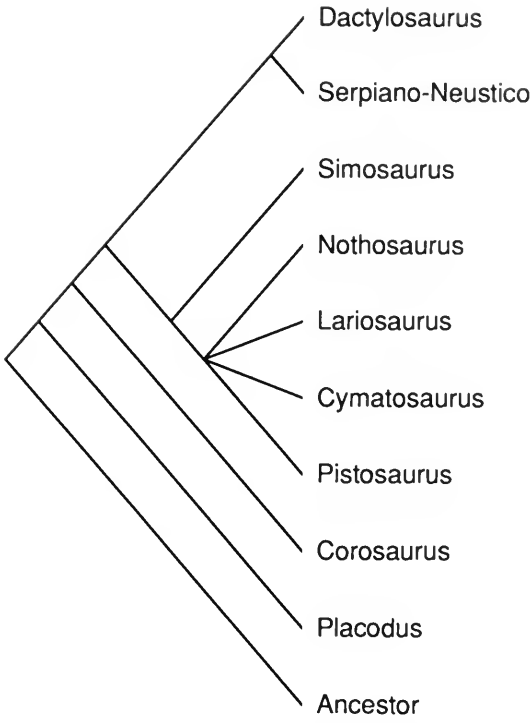

FIG. 66. Strict consensus tree (of six MPRs; TL = 110, CI = 0.673, RC = 0.391) for the Sauropterygia (ingroup) rooted on an all-zero ancestor. For further discussion, see text.

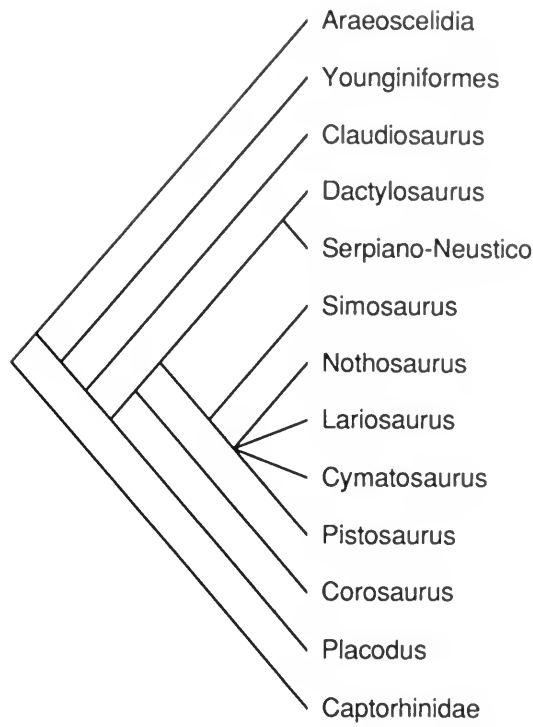

FIG. 67. Strict consensus tree (of six MPRs; TL = 167, CI = 0.707, RC = 0.535) with the Sauropterygia (ingroup) rooted on a paraphyletic outgroup comprising Captorhinidae, Araeoscelidia, Younginiformes, and *Claudiosaurus*. For further discussion, see text.

1 step to 352, CI becomes 0.648, and RC 0.468, but this has no effect on tree topology). Again, lack of resolution was restricted to three crown-groups, that is, among archosauromorph taxa, among lepidosauriforms (Kuehneosauridae, Rhynchocephalia, Squamata), and among the Eusauropterygia (*Cymatosaurus, Lariosaurus–Nothosaurus, Simosaurus,* and *Pistosaurus*) (Fig. 68). However, the 50% majority rule consensus tree shows 100% support for the monophyly of the Eusauropterygia, Lepidosauromorpha, and Archosauromorpha.

The following major dichotomies can be identified on the strict consensus tree (Fig. 68), all with 100% support in the 50% majority rule consensus tree. With DELTRAN character optimization implemented, the Diapsida (Araeoscelidia and its sister-taxon) are diagnosed by the following synapomorphies: 9(1), 10(1), 12(1), 28(1), 34(1), 41(1), 52(1), 66(1), and 89(1). The Neodiapsida (*Claudiosaurus* and its sister-taxon) are diagnosed by the following: 7(1), 18(1), 22(1), 45(1), 60(1), 61(1), 69(1), 82(1), 83(1), 84(1), and 86(1). *Claudiosaurus* is no longer the sister-taxon of the Sauropterygia, as it is with the inclusion of four outgroup taxa only (see above, and Rieppel, 1993a). Instead, it is the second outgroup (among the taxa included in the analysis) to the Sauria, with the Younginiformes representing the first outgroup. The Younginiformes group with the Sauria (Archosauromorpha and Lepidosauromorpha) to the exclusion of *Claudiosaurus* on the basis of the following characters: 29(1), 30(1), 38(1), 39(1), 73(1), and 93(1). The Sauria group to the exclusion of *Youngina* and *Claudiosaurus* on the basis of the following: 17(1), 19(1), 23(1), 47(1), 48(1), 77(1), 91(1), and 94(1). Turtles are united with the Lepidosauriformes (Lepidosauromorpha) and Sauropterygia on the basis of the following: 50(1), 81(1), 87(1), and 90(1). Turtles group with the Sauropterygia to the exclusion of the Lepidosauriformes on the basis of the following: 9(2), 34(0) (see Appendix I), 71(1) (present in *Proganochelys* [Gaffney, 1990]), 73(0), 79(1), 85(1), and 89(0) (loss of the infraorbital foramen is a synapomorphy at this level if turtles are coded for its absence 34[0]).

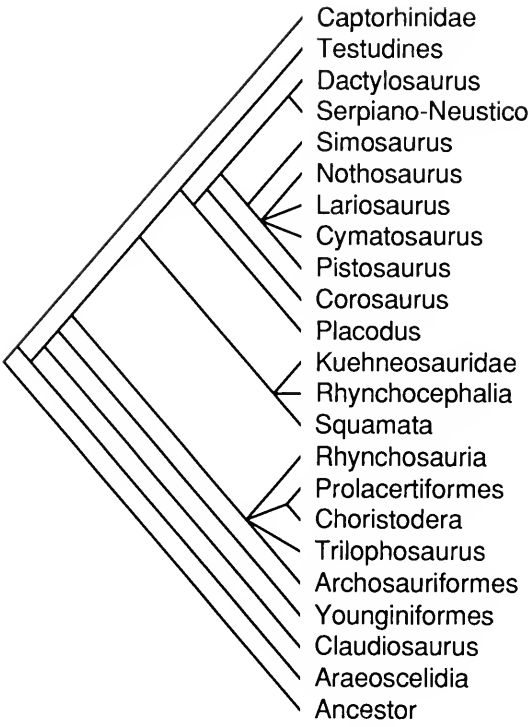

FIG. 68. Strict consensus tree (of 36 MPRs; TL = 351, CI = 0.650, RC = 0.471) for 22 reptile taxa rooted on an all-zero ancestor. For further discussion, see text.

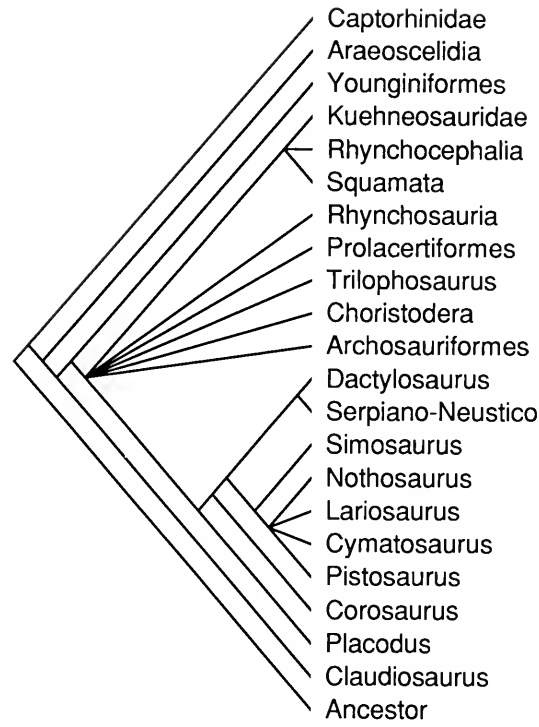

FIG. 69. Sauropterygian interrelationships among the Reptilia with the Testudines omitted from the analysis (strict consensus tree of 48 MPRs; TL = 323, CI = 0.633, RC = 0.491). For further discussion, see text.

Forcing the Sauropterygia to the position of sister-group to younginiforms plus Sauria increases TL by 5 steps, forcing the Sauropterygia to the position of sister-group to *Claudiosaurus* increases TL by 3 steps, and forcing turtles to a sister-group relation with the Captorhinidae (Gaffney & Meylan, 1988) increases TL by 8 steps.

Continuing with DELTRAN character optimization, the synapomorphies of the Sauropterygia are 1(1), 7(2), 22(2), 23(0), 26(1), 32(1), 43(1), 51(1), 56(1), 58(1), 62(1), 65(1), 67(1), 72(1), 74(1), 75(1), 78(2), 92(2), 93(0), and 94(0) (loss of the infraorbital foramen is a synapomorphy at this level if *Placodus* is coded for its absence, turtles for its presence). The Eosauropterygia group to the exclusion of *Placodus* on the basis of the following: 33(2), 53(1), 64(1), 68(1), and 77(0) (character 34[0] is synapomorphic at this level if turtles and *Placodus* are coded for its presence). Pachypleurosaurs group with the Eusauropterygia to the exclusion of *Corosaurus* on the basis of the following: 25(1), 26(2), 35(1), 39(0), 54(1), 61(0), 63(1), and 84(2). Eusauropterygian synapomorphies are: 6(1), 11(1), 14(1), 15(1), 16(1), 27(1), 29(0), 49(1), 76(1), and 92(1). The *Cymatosaurus–Nothosaurus–Lariosaurus–Pistosaurus* clade groups to the exclusion of *Simosaurus* on the basis of the following: 3(1), 24(1), 36(1), 40(1), 44(1), 45(0), and 59(1).

This is not the place to discuss the phylogenetic relationships of turtles (but see Appendix I), which may be related to "parareptiles" (Reisz & Laurin, 1991; Laurin & Reisz, 1994; Lee, 1993) instead of being part of the monophyletic Reptilia (Gauthier et al., 1988b; see also Gaffney & Meylan, 1988, and Appendix I). To remove the bias toward the inclusion of Testudines in a monophyletic Reptilia, the taxon was deleted and a heuristic search conducted rooting the monophyletic ingroup on an all-zero ancestor. The heuristic search employed random stepwise addition, and branch swapping (on minimal trees only) was effected by tree bisection and reconnection. One hundred replications were made. The result was a dramatic decrease of resolution within the Sauria (Fig. 69), with a total of 48 equally parsimonious trees, 323 steps long. The CI is 0.663, and the RC is 0.491. The 50% majority rule consensus tree shows 100%

support for the inclusion of the Sauropterygia in the Sauria in an unresolved polytomy with lepidosauromorph and archosauromorph taxa, 100% support for the monophyly of the Sauropterygia, and no change in the interrelationships of the Sauropterygia as compared to the previous runs.

Summary and Conclusions

Disregarding the problem of turtle interrelationships (but see Appendix I), the most salient results of this analysis are the inclusion of a monophyletic Sauropterygia in the Sauria, the position of placodonts as sister-taxon of the Eosauropterygia, and the position of *Corosaurus* as sister-taxon of an unnamed clade comprising the monophyletic pachypleurosaurs and their sister-group, the monophyletic Eusauropterygia. The tree indicating sauropterygian interrelationships thus reads (Placodontia (*Corosaurus* (Pachypleurosauroidea) (Eusauropterygia))) and contradicts Storrs's (1991, 1993a) concept of a monophyletic Nothosauriformes. The use of the taxon name Euryapsida for the group comprising placodonts and sauropterygians is problematical under the phylogenetic criterion of priority advocated by de Queiroz and Gauthier (1990, 1992, 1993), because *Placodus,* nothosaurs, and plesiosaurs had been grouped under the name Sauropterygia by Owen (1860).

The above analysis showed a number of characters to have a rather high degree of homoplasy (and correspondingly a low CI), yet a number of conclusions can be drawn with respect to the phylogenetic interrelationships of the Sauropterygia based on characters with a fairly consistent distribution and hence with a relatively high CI. In a conservative approach to sauropterygian interrelationships, the diagnoses of the taxa given below are based only on characters (synapomorphies) with a CI of 0.5 or higher (unless otherwise indicated) in the assessment of global parsimony and characters synapomorphic for the respective nodes under the implementation of both ACCTRAN and DELTRAN character optimization strategies. A conservative approach is taken with respect to turtle relationships.

On the assumption of a monophyletic Reptilia (Gauthier, Kluge, & Rowe, 1988, and whether or not turtles are included in that group), the Sauropterygia fall into the Neodiapsida and, among those, into the Sauria. Without inclusion of turtles, the interrelationships of saurian taxa outside the Sauropterygia remain highly unresolved; with the inclusion of turtles, the Sauropterygia appear to be more closely related to the lepidosauromorph than to the archosauromorph clade (as first suggested by Sues, 1987a; see also Carroll & Currie, 1991; Rieppel, 1993a). Synapomorphies of the Neodiapsida, including the Sauropterygia, are as follows: 7(1), exclusion of lacrimal from external naris (preceding the loss of the lacrimal in sauropterygians); 45(1), caniniform teeth on maxilla absent; 60(1), loss of cleithrum; 61(1) clavicles narrow medially (reversals within the Sauropterygia); 69(1), loss of supraglenoid buttress; 82(1), acetabulum circular; 83(1), femoral shaft slender and sigmoidally curved; 84(1), intertrochanteric fossa reduced; and 86(1), anterior femoral condyle not larger than posterior condyle and of subequal extent distally.

The Younginiformes and the Sauria (including the Sauropterygia) share the following synapomorphies: 29(1), quadrate concave posteriorly (CI = 0.333; see discussion below); 30(1), quadrate exposed in lateral view (reversed in the Sauropterygia); 38(1), presence of a retroarticular process; and 93(1), fifth metatarsal short and broad (reversed in the Sauropterygia).

The monophyly of the Sauria including the Sauropterygia is supported by the following characters: 47(1), teeth on pterygoid flange absent (reversal among archosauromorphs implied); 48(1), non-notochordal vertebrae (reversed in *Placodus*); 91(1), loss of distal tarsal 5; and 94(1), presence of a hooked fifth metatarsal (reversed in the Sauropterygia).

The Sauropterygia and the Lepidosauriformes (Lepidosauromorpha) share the following synapomorphies: 22(1), loss of the lower temporal arch (this character interpretation depends on ACCTRAN optimization and inclusion of turtles in the analysis); 50(1), dorsal intercentra absent (shared with turtles); 81(1), thyroid foramen present (shared with turtles); 87(1), perforating artery passing proximal to astragalus (shared with turtles; see Rieppel, 1993c); and 90(1), distal tarsal 1 absent.

The monophyly of the Sauropterygia, including the Placodontia and the Eosauropterygia, is supported by a number of synapomorphies with a CI of 1: 7(2), loss of lacrimal; 32(1), akinetic palate (convergent within turtles, and in crocodiles among the archosaurimorphs); 65(1), clavicles applied to the medial surface of the scapula (a character first recognized by Carroll & Gaskill, 1985); 71(1), coracoid foramen enclosed between scapula and coracoid; and 72(1), pectoral fenestration present (a

character first recognized by Storrs, 1991). A number of additional features with a CI of 0.5–1 support the monophyly of the Sauropterygia: 1(1), large premaxillae, forming most of the snout (convergent in archosauromorphs); 9(2), elongation of the postorbital skull (reversed in pachypleurosaurs and *Pistosaurus,* convergent in some turtles); 22(2), lower temporal fossa open ventrally (convergent, if not homologous [as by ACCTRAN optimization] in lepidosauriforms; see discussion in Rieppel, 1993a); 26(1), paroccipital process trending posteriorly; 34(0), loss of the infraorbital fenestra (see discussion of character 34 above); 43(1), anterior (premaxillary and anterior dentary) teeth procumbent (reversed in pachypleurosaurs); 51(1), cervical intercentra absent; 58(1), three sacral ribs; 62(1), clavicles positioned anteroventral to interclavicle (convergent in choristoderes); 67(1), posterior process on interclavicle short; 74(1), humerus angulated or "curved" (reversed in *Cymatosaurus*); 75(1), humerus with reduced epicondyles; 78(2), radius and ulna of approximately equal length; 79(1), iliac blade reduced; 85(1), distal femoral condyles not projecting markedly beyond shaft; 89(0), foot short and broad; 92(2), two tarsal ossifications (implicated by coding 92[2] for *Placodus* [fide Drevermann, 1933]; more probably, three tarsal ossifications is synapomorphic at the level of the Sauropterygia, two tarsal ossifications derived within the Sauropterygia); 93(0), fifth metatarsal long and slender; and 94(0), fifth metatarsal straight.

The complex relation of basioccipital tubera to pterygoids (character 33) was first recognized as a sauropterygian synapomorphy by Zanon (1989). Under ACCTRAN character optimization, the ventral occipital tubera are synapomorphic at the level of the Sauropterygia, and the lateral basioccipital tubera are synapomorphic at the subordinated level of the Eosauropterygia, the phylogenetic interpretation implying a transformation from ventrally to laterally directed basioccipital tubera. This transformational hypothesis cannot be maintained on the basis of DELTRAN character optimization, which renders ventrally directed basioccipital tubera in complex relation to the pterygoids an autapomorphy of placodonts.

Within the Sauropterygia, placodonts (represented by *Placodus* in this analysis) are the sister-group of the monophyletic Eosauropterygia. Synapomorphies of the Eosauropterygia include the following characters with a CI of 0.5 or higher: 33(2), basioccipital tubera in complex lateral relation to pterygoids (unknown for pachypleurosaurs); 53(1), zygosphene–zygantrum articulation present; 54(1), expanded articular facets of centrum to support the neural arch (coded unknown for *Corosaurus*; DELTRAN optimization delays the origin of the character to the base of the Eosauropterygia exclusive of *Corosaurus*); 64(1), clavicles with expanded anterolateral corners (reversals implied within pachypleurosaurs); and 68(1), scapular blade reduced. Eosauropterygia other than *Corosaurus* constitute an unnamed monophyletic taxon diagnosed by the following synapomorphies with a CI of 0.5–1: 26(2), occiput platelike, without distinct paroccipital processes and with much reduced posttemporal fossae; 39(0), absence of a distinct coronoid process (CI = 0.429, convergent among turtles); 61(0), clavicles broad medially; 63(1), clavicles meet in an anteroventral suture; and 84(2), intertrochanteric fossa absent.

With *Corosaurus* being the sister-group of a clade comprising the pachypleurosaurs and Eusauropterygia, the synapomorphies supporting the monophyly of the Pachypleurosauroidea are the following: 9(1), postorbital skull subequal in length to preorbital skull (secondary reversal); 10(2), upper temporal fossae considerably smaller than orbit; 37(1), ectopterygoid bone absent; 43(0), anterior teeth not procumbent (secondary reversal); and 79(2), iliac blade absent, i.e., reduced to simple dorsal process. The Eusauropterygia are diagnosed by the following: 6(1), separation of nasals by premaxillary–frontal contact (reversals and convergence among pachypleurosaurs implied); 11(1), frontal bones fused in the adult; 14(1), parietal fused in adult; 49(1), platycoelous vertebrae; 76(1), ectepicondylar groove open but without notch; and 92(1), three tarsal ossifications (reversed in *Lariosaurus*; see also discussion above).

Simosaurus is the sister-group to all other eusauropterygian taxa included in the analysis, a result that corroborates earlier findings (Sues, 1987a; Rieppel, 1989a). The following characters (with a CI equal to or larger than 0.5, and with ACCTRAN and DELTRAN optimization implemented) group the *Cymatosaurus–Nothosaurus–Lariosaurus–Pistosaurus* clade to the exclusion of *Simosaurus*: 24(1), quadratojugal absent; 36(1), premaxillae excluded from internal nares; 44(1), premaxillary and anterior dentary fangs present; and 45(1), maxillary fang(s) present. With DELTRAN character optimization implemented, the elongated symphysis (40[1], CI = 0.33) becomes a synapomorphy of the *Cymatosaurus–Nothosaurus–Lariosaurus–Pistosaurus* clade, convergent in *Placodus*; with ACCTRAN character optimiza-

tion implemented, the character is a synapomorphy of the Sauropterygia, reversed in pachypleurosaurs and *Simosaurus*.

The concept of the Nothosauriformes (Storrs, 1991, 1993a), with the Placodontia nested within the Sauropterygia as sister-taxon of the Eusauropterygia, was based on relatively few characters (Storrs, 1991; Rieppel, 1993a), corresponding to characters 9(2), 40(1), 74(1), and 78(2) of this analysis. Within a broader frame of comparison, however, and using ACCTRAN as well as DELTRAN character optimization, the elongation of the postorbital region of the skull (character 9[2]) becomes synapomorphic at the level of the Sauropterygia and reversed in pachypleurosaurs; in this analysis, the elongation of the postorbital region of the skull is considered to be interdependent with the increase in size of the upper temporal fossa (character 10[1]). Angulation of the humerus is synapomorphic at the level of the Sauropterygia (character 74[1], reversed in *Cymatosaurus*), and so is the subequal length of radius and ulna (character 78[2], reversed within pachypleurosaurs).

With a well-corroborated pattern of sauropterygian interrelationships becoming apparent, the ground is prepared for a process interpretation of that pattern (Brooks & McLennan, 1991) in terms of sauropterygian adaptations to the aquatic environment. With *Placodus* as sister-taxon of the Eosauropterygia, it appears that durophagous and piscivorous habits were two options explored at the initial invasion of the western Tethyan sea during the Middle Triassic (early Anisian) marine transgression in central Europe. Whereas *Corosaurus* seems to represent an early sauropterygian offshoot of the eastern Pacific province, stem-group sauropterygians diversified in the Tethyan province (although new evidence indicates a greater diversity of Middle Triassic sauropterygians in the eastern Pacific province than previously assumed; Sander et al., 1994). Sues (1987a) presented the first cladistic analysis of stem-group Sauropterygia (without inclusion of *Corosaurus*), corroborating the basal dichotomy between pachypleurosaurs and the Eusauropterygia (already alluded to in the earlier literature) and providing the basis for the claim that there was, within the Eusauropterygia, a continuous trend toward increasingly marine habits with a shift from limb-mediated propulsion to underwater flight (see also Storrs, 1993b). Whereas the overall trend still remains apparent in the transition from stem-group eusauropterygians to crown-group plesio- and pliosaurs, a more refined hypothesis of interrelationships of the Eusauropterygia is still not available on which to base a more critical assessment of functional and paleoecological correlates of sauropterygian evolution. Resolution of interrelationships among stem-group eusauropterygians remains poor on the basis of presently available data, but the functional interpretation of the skeleton of *Simosaurus* indicates complex synecological relations between the taxa. Niche partitioning appears to have occurred along two principal vectors—prey type and prey size—yet more research on the interrelationships of the stem-group sauropterygians is required (at the level of genera and species) to allow more detailed inferences.

Different character optimization strategies can, in this context, drastically alter paleoecological interpretations of cladistic relationships. A case in point is the posterior concavity on the quadrate bone, taken as indicator for the presence of a relatively large tympanic membrane in correlation with an impedance-matching middle ear. On an earlier occasion, I used (Rieppel, 1989a) the presence of a posteriorly concave quadrate in pachypleurosaurs in support of Sues's (1987a) interpretation that this group was restricted to lagoonal or shallow-water marine environments. In view of the fact that a posteriorly excavated quadrate is also present in placodonts (sister-group of the Eosauropterygia), and accepting the pachypleurosaurs as sister-group of the Eusauropterygia, it seemed that pachypleurosaurs represented the relatively plesiomorphic condition (with respect to that character) and that the loss of the posterior excavation of the quadrate (i.e., the implied loss of the impedance-matching middle ear) was part of the more pronounced adaptations to a marine environment in the Eusauropterygia. Within the broader context of comparison pursued in this analysis, the above interpretation is supported by DELTRAN character optimization only, which treats the loss of the posterior excavation of the quadrate (i.e., the loss of the impedance-matching middle ear) as a synapomorphy of the Eusauropterygia convergent in *Corosaurus*. With ACCTRAN character optimization, the straight posterior edge of the quadrate becomes a synapomorphy of the Eosauropterygia, and the posteriorly excavated quadrate a synapomorphic reversal in pachypleurosaurs. Using the same logic of argumentation, pachypleurosaurs would thus come to represent a clade that invaded the lagoonal basins along the coastal areas of the Tethyan sea coming from a more open marine environment. Again, increased cladistic resolution is required in conjunction with

independent paleoecological clues to provide greater insight into the evolutionary history of the Sauropterygia and their successful invasion into Mesozoic seas.

Acknowledgments

I am greatly indebted to a number of colleagues who provided free access to sauropterygian collections in their care and therewith made this study possible in the first place. My sincere thanks go to R. L. Carroll and L. Kebang, Redpath Museum, Montreal; K. Bartlett, Children's Museum, Indianapolis; H. Hagdorn, Muschelkalkmuseum Ingelfingen; H. Haubold, Martin-Luther Universität, Halle; W.-D. Heinrich, Museum für Naturkunde, Berlin; A. Liebau, Geologisch-Paläontologisches Institut der Universität, Tübingen; A. C. Milner, The Natural History Museum, London; G. Plodowski, Senckenberg Museum, Frankfurt a.M.; H. U. Schlüter, Bundesanstalt für Geowissenschaften und Rohstoffe, Berlin; P. Wellnhofer, Bayerische Staatssammlung für Paläontologie und historische Geologie, Munich; and R. Wild, Staatliches Museum für Naturkunde, Stuttgart. I am particularly indebted to H. Hagdorn and R. Wild, who freely shared their expertise with Muschelkalk fossils with me. Figure 2 was prepared on the basis of data provided by H. Hagdorn. The painstaking printing of the photographs was completed by J. L. Balodimas. Two anonymous reviewers and the following colleagues read part or all of earlier drafts of this manuscript, offering much helpful advice and criticism: R. L. Carroll, Montreal; M. Caldwell, Montreal; J. A. Hopson, Chicago; J. A. Gauthier, San Francisco; H.-D. Sues, Toronto; R. Wild, Stuttgart; H. Hagdorn, Ingelfingen; G. W. Storrs, Bristol; and M. J. Benton, Bristol. I am particularly indebted to Mario de Pinna for setting my mind straight on the nature of unrooted networks. My thanks also go to M. Laurin and R. R. Reisz for many stimulating discussions on turtle relationships and for the permission to quote from their manuscript. This work was supported by NSF grant DEB-9220540.

Literature Cited

AGASSIZ, L. 1833–1845. Recherches sur les Poissons Fossiles. Imprimerie de Petitpierre, Neuchâtel.

ALBERTI, F.v. 1864. Überblick über die Trias mit Berücksichtigung ihres Vorkommens in den Alpen. J. G. Cotta, Stuttgart.

ALEXANDER, R. MCN. 1983. Animal Mechanics, 2nd ed. Hutchinson, London.

ARTHABER, G. 1924. Die Phylogenie der Nothosaurier. Acta Zoologica, Stockholm, **5:** 439–516.

BAUR, G. 1887. On the phylogenetic arrangement of the Sauropsida. Journal of Morphology, **1:** 93–104.

BELLAIRS, A. D'A., AND A. M. KAMAL. 1981. The chondrocranium and the development of the skull in Recent reptiles. *In* Gans, C., and T. S. Parsons, eds., Biology of the Reptilia, **11:** 1–263. Academic Press, London.

BENTON, M. J. 1983. The Triassic reptile *Hyperodapedon* From Elgin: Functional morphology and relationships. Philosophical Transactions of the Royal Society of London, B, **302:** 605–720.

———. 1985. Classification and phylogeny of the diapsid reptiles. Zoological Journal of the Linnean Society, **84:** 97–164.

———. 1990. Phylogeny of the major tetrapod groups; Morphological data and divergence dates. Journal of Molecular Evolution, **30:** 409–424.

———. 1991. Amniote phylogeny, pp. 317–330. *In* Schultze, H.-P., and L. Trueb, eds., Origins of the Higher Groups of Tetrapods, Controversy and Consensus. Comstock, Ithaca, N.Y.

BOULENGER, G. A. 1898. On a nothosaurian reptile from the Trias of Lombardy, apparently referable to *Lariosaurus*. Transactions of the Zoological Society of London, **14:** 1–10.

BROILI, F. 1912. Zur Osteologie des Schädels von *Placodus*. Palaeontographica, **59:** 147–155.

BROOKS, D. R., AND D. A. MCLENNAN. 1991. Phylogeny, Ecology, and Behavior. The University of Chicago Press, Chicago.

BROWN, D. S. 1981. The English Upper Jurassic Plesiosauroidea (Reptilia) and a review of the phylogeny and classification of the Plesiosauria. Bulletin of the British Museum (Natural History), Geology Series, **35:** 253–347.

CARROLL, R. L. 1969. Problems of the origin of reptiles. Biological Reviews, **44:** 393–432.

———. 1975. Permo-Triassic "lizards" from the Karroo. Palaeontographica Africana, **18:** 71–87.

———. 1981. Plesiosaur ancestors from the Upper Permian of Madagascar. Philosophical Transactions of the Royal Society of London, B, **293,** 315–383.

———. 1985. A pleurosaur from the Lower Jurassic and the taxonomic position of the Sphenodontida. Palaeontographica, A, **189:** 1–28.

CARROLL, R. L., AND P. J. CURRIE. 1991. The early radiation of diapsid reptiles, pp. 354–424. *In* Schultze, H.-P., and L. Trueb, eds., Origins of the Higher Groups of Tetrapods, Controversy and Consensus. Comstock, Ithaca, N.Y.

CARROLL, R. L., AND P. GASKILL. 1985. The nothosaur *Pachypleurosaurus* and the origin of plesiosaurs. Philosophical Transactions of the Royal Society of London, B, **309:** 343–393.

CARROLL, R. L., AND W. LINDSAY. 1985. Cranial anatomy of the primitive reptile *Procolophon*. Canadian Journal of Earth Sciences, **22:** 1571–1587.

CHATTERJEE, S. 1974. A rhynchosaur from the Upper

Triassic Maleri Formation of India. Philosophical Transactions of the Royal Society of London, B, **267**: 209–261.

———. 1980. *Malerisaurus*, a new eosuchian reptile from the Late Triassic of India. Philosophical Transactions of the Royal Society of London, B, **291**: 163–200.

COLBERT, E. H. 1955. Evolution of the Vertebrates, 1st ed. John Wiley and Sons, New York.

———. 1970. The Triassic gliding reptile *Icarosaurus*. Bulletin of the American Museum of Natural History, **143**: 85–142.

CORROY, G. 1928. Les vertébrés du Trias de Lorraine et le Trias Lorrain. Annales de Paléontologie, **17**: 83–136.

CURRIE, P. J. 1981. *Hovasaurus boulei*, an aquatic Eosuchian from the Upper Permian of Madagascar. Palaeontologica Africana, **24**: 99–168.

———. 1982. The osteology and relationships of *Tangasaurus mennelli* Haughton (Reptilia; Eosuchia). Annals of the South African Museum, **86**: 247–265.

DEMAR, R., AND H. R. BARGHUSEN. 1972. Mechanics and the evolution of the synapsid jaw. Evolution, **26**: 622–637.

DE QUEIROZ, K., AND J. GAUTHIER. 1990. Phylogeny as a central principle in taxonomy: Phylogenetic definitions of taxon names. Systematic Zoology, **39**: 307–322.

———. 1992. Phylogenetic taxonomy. Annual Review of Ecology and Systematics, **23**: 449–480.

———. 1993. Toward a phylogenetic system of biological nomenclature. Tree, **9**: 27–31.

DREVERMANN, F. 1933. Das Skelett von *Placodus gigas* Agassiz im Senckenberg-Museum. Abhandlungen der Senckenbergischen Naturforschenden Gesellschaft, **38**: 319–382.

EDINGER, T. 1935. *Pistosaurus*. Neues Jahrbuch für Mineralogie, Geologie und Paläontologie, Abhandlungen, Abteilung B, **74**: 321–359.

EDMUND, A. G. 1960. Tooth replacement phenomena in the lower vertebrates. Life Science Division, Royal Ontario Museum, Contributions, **52**: 1–190.

———. 1969. Dentition. *In* Gans, C., and T. S. Parsons, eds., Biology of the Reptilia, **1**: 117–200. Academic Press, London.

EERNISSE, D. J., AND A. G. KLUGE. 1993. Taxonomic congruence versus total evidence, and amniote phylogeny inferred from fossils, molecules, and morphology. Molecular and Biological Evolution, **10**: 1170–1195.

EVANS, S. E. 1980. The skull of a new eosuchian reptile from the Lower Jurassic of South Wales. Zoological Journal of the Linnean Society, **70**: 81–116.

———. 1981. The postcranial skeleton of the Lower Jurassic eosuchian *Gephyrosaurus bridensis*. Zoological Journal of the Linnean Society, **73**: 81–116.

———. 1988. The early history and relationships of the Diapsida. *In* Benton, M. J., ed., The Phylogeny and Classification of the Tetrapods, **1**: 221–260. Clarendon Press, Oxford.

EVANS, S. E., AND H. HAUBOLD. 1987. A review of the Upper Permian genera *Coelurosauravus, Weigeltisaurus*, and *Gracilisaurus* (Reptilia: Diapsida). Zoological Journal of the Linnean Society, **90**: 275–303.

FRAAS, E. 1896. Die Schwäbischen Trias-Saurier. E. Schweizerbart, Stuttgart.

FRASER, N. C. 1982. A new rhynchocephalian from the British Upper Trias. Palaeontology, **25**: 709–725.

———. 1988a. New Triassic sphenodontids from South-West England and a review of their classification. Palaeontology, **29**: 125–186.

———. 1988b. The osteology and relationships of *Clevosaurus* (Reptilia: Sphenodontida). Philosophical Transactions of the Royal Society of London, B, **321**: 125–178.

FRASER, N. C., AND G. M. WALKDEN. 1984. The postcranial skeleton of the Upper Triassic sphenodontid *Planocephalosaurus robinsonae*. Palaeontology, **27**: 575–595.

FREYBERG, B.v. 1972. Die erste erdgeschichtliche Erforschungsphase Mittelfrankens (1840–1847). Eine Briefsammlung zur Geschichte der Geologie. Erlanger Geologische Abhandlungen, **92**: 1–33.

FRITSCH, K.v. 1894. Beitrag zur Kenntnis der Saurier des Halle'schen unteren Muschelkalkes. Abhandlungen der Naturforschenden Gesellschaft zu Halle, **20**: 273–302.

GAFFNEY, E. S. 1972. An illustrated glossary of turtle skull nomenclature. American Museum Novitates, **3486**: 1–33.

———. 1979a. An introduction to the logic of phylogeny reconstruction, pp. 79–111. *In* Cracraft, J., and N. Eldredge, eds., Phylogenetic Analysis and Paleontology. Columbia University Press, New York.

———. 1979b. Comparative cranial morphology of recent and fossil turtles. Bulletin of the American Museum of Natural History, **164**: 65–376.

———. 1990. The comparative osteology of the Triassic turtle *Proganochelys*. Bulletin of the American Museum of Natural History, **194**: 1–263.

GAFFNEY, E. S., AND P. A. MEYLAN. 1988. A phylogeny of turtles. *In* Benton, M. J., ed., The Phylogeny and Classification of the Tetrapods, **1**: 157–219. Clarendon Press, Oxford.

GANS, C., AND W. J. BOCK. 1965. The functional significance of muscle architecture—A theoretical analysis. Ergebnisse der Anatomie und Entwicklungsgeschichte, **38**: 115–142.

GANS, C., AND F. DE VREE. 1987. Functional bases of fibre length and angulation in muscle. Journal of Morphology, **192**: 63–85.

GANS, C., F. DE VREE, AND D. CARRIER. 1985. Usage pattern of the complex masticatory muscles in the shingleback lizard, *Trachydosaurus rugosus*: A model for muscle placement. American Journal of Anatomy, **173**: 219–240.

GAUTHIER, J. A. 1984. A cladistic analysis of the higher systematic categories of the Diapsida. Ph.D. thesis, University of California, Berkeley. Univ. Microfilm, Int., No. 85-128525, Ann Arbor, Mich.

GAUTHIER, J. A., R. ESTES, AND K. DE QUEIROZ. 1988. A phylogenetic analysis of Lepidosauromorpha, pp. 15–98. *In* Estes, R., and G. Pregill. G., eds., Phylogenetic Relationships of the Lizard Families. Clarendon Press, Oxford.

GAUTHIER, J. A., A. G. KLUGE, AND T. ROWE. 1988. Amniote phylogeny and the importance of fossils. Cladistics, **4:** 104–209.

GERVAIS, P. 1859. Zoologie et Paléontologie Françaises, 2nd ed. Arthus Bertrand, Paris.

GIEBEL, C. G.1847. Fauna der Vorwelt mit steter Berücksichtigung der lebenden Thiere. Brockhaus, Leipzig.

GODFREY, S. J. 1984. Plesiosaur subaqueous locomotion: A reappraisal. Neues Jahrbuch für Geologie und Paläontologie, Monatshefte, **1984:** 661–672.

GOW, C. 1975. The morphology and relationships of *Youngina capensis* Broom and *Prolacerta broomi* Parrington. Paleontologica Africana, **18**, 89–131.

GREGORY, J. T. 1944. Osteology and relationships of *Trilophosaurus*. The University of Texas Publications, Contributions to Geology, **4401:** 273–359.

HAAS, G. 1966. On the vertebral centra of nothosaurs and placondonts from the Muschelkalk of Wadi Ramon, Israel. Colloques Internationaux du Centre de la Recherche Scientifique, Paris, **163:** 329–334.

HAGDORN, H. 1991. The Muschelkalk in Germany—An introduction, pp. 7–21. *In* Hagdorn, H., ed., Muschelkalk, A Field Guide. Korb, Stuttgart.

HEATON, M. J. 1979. Primitive captorhinid reptiles from the Late Pennsylvanian and Early Permian of Oklahoma and Texas. Oklahoma Geological Survey, Bulletin, **127:** 1–84.

HEATON, M. J., AND R. R. REISZ. 1980. A skeletal reconstruction of the early Permian captorhinid reptile *Eocaptorhinus laticeps* (Williston). Journal of Paleontology, **54:** 136–143.

———. 1986. Phylogenetic relationships of captorhinomorph reptiles. Canadian Journal of Earth Sciences, **23:** 402–418.

HUENE, F.v. 1921. Neue Beobachtungen an *Simosaurus*. Acta Zoologica, Stockholm, **1921:** 201–239.

———. 1936. *Henodus chelydrops,* ein neuer Placodontier. Palaeontographica, A, **84:** 99–148.

———. 1944. Ein beachtenswerter Humerus aus dem untersten Muschelkalk und seine Bedeutung. Neues Jahrbuch für Mineralogie, Geologie und Paläontologie, Monatshefte, Abteilung B, (8): 223–227.

———. 1948. *Simosaurus* and *Corosaurus*. American Journal of Science, **246:** 41–43.

———. 1952. Skelett und Verwandtschaft von *Simosaurus*. Palaeontographica, A, **113:** 163–182.

———. 1956. Paläontologie und Phylogenie der Niederen Tetrapoden. Gustav Fischer, Jena.

———. 1958. Aus den Lechtaler Alpen ein neuer *Anarosaurus*. Neues Jahrbuch für Geologie und Paläontologie, Monatshefte, **1958**(8/9): 382–384.

———. 1959. *Simosaurus guilielmi* aus dem unteren Mittelkeuper von Obersontheim. Palaeontographica, A, **113:** 180–184.

JAEKEL, O. 1905. Über den Schädelbau der Nothosauridae. Sitzungsberichte der Gesellschaft Naturforschender Freunde in Berlin, **1905:** 60–84.

———. 1907. *Placochelys placodonta* aus der Obertrias des Bakony. Resultate der Wissenschaftlichen Erforschung des Balatonsees. I. Band. 1. Teil. Palaeontologie—Anhang. Victor Hornyánzky, Budapest, pp. 1–91, Pls. I–X.

———. 1910. Über das System der Reptilien. Zoologischer Anzeiger, **35:** 324–341.

KOKEN, E. 1893. Beiträge zur Kenntnis der Gattung *Nothosaurus*. Zeitschrift der Deutschen Geologischen Gesellschaft, **45:** 338–377.

KUHN, O. 1934. Fossilium Catalogus. I: Animalia. Pars 69: Sauropterygia. W. Junk's–Gravenhage.

KUHN-SCHNYDER, E. 1942. Über einen weiteren Fund von *Paraplacodus broili* PEYER aus der Trias des Monte San Giorgio. Eclogae Geologicae Helvetiae, **35:** 174–183.

———. 1959. Ein neuer Pachypleurosaurier von der Stulseralp bei Bergün (Kt. Graubünden, Schweiz). Eclogae Geologicae Helvetiae, **52:** 639–658.

———. 1961. Der Schädel von *Simosaurus*. Paläontologische Zeitschrift, **35:** 95–113.

———. 1962. La position des nothosauroidés dans le système des reptiles. Colloques Internationaux du Centre National de la Recherche Scientifique, Paris, **104:** 135–144.

———. 1963. Wege der Reptiliensystematik. Paläontologische Zeitschrift, **37:** 61–87.

———. 1965. Sind die Reptilien stammesgeschichtlich eine Einheit? Umschau in Wissenschaft und Technik, **1965**(5): 149–154.

———. 1967. Das Problem der Euryapsida. Colloques Internationaux du Centre National de la Recherche Scientifique, Paris, **163:** 335–348.

———. 1980. Observations on the temporal openings of reptilian skulls and the classification of reptiles, pp. 153–175. *In* Jacobs, L. L., ed., Aspects of Vertebrate History. Museum of Northern Arizona Press, Flagstaff.

———. 1987. Die Triasfauna der Tessiner Kalkalpen. XXVI. *Lariosaurus lavizzarii* n. sp. (Reptilia, Sauropterygia). Schweizerische Paläontologische Abhandlungen, **110:** 335–348.

———. 1990. Über Nothosauria (Sauropterygia, Reptilia)—Ein Diskussionsbeitrag. Paläontologische Zeitschrift, **64:** 313–316.

LAURIN, M. 1991. The osteology of a Lower Permian eosuchian from Texas and a review of diapsid phylogeny. Zoological Journal of the Linnean Society, **101:** 59–104.

LAURIN, M., AND R. R. REISZ. 1993. The origin of turtles. Journal of Vertebrate Paleontology, **13:** 46A.

———. 1994. A reevaluation of early amniote phylogeny. Zoological Journal of the Linnean Society, in press.

LEE, M. S. Y. 1993. The origin of the turtle body plan: Bridging a famous morphological gap. Science, **261:** 1716–1720.

LYDEKKER, R. 1889. Catalogue of the Fossil Amphibia and Reptilia in the British Museum (Natural History). British Museum, London.

MAZIN, J. M. 1985. A specimen of *Lariosaurus balsami* Curioni 1847, from the eastern Pyrenees (France). Palaeontographica, A, **189:** 159–169.

MEYER, H.v. 1834. Museum Senckenberg 1. Senck-

enbergische naturforschenden Gesellschaft, Frankfurt a.M. (not seen).

———. 1842. *Simosaurus,* die Stumpfschnauze, ein Saurier aus dem Muschelkalke von Luneville. Neues Jahrbuch für Mineralogie, Geognosie, Geologie und Petrefakten-Kunde, **1842:** 184–197.

———. 1847–1855. Zur Fauna der Vorwelt. Die Saurier des Muschelkalkes mit Rücksicht auf die Saurier aus buntem Sandstein und Keuper. Heinrich Keller, Frankfurt a.M.

———. 1860. *Lamprosaurus Göpperti,* aus dem Muschelkalke von Krappitz in Ober-Schlesien. Palaeontographica, **7:** 245–247.

———. 1863. Die Placodonten, eine Familie von Sauriern der Trias. Palaeontographica, **11:** 175–221.

Meyer, H.v., and T. Plieninger. 1844. Beiträge zur Paläontologie Württembergs. E. Schweizerbart, Stuttgart.

Moodie, R. L. 1908. Reptilian epiphyses. The American Journal of Anatomy, **7:** 442–467.

Nopcsa, F. 1928. Palaeontological notes on reptiles. Geologica Hungaria, Series Palaeontologia, **1:** 3–84.

Nosotti, S., and G. Pinna. 1993a. *Cyamodus kuhnschnyderi* n.sp., nouvelle espèce de Cyamodontidae (Reptilia, Placodontia) du Muschelkalk supérieur allemand. Comptes Rendues à l'Académie des Sciences, Paris, Série II, **317:** 847–850.

———. 1993b. New data on placodont skull anatomy. Paleontologia Lombarda, n.s., **2:** 109–114.

Oelrich, T. M. 1956. The anatomy of the head of *Ctenosaura pectinata* (Iguanidae). Miscellaneous Publications Museum of Zoology, University of Michigan, **94:** 1–122.

Olson, E. C. 1961. Jaw mechanics: Rhipidistians, amphibians, reptiles. American Zoologist, **1:** 205–215.

Owen, R. 1860. Palaeontology. Adam and Charles Black, Edinburgh.

Patterson, C., D. M. Williams, and C. J. Humphries. 1993. Congruence between molecular and morphological phylogenies. Annual Review of Ecology and Systematics, **24:** 153–188.

Peyer, B. 1931a. Die Triasfauna der Tessiner Kalkalpen. IV. *Ceresiosaurus calcagnii* nov. gen. nov. spec. Abhandlungen der Schweizerischen Paläontologischen Gesellschaft, **51:** 1–68.

———. 1931b. *Paraplacodus broilii* nov. gen. nov. spec., ein neuer Placodontier aus der Tessiner Trias. Centralblatt für Mineralogie, Geologie und Palaeontologie, **1931:** 570–573.

———. 1933–1934. Die Triasfauna der Tessiner Kalkalpen. VII. Neubeschreibung der Saurier von Perledo. Abhandlungen der Schweizerischen Paläontologischen Gesellschaft, **53-54:** 1–130.

———. 1935. Die Triasfauna der Tessiner Kalkalpen, VIII. Weitere Placodontierfunde. Abhandlungen der Schweizerischen Paläontologischen Gesellschaft, **55:** 1–26.

———. 1939. Die Triasfauna der Tessiner Kalkalpen, XIV. *Paranothosaurus amsleri* nov. gen. nov. spec. Abhandlungen der Schweizerischen Paläontologischen Gesellschaft, **62:** 1–87.

Pinna, G. 1989. Sulla regione temporo–jugale dei rettili placodonti e sulle relazione fra placodonti e ittiotterigi. Atti della Società Italiana di Scienze Naturali e del Museo Civico di Storia Naturale di Milano, **130:** 149–158.

———. 1990. Notes on stratigraphy and geographical distribution of placodonts. Atti della Società Italiana di Scienze Naturali e del Museo Civico di Storia Naturale di Milano, **131:** 145–156.

Pinna, G., and S. Nosotti. 1989. Anatomia, morfologia funzionale e paleoecologia del rettile placodonte *Psephoderma alpinum* Meyer, 1858. Memorie della Società Italiana de Scienze Naturali e del Museo Civico di Storia Naturale di Milano, **25:** 15–50.

Platnick, N. I., C. E. Griswold, and J. A. Coddington. 1991. On missing entries in cladistic analysis. Cladistics, **7:** 337–343.

Reisz, R. R. 1981. A diapsid reptile from the Pennsylvanian of Kansas. Special Publications, Museum of Natural History, University of Kansas, **7:** 1–74.

Reisz, R. R., D. S. Berman, and D. Scott. 1984. The anatomy and relationships of the Lower Permian reptile *Araeoscelis.* Journal of Vertebrate Paleontology, **4:** 57–67.

Reisz, R. R., and M. Laurin. 1991. *Owenetta* and the origin of turtles. Nature (London), **349:** 324–326.

Rieppel, O. 1977. Über die Entwicklung des Basicraniums bei *Chelydra serpentina* Linnaeus (Chelonia) und *Lacerta sicula* Rafinesque (Lacertilia). Verhandlungen der Naturforschenden Gesellschaft Basel, **86:** 153–170.

———. 1978. Streptostyly and muscle function in lizards. Experientia, **34:** 776–777.

———. 1984. Miniaturization of the lizard skull: Its functional and evolutionary implications. *In* Ferguson, M. W. J., ed., The Structure, Development and Evolution of Reptiles. Symposia of the Zoological Society of London, **52:** 503–520. Academic Press, London.

———. 1985. Minaturization of the tetrapod head: Muscle fibre length as a limiting factor. *In* Riess, J., and E. Frey, eds., Principles of Construction in Fossil and Recent Reptiles. Konzepte SFB, **230**(4): 121–138. Attempo Verlag, Tübingen.

———. 1987. The Pachypleurosauridae: An annotated bibliography. With comments on some lariosaurs. Eclogae Geologicae Helvetiae, **80:** 1105–1118.

———. 1989a. A new pachypleurosaur (Reptilia: Sauropterygia) from the Middle Triassic of Monte San Giorgio, Switzerland. Philosophical Transactions of the Royal Society of London, B, **323:** 1–73.

———. 1989b. The hind limb of *Macrocnemus bassanii* (Reptilia, Diapsida): Development and functional anatomy. Journal of Vertebrate Paleontology, **9:** 373–387.

———. 1993a. Euryapsid relationships: A preliminary analysis. Neues Jahrbuch für Geologie und Paläontologie, Abhandlungen, **188:** 241–264.

———. 1993b. Status of the pachypleurosauroid *Psilotrachelosaurus toeplitschi* Nopcsa (Reptilia, Sauropterygia), from the Middle Triassic of Austria. Fieldiana: Geology, n.s., **27:** 1–17.

———. 1993c. Studies on skeleton formation in rep-

tiles. IV. The homology of the reptilian (amniote) astragalus revisited. Journal of Vertebrate Paleontology, **13:** 31–47.

———. 1993d. Review of the Pachypleurosauroidea. Journal of Vertebrate Paleontology, **13:** 54A (abstract).

———. 1993e. Studies on skeleton formation in reptiles: Patterns of ossification in the skeleton of *Chelydra serpentina* (Reptilia, Testudines). Journal of Zoology, London, **231:** 487–509.

———. 1994a. The braincases of *Simosaurus* and *Nothosaurus*: Monophyly of the Nothosauridae (Reptilia: Sauropterygia). Journal of Vertebrate Paleontology, **14:** 9–23.

———. 1994b. Status of *Nothosaurus juvenilis* Edinger 1921 (Reptilia, Sauropterygia), from the Middle Triassic of Germany. Palaeontology, in press.

———. 1995. The status of *Anarosaurus multidentatus* Huene (Reptilia, Sauropterygia), from the Lower Anisian of the Lechtaler Alps (Arlberg, Austria). Paläontologische Zeitschrift, in press.

RIEPPEL, O., AND L. LABHARDT. 1979. Mandibular mechanics in *Varanus niloticus* (Reptilia, Lacertilia). Herpetologica, **35:** 158–163.

RIEPPEL, O., AND R. WILD. 1994. *Nothosaurus edingerae* Schultze 1970: Diagnosis of the species and comments on its stratigraphical occurrence. Stuttgarter Beiträge zur Naturkunde, Serie B (Geologie und Paläontologie), in press.

ROBINSON, P. L. 1962. Gliding lizards from the Upper Keuper of Great Britain. Proceedings of the Geological Society of London, **1601:** 137–146.

———. 1973. A problematical reptile from the British Upper Triassic. Journal of the Geological Society of London, **129:** 457–479.

ROMER, A. S. 1956. Osteology of the Reptiles. The University of Chicago Press, Chicago.

———. 1968. Notes and Comments on Vertebrate Paleontology. University of Chicago Press, Chicago.

SANDER, P. M. 1989. The pachypleurosaurids (Reptilia: Nothosauria) from the Middle Triassic of Monte San Giorgio, (Switzerland), with the description of a new species. Philosophical Transactions of the Royal Society of London, B, **325:** 561–670.

SANDER, P. M., O. C. RIEPPEL, AND H. BUCHER. 1994. A new marine vertebrate fauna from the Middle Triassic of Nevada. Journal of Paleontology, **68:** 676–680.

SANZ, J. L. 1983. Consideraciones sobre el genero *Pistosaurus*. El suborden Pistosauria (Reptilia, Sauropterygia). Estudios Geologicos, **39:** 451–458.

SCHMIDT, K. P. 1927. New reptilian generic names. Copeia, **1927**(163): 58–59.

SCHMIDT, M. 1928. Die Lebewelt unserer Trias. F. Rau, Öhringen.

SCHMIDT, S. 1987. Phylogenie der Sauropterygier (Diapsida; Trias-Kreide). Neues Jahrbuch für Geologie und Paläontologie, Abhandlungen, **173:** 339–375.

———. 1988. Die Nothosaurier des Crailsheimer Muschelkalks, pp. 144–150. *In* Hagdorn, H., ed., Neue Forschungen zur Erdgeschichte von Crailsheim. W. K. Weidert, Stuttgart.

SCHRAMMEN, A. 1899. 3. Beitrag zur Kenntnis der Nothosauriden des unteren Muschelkalkes in Oberschlesien. Zeitschrift der Deutschen Geologischen Gesellschaft, **51:** 388–408.

SCHRÖDER, H. 1914. Wirbeltiere der Rüdersdorfer Trias. Abhandlungen der Königlich Preussischen Geologischen Landesanstalt, Neue Folge, **65:** 1–98.

SCHULTZE, H.-P. 1970. Über *Nothosaurus*. Neubeschreibung eines Schädels aus dem Keuper. Senckenbergiana Lethaea, **51:** 211–237.

SCHUSTER, J., AND R. BLOCH. 1925. Der Unterkiefer von *Nothosaurus raabi*. Centralblatt für Mineralogie, Geologie und Paläontologie, B, **1925:** 60–62.

SIEBENROCK, F. 1894. Das Skelet der *Lacerta simony* und der Lacertidenfamilie überhaupt. Sitzungsberichte der Kaiserlichen Akademie der Wissenschaften in Wien, Mathematisch—Naturwissenschaftliche Klasse, **103:** 205–292.

SIGOGNEAU-RUSSELL, D. 1979. Les champsosaures Européns: Mise au point sur le champsosaure d'Erquelinnes (Landénien Inférieur, Belgique). Annales de Paléontologie (Vertébrés), **65:** 93–154.

———. 1981. Étude ostéologique du reptile *Simoedosaurus* (Choristodera). IIe partie. Squelette postcrânien. Annales de Paléontologie (Vertébrés), **67:** 61–140.

SIGOGNEAU-RUSSELL, D., AND D. E. RUSSELL. 1979. Étude ostéologique du reptile *Simoedosaurus* (Choristodera). Annales de Paléontologie (Vertébrés), **64:** 1–84.

STORRS, G. W. 1991. Anatomy and relationships of *Corosaurus alcovensis* (Diapsida: Sauropterygia) and the Triassic Alcova Limestone of Wyoming. Bulletin of the Peabody Museum of Natural History, **44:** 1–151.

———. 1993b. Function and phylogeny in sauropterygian (Diapsida) evolution. American Journal of Science, **293-A:** 63–90.

———. 1993a. The systematic position of *Silvestrosaurus* and a classification of Triassic sauropterygians (Neodiapsida). Paläontologische Zeitschrift, **67:** 177–191.

STORRS, G. W., AND M. A. TAYLOR. 1993. Cranial anatomy of a plesiosaur from the Triassic/Jurassic boundary of Street, Somerset, England. Journal of Vertebrate Paleontology, **13:** 59A.

SUES, H.-D. 1987a. Postcranial skeleton of *Pistosaurus* and interrelationships of Sauropterygia (Diapsida). Zoological Journal of the Linnean Society, **90:** 109–131.

———. 1987b. The skull of *Placodus* and the relationship of the Placondontia. Journal of Vertebrate Paleontology, **7:** 138–144.

SUES, H. D., AND R. L. CARROLL. 1985. The pachypleurosaurid *Dactylosaurus schroederi* (Diapsida: Sauropterygia). Canadian Journal of Earth Science, **22:** 1602–1608.

SWOFFORD, D. L. 1990. PAUP—Phylogenetic Analysis Using Parsimony, Version 3.0. Illinois Natural History Survey, Champaign.

SWOFFORD, D. L., AND D. P. BEGLE. 1993. PAUP—Phylogenetic Analysis Using Parsimony, Version 3.1.

Laboratory of Molecular Systematics, Smithsonian Institution, Washington, D.C.

TAYLOR, M. A. 1987. How tetrapods feed in water: A functional analysis by paradigm. Zoological Journal of the Linnean Society, **91:** 171–195.

———. 1992. Functional anatomy of the head of the large aquatic predator *Rhomaleosaurus zetlandicus* (Plesiosauria, Reptilia) from the Toarcian (Lower Jurassic) of Yorkshire, England. Philosophical Transactions of the Royal Society of London, B, **335:** 247–280.

TINTORI, A., AND S. RENESTO. 1990. A new *Lariosaurus* from the Kalkschieferzone (uppermost Ladinian) of Valceresio (Varese, N. Italy). Bolletino della Società Paleontologica Italiana, **29:** 309–319.

TSCHANZ, K. 1989. *Lariosaurus buzzii* n. sp. from the Middle Triassic of Monte San Giorgio (Switzerland), with comments on the classification of nothosaurs. Palaeontographica, A, **208:** 153–179.

VAUGHN, P. 1955. The Permian reptile *Araeoscelis* restudied. Bulletin of the Museum of Comparative Zoology, **113:** 305–467.

WENGER, R. 1957. Die Germanischen Ceratiten. Palaeontographica, A, **108:** 57–129.

WHITESIDE, D. I. 1986. The head skeleton of the Rhaetian sphenodontid *Diphydontosaurus avonis* gen. et sp. nov and the modernizing of a living fossil. Philosophical Transactions of the Royal Society of London, B, **312:** 379–430.

WILD, R. 1973. Die Triasfauna der Tessiner Kalkalpen. XXIII. *Tanystropheus longobardicus* Bassani (Neue Ergebnisse). Abhandlungen der Schweizerischen Paläontologischen Gesellschaft, **95:** 1–162.

———. 1987. Die Tierwelt der Keuperzeit (unter besonderer Berücksichtigung der Wirbeltiere). Natur an Rems und Murr, **1987**(6): 17–43.

WILLISTON, S. W. 1914. The osteology of some American Permian vertebrates. Journal of Geology, **22:** 364–419.

———. 1925. The Osteology of the Reptiles. Harvard University Press, Cambridge, Massachusetts.

YOUNG, C.-C. 1958. On the new Pachypleurosauroidea from Keichow, southwest China. Vertebrata PalAsiatica, **2:** 68–81.

ZANON, R. T. 1989. *Paraplacodus* and the diapsid origin of Placondontia. Journal of Vertebrate Paleontology, **9:** 47A.

Appendix I: Cladistic Analysis— Addition of Taxa and the Relationships of Turtles

The position of the Sauropterygia within the Sauria seems well supported in the analysis discussed above, but it may seem problematic in view of the similarities they have been described to share with *Claudiosaurus* (Carroll, 1981; Storrs, 1991, 1993a) and may be the result of not including certain lepidosauromorph taxa, such as *Palaeagama, Paliguana, Saurosternon,* and *Coelurosauravus* (J. A. Gauthier, pers. comm.). Data for the inclusion of these taxa were taken from Carroll (1975), Evans (1982), and Evans and Haubold (1987). A similar argument pertains to the position of turtles, since their relationships were not tested against pareiasaurs and procolophonids (Reisz & Laurin, 1991; Laurin & Reisz, 1993; Lee, 1993). Accordingly, pareiasaurs and procolophonids were entered into the analysis. The data for these groups were taken from Romer (1956), Carroll and Lindsay (1985), Laurin and Reisz (1993, 1994), Reisz and Laurin (1991), Lee (1993), and unpublished observations communicated by M. deBraga. The codings reflect a basal morphology for these latter two groups.

To bias the analysis toward parareptile relationships of turtles, the infraorbital fenestra was coded as present in turtles, pareiasaurs, and procolophonids (Laurin & Reisz, 1994) but absent in *Placodus.* Character 22 was the only multistate character coded as ordered. Rooting was on an all-zero ancestor. Heuristic search settings were random stepwise addition sequence and TBR (tree-bisection-reconnection) branch swapping with 10 replications. A total of 108 MPRs were obtained, with a TL of 395 steps, a CI of 0.580, and an RC of 0.404. The resulting strict consensus tree (Fig. 70) shows poor resolution for the incompletely known fossils *Palaeagama, Paliguana, Saurosternon,* and *Coelurosauravus.* Procolophonids and pareiasaurs are sister-taxa and together come out as sister-group to the Diapsida. Interestingly, however, the turtles are retained within the Sauria as sister-group of the Sauropterygia, even though pareiasaurs and procolophonids are included in the analysis.

To remove noise imported into the analysis by incompletely known taxa, another search was run with the identical search settings as before, but excluding *Palaeagama, Paliguana, Saurosternon,* and *Coelurosauravus.* Thirty-six trees were retained with a TL of 375 steps, a CI of 0.611, and an RC of 0.435. The turtles remain sister-group of the Sauropterygia, the turtles plus Sauropterygia come out as sister-group of the Lepidosauriformes, and all of those as sister-taxon to the archosauromorph taxa within a monophyletic Sauria in all 36 trees. Araeoscelidia, Younginiformes, and *Claudiosaurus* appear in their conventional position, whereas procolophonids and pareiasaurs again come out as sister-group to the Diapsida (Fig. 71).

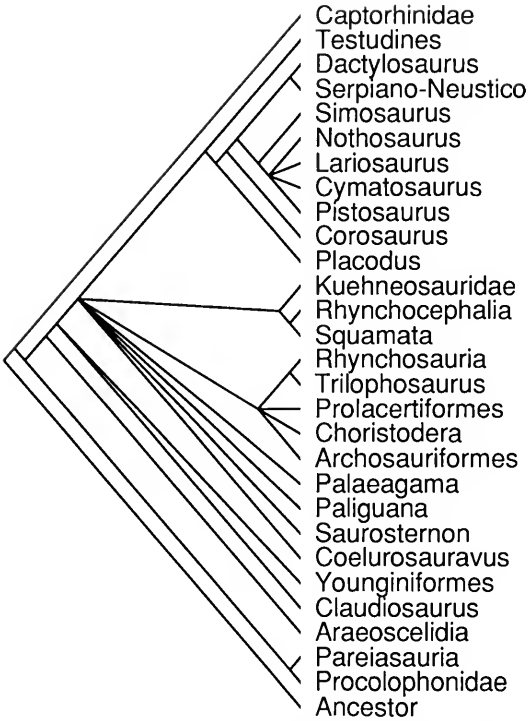

FIG. 70. Testing sauropterygian versus turtle interrelationships by the inclusion of additional taxa, some of them very incompletely known (see Table 8) (strict consensus tree of 108 MPRs; TI = 395, CI = 0.580, RC = 0.404). For further discussion, see text.

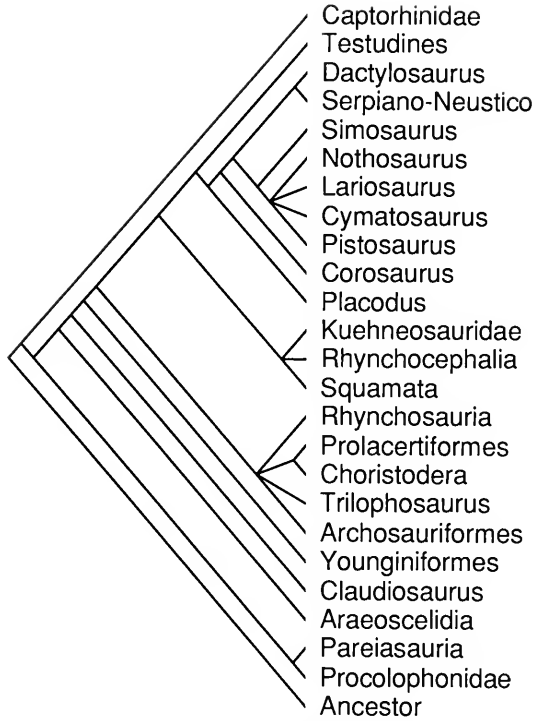

FIG. 71. Testing sauropterygian versus turtle interrelationships by the inclusion of pareiasaurs and procolophonids, but excluding very incompletely known taxa (see Table 8) (strict consensus tree of 36 MPRs; TL = 375, CI = 0.611, RC = 0.435). For further discussion, see text.

A position of turtles among crown-group diapsids is also supported by some molecular data (summarized in Benton, 1990, 1991, and Patterson et al., 1993), but not by total evidence (Eernisse & Kluge, 1993). The results remain problematical because many characters that indicate a parareptilian affinity of turtles (Laurin & Reisz, 1994) are not included in this analysis, chiefly because they are not comparable to sauropterygians and/or crown-group diapsids. The results remain interesting, however, because if nature is hierarchically ordered, and if that hierarchy is decomposable into subordinated three-taxon statements, as is generally agreed (Gaffney, 1979a), then the relative relationships of any three taxa should remain stable (if they reflect history) no matter how many taxa are later added to the analysis: the lungfish should always come out closer to the cow than to the trout, no matter how many other "fishes" or tetrapods are subsequently added to the analysis. There is, however, evidence that the addition of taxa can, under circumstances that are currently not well understood, reverse relative relationships (Gauthier et al., 1988b). In that sense, the results of the present analysis indicate the need for a more global assessment of turtle relationships, as is projected in collaboration with M. deBraga and R. R. Reisz.

Appendix II: Material Included in This Study

Institutional Abbreviations

BGR = Bundesanstalt für Geowissenschaften und Rohstoffe, Berlin (only type material or otherwise published and figured specimens are catalogued in this institution; other specimens are referred to by drawers; the prefix S specifies the stratigraphic collection; each cabinet has two rows of drawers [left and right] numbered from top to bottom); BSP = Bayerische Staatssammlung für Paläontologie und historische Geologie, Munich; BT = Oberfränkisches Erdgeschichtliches Museum, Bayreuth; CM

= Children's Museum, Indianapolis; FMNH = Field Museum of Natural History, Chicago; GPTI = Geologisch–Paläontologisches Institut der Universität, Tübingen; MB = Natural History Museum, Berlin; MHI = Muschelkalkmuseum Hagdorn, Ingelfingen; SMF = Senckenberg Museum, Frankfurt a.M.; SMNS = Staatliches Museum für Naturkunde, Stuttgart.

Material

Corosaurus alcovensis: FMNH PR480, PR1369, Alcova Limestone, Wyoming.

Cyamodus kuhn-schnyderi: SMNS 15855, 16270, upper Muschelkalk, Tiefenbach near Crailsheim (holotype and one paratype, originals of Nosotti and Pinna, 1993); SMNS 59828, upper Muschelkalk, Hegnabrunn (femur); SMNS 59825, upper Muschelkalk, Hegnabrunn (isolated dorsal vertebra).

Cymatosaurus sp: BGR uncatalogued (parietal, drawer S44/3 left), lower Muschelkalk (*Pecten*- and *Dadocrinus*-beds), Sacrau near Gogolin, Poland (former upper Silesia); BGR uncatalogued (partial skull, drawer S44/3 left), lower Muschelkalk (*Pecten*- and *Dadocrinus*-beds), Sacrau near Gogolin, Poland (former upper Silesia); BGR uncatalogued (lower jaw, drawer S44/3 left), lower Muschelkalk (*Pecten*- and *Dadocrinus*-beds), Gogolin, Poland (former upper Silesia); SMNS 58463, lower Muschelkalk, Winterswijk (humerus); Martin-Luther University Halle, uncatalogued, lower Muschelkalk (Schaumkalk), Freyburg/Unstrut (humerus).

Cymatosaurus cf. *C. silesiacus*: SMNS 10977, lower Muschelkalk, Jenzig near Jena (skull).

Cymatosaurus friedericianus: Martin-Luther Universität Halle, Institut für geologische Wissenschaften, lowermost Muschelkalk, Zementfrabrik Halle (skull, holotype, original of Fritsch, 1894).

Dactylosaurus schroederi: BGR uncatalogued, lower Muschelkalk of Gross-Stein, upper Silesia, now Kamien Gorny Slaski, Poland (original of Nopcsa, 1928); SMF R-4097a,b (cast of the holotype).

Keichousaurus sp.: CM 91.92.1., complete skeleton, Triassic, Hunan (China).

Lamprosauroides: Lower Muschelkalk [mu1], Sacrau near Gogolin (Poland), BGR uncatalogued (fragmentary maxilla).

Lariosaurus balsami: SMF R-13, Upper Triassic, Perledo; BSP AS I 802, Upper Triassic, Perledo.

Nothosaurus mirabilis: BM(NH) 42829, Muschelkalk, probably Bayreuth (skull, original of Lydekker, 1889, Fig. 83), BT uncatalogued, upper Muschelkalk, Bayreuth (original of Meyer, 1847–1855, Pl. 2, Figs. 1–2, Pl. 3, Fig. 1); SMNS 56286, upper Muschelkalk, Berlichingen a.d. Jagst (skull); SMNS 59817, upper Muschelkalk [*nodosus* biozone], Hegnabrunn (mandibular symphysis); SMNS 59818, upper Muschelkalk (*nodosus–spinosus* biozone), Hegnau (lower jaw fragment); SMNS 13155, upper Muschelkalk, Crailsheim (partial skull); SMNS 56838, upper Muschelkalk (*nodosus* biozone), Berlichingen a.d. Jagst (partial skull).

Nothosaurus oldenburgi: MB R.1, lower Muschelkalk, Rüdersdorf near Berlin (holotype, original of Schröder, 1914).

Nothosaurus procerus: MB R.4, lower Muschelkalk, Rüdersdorf near Berlin (holotype, original of Schröder, 1914).

Nothosaurus procerus var. *parva*: MB R.5, lower Muschelkalk, Rüdersdorf near Berlin (holotype, original of Schröder, 1914).

Nothosaurus raabi: MB I.007.18, lower Muschelkalk, Rüdersdorf near Berlin (holotype, original of Schröder, 1914); MB R.6, lower Muschelkalk, Rüdersdorf (lower jaw, original of Schuster & Bloch, 1925); SMF R-4546, lower Muschelkalk, Oberdorla, Thüringen (tarsus).

Nothosaurus sp.: BM(NH) 38669, Lettenkeuper?, Hoheneck (pectoral girdle); BM(NH) R-40052, Muschelkalk, Nürnberg? (humerus, original of Lydekker, 1889, Pt. II, Fig. 84. The specimen may have been purchased in Nürnberg, but since no Muschelkalk crops out in that region, it could not have been collected there.); BT uncatalogued, upper Muschelkalk, Bayreuth (pubis, original of Meyer, 1847–1855, Pl. 41, Fig. 3); MB R.150, lower Muschelkalk [Schaumkalk], Oberdorla Thüringen (torso, original of Peyer, 1939, Fig. 23); MB R.328, upper Muschelkalk, Bayreuth (interclavicle and parts of clavicles); MB R.714 (upper Muschelkalk, gastral rib, original of Koken, 1893, Pl. 11, Fig. 9); MB R.728, lower Muschelkalk, Gogolin, Poland (former upper Silesia) (clavicle); MHI 1175/1, upper Muschelkalk (Discoceratitenschichten), Wittighausen (scapula); MHI 1277, upper Muschelkalk [*dorsoplanus* biozone], Schwäbisch Hall—Gottwollshausen (scapula); SMNS 7175, upper Lettenkeuper, Hoheneck near Ludwigsburg (ulna); SMNS 1892, Lettenkeuper, Hoheneck near Ludwigsburg (ulna); SMNS 16250b, upper Muschelkalk, Bindlach near Bayreuth (humerus); SMNS 18516, upper Muschelkalk, Heldenmühle near Crailsheim (pubis); SMNS 55853, Grenzbonebed, Zwingelhausen (pubis); SMNS 56618, upper Muschelkalk (uppermost *nodosus* biozone), Hohenloher Schotterwerke, Berlichingen (complete skeleton);

SMNS 56686, upper Muschelkalk, Sommerhausen near Würzburg (ulna); SMNS 59829, upper Muschelkalk, Bindlach near Bayreuth (femur); SMNS 59821, upper Muschelkalk [Trochitenkalk], ?Bindlach near Bayreuth (ilium); SMNS 59822, upper Muschelkalk, Hegnabrunn (clavicle); SMNS 59820, upper Muschelkalk, Bindlach near Bayreuth (dorsal centrum); Martin-Luther University Halle, uncatalogued, lower Muschelkalk, Halle (humerus).

Opeosaurus suevicus: SMNS 4141, upper Muschelkalk, Stuttgart-Zuffenhausen (original of Meyer (1847–1855, p. 82, Pl. 14, Figs. 7–9).

Pachypleurosauroidea: MHI uncatalogued; lower Muschelkalk [lower Dolomites], Neidenfels (dorsal centrum).

Paraplacodus broilii: BSP 1953 XV 5, Middle Triassic, Monte San Giorgio (Switzerland).

Pistosaurus longaevus: BT, uncatalogued, upper Muschelkalk, Bayreuth (original of Meyer, 1847–1855, pp. 23–27, Pl. 22, Fig. 1; the "first specimen" of Meyer is now lost—see Edinger, 1935); MHI 1278, upper Muschelkalk (Trochitenbank 5), Neidenfels near Crailsheim (dorsal centrum).

Placochelys placodonta: MB R.1765, lower Keuper, Jerusalemer Berg near Veszprém, Hungary (original of Jaekel, 1907, Pl. 3, Fig. 1).

Placodus gigas: BSP AS VII 1209, upper Muschelkalk, Bayreuth (lower jaw); BSP 1968.I.75, upper Muschelkalk, Hegnabrunn near Kulmbach (skull, original of Broili, 1912, Pl. 14, Figs. 1–4); BT 13, upper Muschelkalk, Bayreuth (skull, original of Sues, 1987b); BT, uncatalogued, upper Muschelkalk, Bayreuth (holotype of *Placodus hypsiceps* Meyer, 1863); MHI 776, upper Muschelkalk (Discoceratitenschichten), Grombach (humerus); SMF 359, upper Muschelkalk, Bayreuth (skull, original of Broili, 1912); SMF 1035, skeleton, original of Drevermann (1933; accessible as cast only); SMF 4162, upper Muschelkalk, Bayreuth (partial skull); SMNS 18641, upper Muschelkalk [Trochitenkalk]), Crailsheim (partial skull); SMNS 59827, upper Muschelkalk (*spinosus* biozone, layer #49), Hegnabrunn (humerus); SMNS 59826, upper Muschelkalk, Hegnabrunn (dorsal centrum); SMNS uncatalogued, coll. M. Wild #1798, upper Muschelkalk, Bindlach near Bayreuth (femur).

Sauropterygia indet.: MB R.328, upper Muschelkalk, Bayreuth (incomplete pectoral girdle); SMNS 16253, lower Muschelkalk, Gogolin, Poland (former upper Silesia) (humerus, original of Huene, 1944); SMNS 59824, upper Muschelkalk (*pulcher–robustus* biozone), Bindlach near Bayreuth (interclavicle, probably *Placodus*).

Simosaurus gaillardoti:

PARTIALLY ARTICULATED SKELETONS—SMNS 14733, upper Muschelkalk, Tiefenbach near Crailsheim, skeleton described by Huene, 1952; GTPI uncatalogued, lower Gipskeuper, Obersontheim, skeleton described by Huene, 1959.

SKULLS—BSP 1932.I.13, Muschelkalk, Tiefenbach near Crailsheim; SMNS 10360, upper Muschelkalk, Neidenfels near Crailsheim (original of Jaekel, 1905; Kuhn-Schnyder, 1961; Rieppel, 1989, 1994); SMNS 11364, upper Muschelkalk, Neidenfels near Crailsheim (original of Jaekel, 1905, Fig. 4); SMNS 15860, upper Muschelkalk (Discoceratitenschichten), Tiefenbach near Crailsheim; SMNS 16639, upper Muschelkalk (Discoceratitenschichten, layer "Krüppel" below the Grenzbonebed), Tiefenbach near Crailsheim; SMNS 16700, Lettenkeuper, Hoheneck (holotype of *Simosaurus guilielmi*); SMNS 16735a, upper Muschelkalk, Tiefenbach near Crailsheim; SMNS 16767, upper Muschelkalk (Discoceratitenschichten, layer #5), Tiefenbach near Crailsheim; SMNS 18220, upper Muschelkalk (Discoceratitenschichten, layer #5), Heldenmühle near Crailsheim; SMNS 18274, upper Muschelkalk (Discoceratitenschichten), Heldenmühle near Crailsheim; SMNS 18520, upper Muschelkalk (Discoceratitenschichten), Heldenmühle near Crailsheim; SMNS 18550, upper Muschelkalk (Discoceratitenschichten, layer #19), Heldenmühle near Crailsheim; SMNS 18637, upper Muschelkalk (Discoceratitenschichten, layer #2), Heldenmühle near Crailsheim; SMNS 50714, upper Muschelkalk (Discoceratitenschichten), Schmalfelden; SMNS 50715, upper Muschelkalk (Discoceratitenschichten), Rüblingen near Kupferzell; SMNS, uncatalogued, upper Muschelkalk, Crailsheim (original of Meyer, 1847–1855, Pl. 65, Figs. 1–2); GPTI Re 1387, upper Muschelkalk, Tiefenbach near Crailsheim (original of Huene, 1921, Pls. 1–3).

LOWER JAW—SMNS 7861, upper Muschelkalk (Discoceratitenschichten), Crailsheim (original of Fraas, 1896, p. 11, Pl. 3); SMNS 16638, upper Muschelkalk (Discoceratitenschichten, layer #6, or #7), Tiefenbach near Crailsheim (original of Huene, 1952, p. 173, Fig. 58).

VERTEBRAE—SMNS 54763, upper Muschelkalk, Crailsheim (dorsal centrum).

PECTORAL GIRDLE—SMNS 7862, upper Muschelkalk, Crailsheim (original of Fraas, 1896, p. 12; Huene, 1952, p. 174, Fig. 59); SMNS 10046, upper Muschelkalk, Crailsheim (original of Huene, 1952, p. 174, Fig. 64); SMNS 15012, upper Muschelkalk (Discoceratitenschichten, layer #11), Tiefenbach

near Crailsheim (original of Huene, 1952, p. 174, Fig. 60; Sues, 1987a, p. 127; SMNS 15955, upper Muschelkalk, Tiefenbach near Crailsheim (original of Huene, 1952, p. 174, Fig. 61); SMNS 16736, upper Muschelkalk (Discoceratitenschichten, layer #8), Tiefenbach near Crailsheim (original of Huene, 1952, p. 174, Fig. 65); SMNS 17097, upper Muschelkalk (Discoceratitenschichten, layer #13), Tiefenbach near Crailsheim (right clavicle); SMNS 59823, interclavicle, upper Muschelkalk (*spinosus* biozone, layers #47–#49, Hegnabrunn near Kulmbach); SMNS 18373, upper Muschelkalk (Discoceratitenschichten, layer #7), Heldenmühle near Crailsheim (right scapula).

HUMERUS—SMNS 7956, upper Muschelkalk, Wahlheim; SMNS 17590, upper Muschelkalk, Heldenmühle near Crailsheim; SMNS 18287, upper Muschelkalk (Discoceratitenschichten, layer #2), Heldenmühle near Crailsheim; SMNS 18658, upper Muschelkalk, Lobenhausen near Crailsheim; SMNS 18686, upper Muschelkalk (Discoceratitenschichten, layer #7), Heldenmühle near Crailsheim; SMNS 52095, upper Muschelkalk, Schwenningen; SMNS uncatalogued, upper Muschelkalk, Ludwigsburg.

FEMUR—SMNS 17223, upper Muschelkalk, Heldenmühle near Crailsheim; SMNS 18038, upper Muschelkalk, Heldenmühle near Crailsheim; SMNS 18676, upper Muschelkalk (Discoceratitenschichten, layer #2), Heldenmühle near Crailsheim; SMNS 18689a, upper Muschelkalk (Discoceratitenschichten, layer #4), Heldenmühle near Crailsheim; SMNS 19052, upper Muschelkalk, Wolfsbuch near Creglingen.

TIBIA—SMNS 15978, upper Muschelkalk (Discoceratitenschichten, layer #13), Heldenmühle near Crailsheim.

A Selected Listing of Other *Fieldiana: Geology* Titles Available

A Preliminary Survey of Fossil Leaves and Well-Preserved Reproductive Structures from the Sentinel Butte Formation (Paleocene) near Almont, North Dakota. By Peter R. Crane, Steven R. Manchester, and David L. Dilcher. *Fieldiana: Geology,* n.s., no. 20, 1990. 63 pages, 36 illus.

Publication 1418, $13.00

Protoptychus hatcheri Scott, 1895. The Mammalian Faunas of the Washakie Formation, Eocene Age, of Southern Wyoming. Part II. The Adobetown Member, Middle Division (= Washakie B), Twka/2 (In Part). By William D. Turnbull. *Fieldiana: Geology,* n.s., no. 21, 1991. 33 pages, 12 illus.

Publication 1421, $13.00

A Catalogue of Type Specimens of Fossil Vertebrates in the Field Museum of Natural History. Classes Amphibia, Reptilia, Aves, and Ichnites. By John Clay Bruner. *Fieldiana: Geology,* n.s., no. 22, 1991. 51 pages, 1 illus.

Publication 1430, $15.00

The Ear Region in Xenarthrans (= Edentata: Mammalia). Part II. Pilosa (Sloths, Anteaters), Palaeanodonts, and a Miscellany. By Bryan Patterson, Walter Segall, William D. Turnbull, and Timothy J. Gaudin. *Fieldiana: Geology,* n.s., no. 24, 1992. 79 pages, 24 illus.

Publication 1438, $20.00

Comparative Microscopic Dental Anatomy in the Petalodontida (Chondrichthyes, Elasmobranchii). By Rainer Zangerl, H. Frank Winter, and Michael C. Hansen. *Fieldiana: Geology,* n.s., no. 26, 1993. 43 pages, 35 illus.

Publication 1445, $16.00

Status of the Pachypleurosauroid *Psilotrachelosaurus toeplitschi* Nopcsa (Reptilia, Sauropterygia), from the Middle Triassic of Austria. By Olivier Rieppel. *Fieldiana: Geology,* n.s., no. 27, 1993. 17 pages, 9 illus.

Publication 1448, $10.00

Order by publication number and/or ask for a free copy of our price list. All orders must be prepaid. Illinois residents add current destination tax. All foreign orders are payable in U.S. dollar-checks drawn on any U.S. bank or the U.S. subsidiary of any foreign bank. Prices and terms subject to change without notice. Address all requests to:

FIELD MUSEUM OF NATURAL HISTORY
Library—Publications Division
Roosevelt Road at Lake Shore Drive
Chicago, Illinois 60605-2498, U.S.A.

Field Museum of Natural History
Roosevelt Road at Lake Shore Drive
Chicago, Illinois 60605-2496
Telephone: (312) 922-9410